Investigation of the Influences on Surface Resistivity used for Quality Control of Concrete

Tao Fan

A Thesis

In the Department

of

Building, Civil and Environmental Engineering

Presented in Partial Fulfillment of the Requirements

for the Degree of Master of Applied Science Building Engineering at

Concordia University

Montreal, Quebec, Canada

March 2023

CONCORDIA UNIVERSITY

School of Graduate Studies

This is to certify that the thesis,

prepared by: Tao Fan

Entitled: Investigation of the Influences on Surface Resistivity used for Quality Control of Concrete

and submitted in partial fulfillment of the requirements for the degree of

Master of Applied Science (Civil Engineering)

complies with the regulations of the University and meets the accepted standards with respect to originality and quality.

Signed by the final Examining Committee:

Dr. Lan Lin	Chair
Dr. Ahmed Soliman	Examiner
Dr. Lan Lin	Examiner
Dr. Michelle R. Nokken	Supervisor

Approved by

Dr. Ashutosh Bagchi
Chair of Department or Graduate Program Director

March 2023

Dr. Mourad Debbabi
Dean of Faculty

Abstract

Investigation of the Influences on Surface Resistivity used for Quality Control of Concrete

Supervisor: Dr. Michelle R. Nokken

Tao Fan, Master

Concordia University, 2023

The destructive techniques that can be used to estimate the concrete quality are expensive and time consuming and are often accompanied by following reinforcing and repair. Therefore, non-destructive testing (NDT) methods have drawn the attention of some researchers. There is an increasing interest in electrical resistivity as non-destructive tests for quality control of concrete structures in the last decades. Electrical resistivity is a technique that is rapid and inexpensive. This project studied how the electrical resistivity of concrete and mortar cylinders immersed in different solutions changed with time in order to investigate various factors. In the two rounds tests of concrete and mortar specimens, it was found that the electrical resistance is highly influenced by the moisture content of the specimens, the immersion solutions, the water-cement ratio of the concrete as well as the addition of supplementary cementitious materials (SCMs). In addition, it was observed in the experiments that the electrical resistivity of the concrete specimens decreased rapidly within 24 hours after immersion in the solution (the specimens were dried in advance for 30 days), and the rate of decrease gradually slowed down over the next 27 days. It is also showed that the electrical resistivity of mortar specimens was significantly lower than the concrete with a similar mixture design. However, for the portion of the research that investigated the solution penetration with time by using internal sensors, the tests results are not adequate data to draw a conclusion.

Acknowledgements

It is with sincere and deepest gratitude that I would like to thank my supervisor, Dr, Michelle R. Nokken for providing this precious chance to me as one of her students. Throughout the writing of the thesis, I have received a great deal of support and assistance from her. The process of completing the dissertation was much harder and longer than I thought due to the Covid-19 and the closure of laboratory, but Dr. Nokken was always patient and kind with me. She always motivated me when I was in trouble and helped me with her knowledge and patience. Thanks again Professor for your supervision, guidance and help in this work.

I would also like to acknowledge Ms. Hong Guan, who helped a lot during the process of my experiments. Your patient support and help are so important for me to complete my dissertation.

In addition, I would like to thank Dr. Sameh Diab and Mr. Roberto Avila for providing help to me on making the experimental specimens. I could not have completed the experiments without your support.

Finally, I would like to thank my family for their continuous support and patient comfort. You are always there for me.

To the greatest of my life, mom, dad and my brother

Table of Contents

List of Figures

List of Tables

1 Introduction

Concrete is widely used as a building material presently. It is used to construct most of the infrastructure that greatly facilitates our lives, for example, highways, bridges, buildings, tunnels, subway and dams. The service life of these concrete structures is closely related to the quality of the concrete used. Among all the properties of the concrete, compressive strength and durability are the two of most important that are directly related to the quality of concrete (Sanchez, 2015). The durability of concrete is defined as "its ability to resist weathering action, chemical attack, abrasion, or any other deterioration process to retain its original form, quality, and serviceability when exposed to harsh environment" (Mehta, 2006). Durability of concrete depends largely on the properties of its microstructure, such as pore size distribution and the shape of the interconnections (tortuosity), which can be significantly affected by the use of SCMs (Elkey, 1995). High-quality concrete can continue to serve without deterioration or major rehabilitation before reaching the end of its intended service life, and proper maintenance and monitoring of the concrete are required to ensure the safety and serviceability of the structure (Wang, 2014). Since the durability of concrete is closely related to the service life of the building, there has been increasing interest in studying durability related research.

The rapid chloride permeability test (RCPT) proposed by Whiting (1981) and standardized as ASTM-C 1202 and AASHTO T 227 is widely used for assessing the durability of concrete. However, this RCPT method is neither rapid nor capable of direct measurement of chloride permeability. Therefore, the development of electrical resistivity measurement methods as a non-destructive technique (NDT) to assess the durability of concrete structures has drawn a lot of attention over the past few decades.

As an alternative of RCP test, the electrical resistivity measurement can be used to evaluate concrete's performance. The sample preparation process for resistivity tests is substantially simpler and quicker than it is for RCP tests. The Nernst-Einstein equation can also be used to directly relate the resistivity value to the concrete's chloride diffusion coefficient (Lu, 1997). Several techniques including the surface resistivity and bulk resistivity have been developed for measuring the electrical resistivity of concrete. Electrical resistivity has been standardized in 2019 by ASTM C1876 to measure the concrete bulk resistivity and also by AASHTO T358 to quantify the surface resistivity of concrete. The correlations between the resistivity measurements and certain durability characteristics of concrete have been proved by much research.

Electrical resistivity is a technique that is rapid and inexpensive. However, electrical resistivity can be affected by concrete mixture design, age of concrete and external factors such as temperature and moisture content. On the concrete mixture side, the selection of the materials not only affect the pore structure, but the electrical resistivity itself. As cement and cement replacements come into contact with the mixing water, a highly ionic solution with high pH is formed. The ionic content of this pore solution plays a significant role in its conductivity as well as the size and continuity of the pore system. Over time as cementing materials react, the pore sizes and continuity change causing an increase in resistivity.

Electrical resistivity can be carried out on standard sized cylinders. Given the non-destructive nature of the test, the electrical resistivity can be carried out immediately prior to testing the

same sample for compressive strength. However, standard compressive strength tests are typically performed at the age of 28 days after casting. In some cases, this requires advance planning and a possible change to the curing method. Surface resistivity, according to AASHTO 358, requires the concrete cylinder to be immersed in a limewater solution for a minimum of 21 days. As limewater is one of the acceptable curing methods for compressive strength, little needs to do to add resistivity to the testing protocol. However, ASTM C 1876 (the bulk resistivity method), involves immersion for a minimum of 6 days in a simulated pore solution requiring a change in solution which adds a conflict with the strength testing standard. This issue can be rectified by casting additional cylinders. As mentioned previously, mixture design, hydration, pore solution conductivity all plays a role in the measured resistivity. This research endeavours to investigate variables related to the development of resistivity with time. One key research objective is to compare the two resistivity tests and the standard immersion solutions.

1.1 Research Objectives

The main focus of this study is to analyze some of the influencing factors of electrical resistivity by the use of a resistivity measuring device. As mentioned before, electrical resistivity can be affected by many factors: concrete mixture, age of concrete and external environment, etc. The main research objectives are:

- Investigate how the surface resistivity and bulk resistivity change after immersion in the solutions in different initial moisture states.
- Determine how the inclusion of supplementary cementitious materials in concrete influence the electrical resistivity changes with time of the concrete.
- Investigate how the electrical resistivity of concrete is influenced by different immersion solutions (limewater, simulated pore solution and double strength pore solution).
- Analyse the difference in surface and bulk resistivity over time and between variables of mixture design, saturation, and immersion solutions.
- Examine how the age of concrete affects the electrical resistivity of the concrete.
- Investigate the penetration of solution after immersed the concrete samples into solutions (monitoring the resistivity at varying depths).

1.2 Thesis Outline

This thesis consists of 5 Chapters. Chapter 1 gives a brief background and the research objectives. A review of literature relevant to the topic of the research is the subject of Chapter 2. The research methodology including the mixture designs, the experimental techniques and the details of the testing protocol are given in Chapter 3. Chapter 4 contains the experimental results with a discussion of the relevance to the research objectives. The major conclusions and some recommendations for future work are the topic of Chapter 5.

1.3 List of Abbreviations

ASTM	American Society for Testing Materials
AASHTO	American Association of State Highway and Transportation Officials
W/C	Water to cement ratio
LW	Limewater solution
SPS	Simulated pore solution
DSPS	Double-strength pore solution
SSD	Saturated surface dry
SCMs	Supplementary cementitious materials
ILS	Interlaboratory study
NIST	National Institute of Standards and Technology
ERT	Electrical resistivity tomography
PCB	Printed circuit board

2 Literature Review

2.1 Concrete Durability

Over the last century, the research on the durability of concrete has attracted significant attention and it is still a research hotspot at present. Generally, there is an agreement that freezing and thawing, corrosion of reinforcing steel, alkali-silica reaction and sulphate attack are the most common deterioration mechanisms. They have different paths to affect the concrete, but all will destroy the concrete structures eventually.

Generally, the deterioration mechanisms of concrete can be divided into three parts: (1) Physical deterioration (freezing and thawing, for example); (2) Chemical Deterioration (alkali-silica sulphate attack and sulphate attack); and (3) Reinforcement corrosion. For freezing and thawing, the mechanism has been researched a lot and is widely known. It is mainly because of water entering the pore system and when exposed to a cold environment, water freezes and expands. The water expands by 9% of the volume as it freezes, producing huge hydraulic pressures in the capillaries and pores of the cement paste. Cracks will form when the pressures exceed the tensile strength of the concrete. Then the ice thaws and more water get into the cracks, followed by a repeated process of water freezing, expanding and thawing, generating more cracks. The durability of concrete will be greatly affected by this deterioration process. With cycling, the effect is cumulative, it can lead to cracking, scaling, delamination, or spalling. Therefore, the common methods to improve the concrete's resistance to freezing-and-thawing are: (1) keep concrete below critical saturation (but not always possible); (2) reduce the amount of freezable water by reducing capillary porosity (low water and cement ratio w/c); (3) addition of entrainment (providing a relief for hydraulic pressure).

For the chemical deterioration (alkali-silica reaction and sulphate attack), there are very complicated chemical reactions present in the deterioration process. The mechanisms are complex, and some are even not clear at present, requiring further studies. However, the non-reactive aggregate, low alkali cement and the supplementary cementitious materials are recommended to use to decrease the influence of chemical deterioration of alkali-silica reaction. Limiting calcium aluminates is the many preventative method for sulphate attack.

For reinforcement corrosion, the research and experience have shown that the corrosion can take place after a short time when the reinforced concrete structures are put in service. The main reason for cracks in reinforced concrete is the corrosion of the rebars. Generally, concrete provides an alkaline environment (pH=12.5-13.5) around the steel surface which can prevent it from corrosion. However, once this alkaline environment is weakened (pH lower than 8) due to the occurrence of carbonization (carbon dioxide from the air reacts with calcium dioxide), corrosion of steel bars ensues (Woelfl, 1979). Another reason is the ingress of chloride ions, which will also destroy the passive layer between steel and concrete (Xie et al, 2012). When the chloride exceeds the critical concentration, it will weaken the passivity and increase the active corrosion rate of carbon steel in neutral and alkaline pore water solution. The resulting iron corrosion products can form acidic solutions with chlorides, which then neutralize the alkaline concrete environment and further enhance corrosion (Liu, 2008). Therefore, the reinforced concrete structures require regular maintenance to make a longer service life.

2.2 Concrete Electrical Resistivity

2.2.1 Introduction

The electrical resistivity of concrete can be described as the ability of concrete to withstand the transfer of ions subjected to an electrical field (Gowers and Millard, 1999). It is an inherent property of a material which is represented as ρ. It can be calculated through measuring electrical resistance, $\boldsymbol{R}$, in an appropriately designed circuit, and applying a certain geometry factor, γ. The relationship between resistivity and resistance is shown in equation 1 (Layssi et al, 2015).

$$\boldsymbol{\rho = \gamma * R} \ \text{(ohm·cm) or (Ω·cm)} \tag{1}$$

Based on equation (1), the concrete resistivity is determined by measuring electrical resistance and applying a geometry factor. The geometry factor depends on the size and shape of the sample as well as the distance between the probes on the testing device. For instance, for a concrete cylinder sample with the length of L and cross section area of A with the electrical current flow unidirectionally along the length, the geometry factor γ for this concrete sample is:

$$\gamma = \frac{A}{L} \tag{2}$$

The electrical resistivity of the sample will be:

$$\rho = R\ (\frac{A}{L}) \tag{3}$$

The electrical conductivity is the ability of the material to carry an electric current, which is inversely related to electrical resistivity, as shown in equation (4).

$$\sigma = \frac{1}{\rho} \ \ (\mathrm{S/m}) \tag{4}$$

Based on the equations, the resistivity of the concrete can be known once the resistance is detected. It is important to note that resistivity and resistance are two different properties of one material. The resistivity is an inherent property of a material regardless its size and shape. Generally, one material has approximately the same resistivity, while the resistance of one material could change when it has different size and shape, for instance, for a copper conductor, the resistance of long and thin copper wires is much greater than that of thick and short copper wires.

The ability of concrete to resist electrical current is related to its ability to resist chloride ion movement. Over the last few decades, a great deal of attention has been paid on electrical resistivity measurement techniques as a non-destructive technique (NDT) to evaluate the durability of concrete structures (Azarsa and Gupta, 2017). Concrete pore fluid is an electrolytic solution containing various ions, K^+, Na^+, Ca^{2+}, SO_4^{2-}, OH^-, etc. Other ions (such as chlorides which is an aggressive ions) could also be present in pore water due to intrusion into concrete from the external source (seawater) which will increase the ions concentration in the pore solution and reduce the resistance of the concrete. Based on the previous research, the deterioration processes of concrete structures will decrease the durability that are partially controlled by transport of aggressive ions through the concrete microstructure (Layssi et al,

2015). The concrete resistivity indicates its ability to withstand transfer of charged ions. Therefore, the increase of ionic concentration in the pore water leads to the decrease of electrical resistivity. Additionally, the degree of saturation and pore structure are also major factors for concrete resistivity. A structure with a lower permeability will increase the resistance to intrusion of aggressive ions and transfer of ions, meaning higher electrical resistivity. As a conclusion, the concrete electrical resistivity is a combined result of many factors.

2.2.2 Influencing Parameters on Resistivity

Based on numerous previous research studies, it was found that the electrical resistivity of concrete could be affected by many factors (Weydert, 1999 and Elkey, 1995). The electrical resistivity of concrete is related to the microstructure of the concrete, pore structure, porosity, concentration of ions, etc. This part briefly introduces some parameters that influence the electrical resistivity. It is divided into two parts: (1) factors influencing electrical resistivity and (2) factors influencing the electrical resistivity measurements.

Factors Influencing Electrical Resistivity

Effect of Water-cement Ratio (w/c ratio)

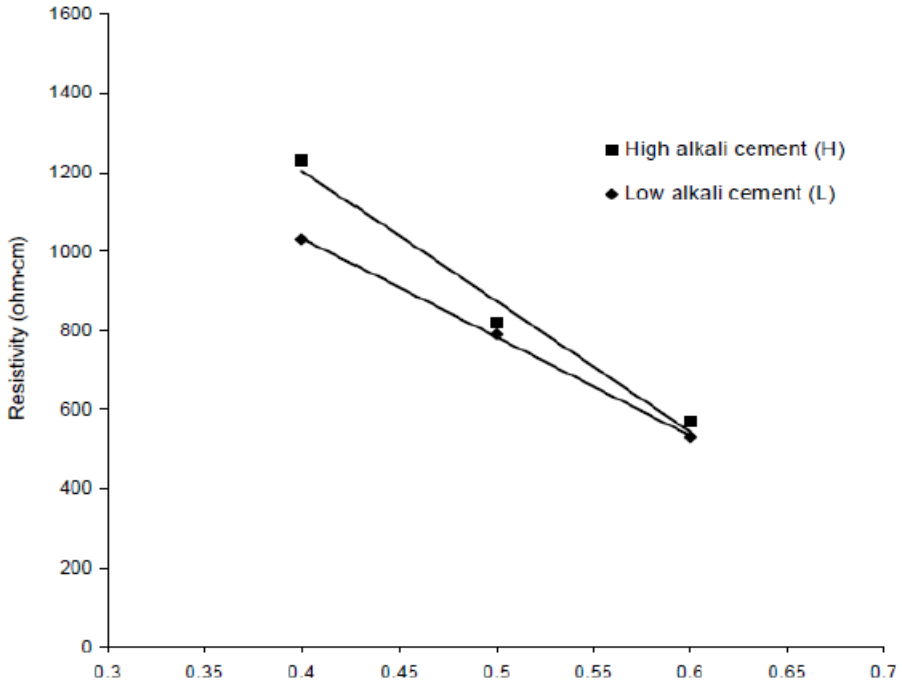

Figure 1: Effect of w/c ratio on electrical resistivity (Monfore, 1968).

The water-cement ratio is one of the most important factors that affect the concrete resistivity, because it plays an important role in the formation of microstructure of the cement paste as well as the ionic concentration of pore solution. Generally, a higher w/c ratio of concrete means a

high percentage of porosity, leading to a more permeable concrete, and results in a lower electrical resistivity. A previous study (Monfore, 1968) showed that increasing w/c ratio from 0.40 to 0.60 resulted in a twofold reduction in resistivity as shown in Figure 1.

However, some other studies found that this rule doesn't apply in some cases, for instance, in the research of Sanchez (2015), in the samples containing blast furnace slag, it was found that there was not a consistent decrease in resistivity with increasing w/c ratio. But there is no doubt that the water to cement ratio has a significant impact on the resistivity of concrete.

Effect of Cement and Aggregate Type and Size

Concrete is a complicated material formed by aggregates and hydrated cement paste which is acting as binding material resulting from the reaction product of cement and water. Different kinds of concrete are made of different aggregates and cements, forming different microstructure, and therefore influence the electrical resistivity of the concrete. For example, the resistivity of blended cements is higher than that of ordinary Portland cements. The reason is that the supplementary cementitious materials (SCMs) in the blended cements like fly ash and furnace slag has a filler effect leading to a fine pore structure (Banea, 2015). This will increase the tortuosity and decrease the permeability of the concrete, affecting the transport properties and the resistance to the penetration of aggressive agents of concrete, thus improving the durability of the concrete. However, the blended cements hydrate very slowly, requiring a long time to achieve the desired condition.

Effect of Supplementary Cementitious Materials (SCMs)

It has been proven by many studies that the use of SCMs could increase the electrical resistivity of concrete, as mentioned above. The first reason is that the addition of SCMs could provide reactive amorphous silica leading to a Pozzolanic reaction which could enhance the mechanical properties and durability. The second is that SCMs can lead to a physical filler effect which reduces the porosity between cement grains. It was observed that the increasing of percentage of Portland cement replaced by SCMs could increase the value of surface resistivity (Kessler et al, 2008 and Rupnow and Icenogle, 2011).

Factors Influencing the Electrical Resistivity Measurements

Effect of Moisture Content

Moisture content has been reported as another important factor that affects the electrical resistivity of concrete. This is because the electrical current passing through concrete is carried by the pore solution. Generally, electrical resistivity increases with decreasing moisture content. As the moisture content of concrete decreases, there is less pore solution existing in the pore system to carry the current, leading to an increase of resistivity (Banea, 2015).

However, in Larsen's (2007) research, the electrical resistivity of 8 concrete mixtures samples under different moisture states was measured. Based on the results, it was found that when the moisture degree (MD) decreases from 88% to 77%, the surface resistivity increases as average of 2 times. And there is a more obvious change on surface resistivity almost average 6 times increase when the moisture degree decreases from 88% to 66% as Figure 2 shows.

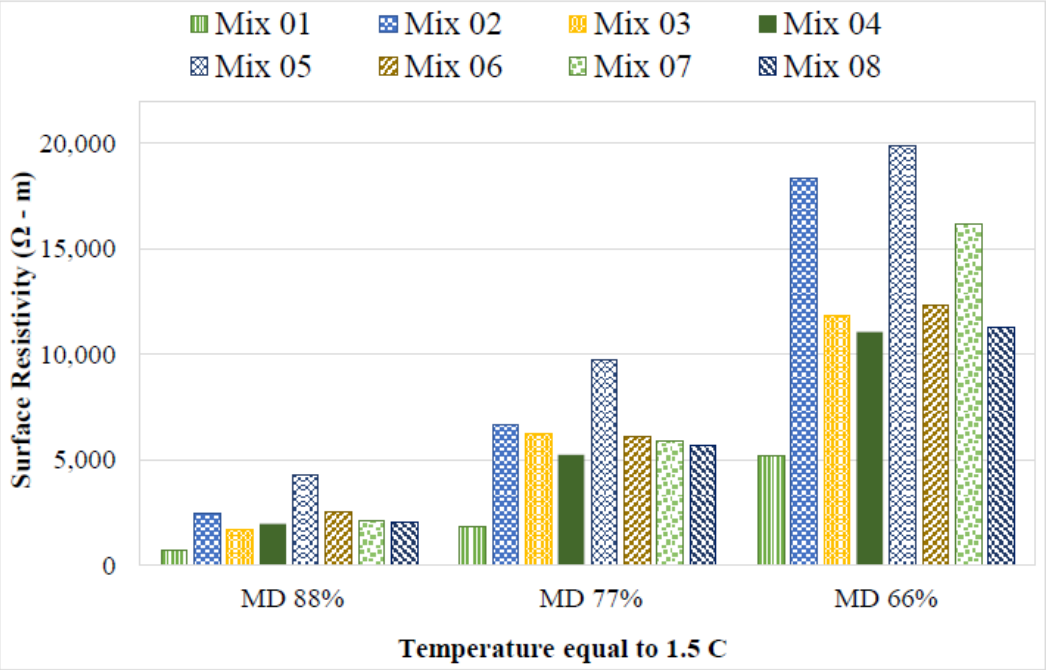

Figure 2: Moisture degree effect on surface resistivity (Larsen et al, 2007).

Effect of Temperature

Temperature has a great influence on electrical resistivity of concrete. A temperature increase will lead to a decrease in resistivity (Azarsa et al, 2017). When the temperature increases, the viscosity of the pore solution decreases, therefore increasing the mobility of the ions that carry the current (Banea, 2015). According to the data from the research of Larsen et al (2007), when the temperature is increased from 1.5 ° C to 20.5 ° C, the resistivity is reduced by an average of 2.20 times, and at 40 ° C, it is reduced by nearly 5 times. The research of Elkey and Sellevold (1995) studied the effect of temperature. They found that a 5% change of resistivity per °C at 21 °C under 30% saturation, and a 3% change of resistivity per °C under 70% saturation.

Effect of Saturation

In the research of Sanchez Marquez and Nokken (2014), the influence of saturation on electrical resistivity was studied. In this research, samples with different binder combinations and water-cement ratios were studied to determine the saturation duration required to reach a constant resistivity and found that 24 hours saturation resulted in stable resistivity measurements.

In this study, five kinds of binder combinations were researched. Each binder combination has five mixtures with w/c ratio ranging from 0.32 to 0.64. The samples were stored in limewater solution at 23 °C for 7 days. The samples of cylinders were removed from the containers at the age of 28, 56 and 91 days to measure the surface resistivity over 3 days to study the influence of saturation. The results at the age 28 days for 3 binder combinations are shown in Figure 3 to 5:

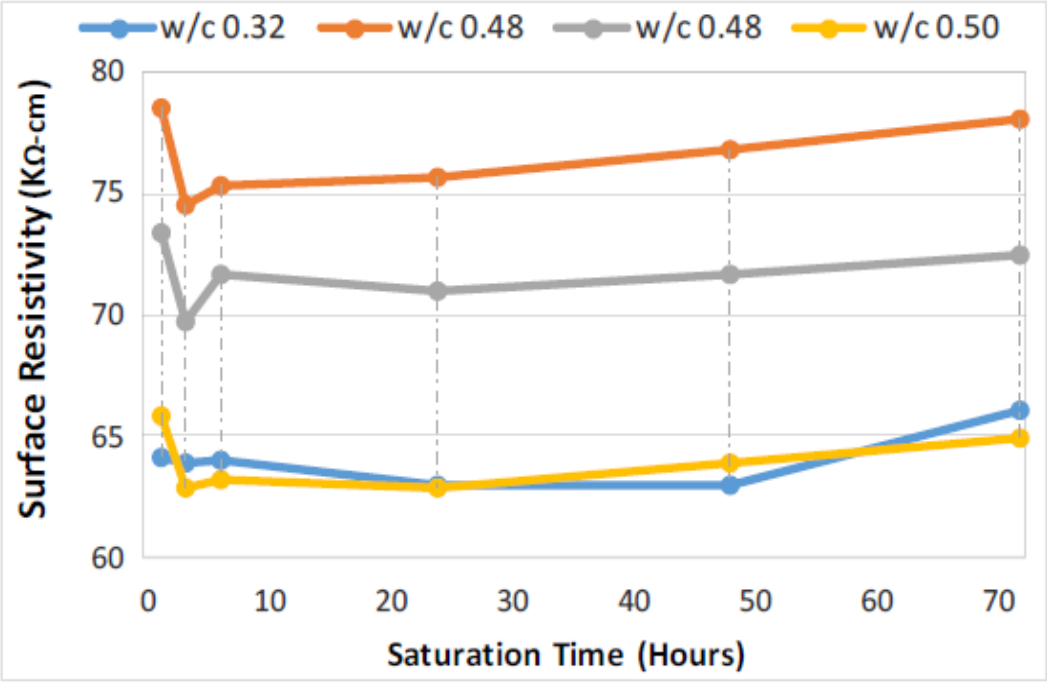

Figure 3: Resistivity values against saturation time mixture 100TI (Sanchez et al, 2014).

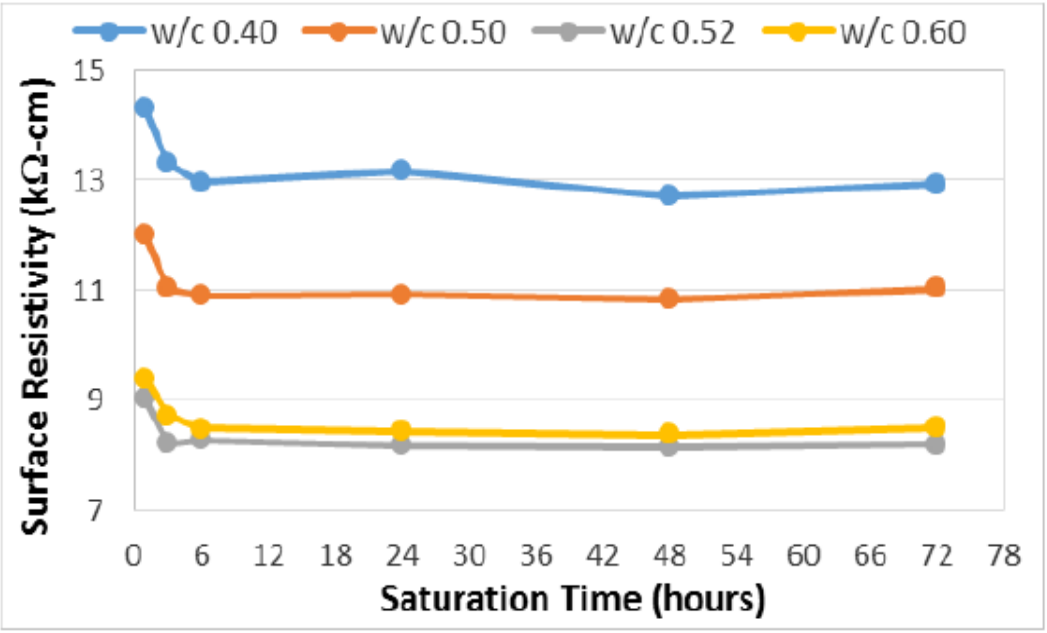

Figure 4: Resistivity values against saturation time mixture 50L–50S (Sanchez et al, 2014).

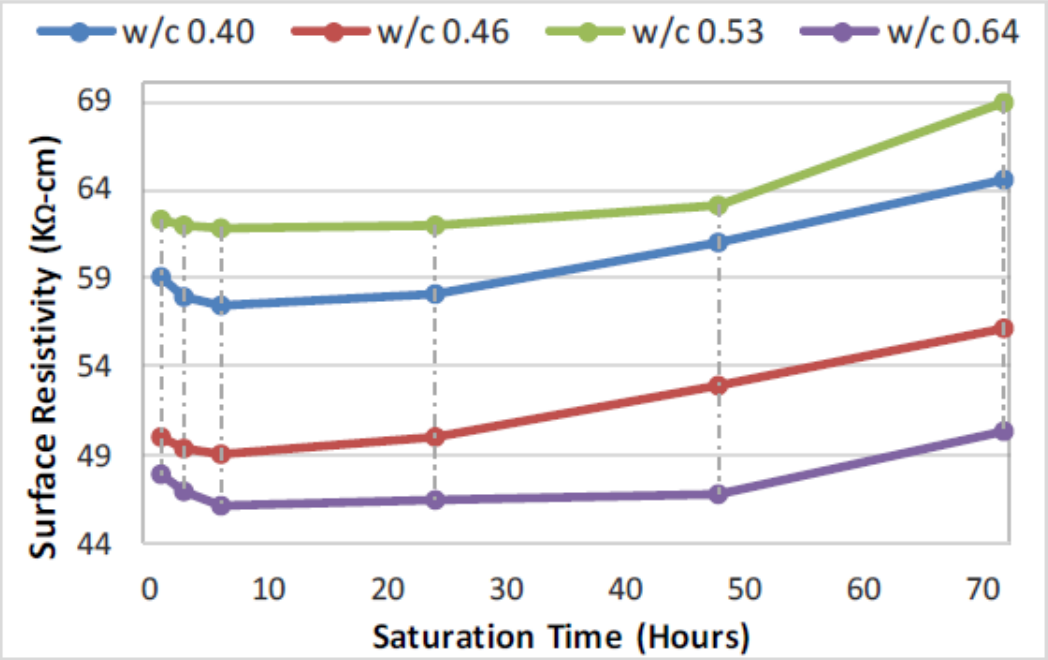

Figure 5: Resistivity values against saturation time mixture 50TI-20FA-30S (Sanchez et al, 2014).

It can be seen that the behaviors of the three mixtures are very different. For the mixture only including Portland cement (100TI), the resistivity decreases at the first 6 hours and then becomes stable. For the mixtures containing slag (Figure 4 and 5), a drop of resistivity was first observed, and then there is a gradual increase. In this study, 24 hours was considered sufficient to obtain reliable measurements.

Determination of Degree of Saturation

According to Qiao's (2019) study, the samples submerged in simulated pore solution reach a degree of saturation relating to the filling of pores, (the Nick Point as in Figure 6). As shown in Figure 6, after immersed in the simulated pore solution, the electrical resistivity of the samples decreased as the mass increased (the solution entered the pore structure). It can be seen from the figure that the mass of samples increased rapidly before the Nick Point, and the increase slowed down after Nick Point. While for the resistivity, it can be found that before the Nick Point, the resistivity decreased significantly and showed a slight increase in resistivity. Therefore, at Nick Point, the samples achieve a degree of saturation, defined as S_{NK} in Qiao's (2019) study. The degree of saturation at Nick Point (S_{NK}) can be calculated by the following equation:

$$S_{NK} = \frac{m_{NK} - m_{OD}}{m_{SAT} - m_{OD}} \quad (4)$$

where m_{NK}, m_{OD} and m_{SAT} are the mass (g [lb]) at S_{NK}, oven dry, and saturation respectively.

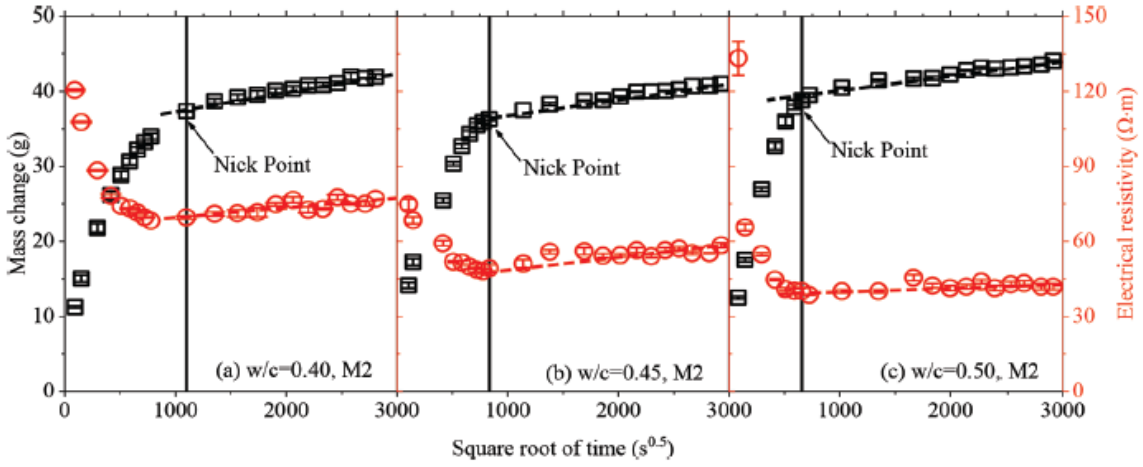

Figure 6: Determination of saturation degree (Qiao et al, 2019).

2.3 Concrete Resistivity Measurements

Firstly, there are some different commercially available electrical test setups that could be used to measure the bulk and surface resistivity of concrete. Milena (2018) summarized three setups that are most widely used: surface resistivity (SR), axial resistivity (AR) and electrical impedance spectroscopy (EIS) measurements.

Figure 7: Surface resistivity test device (Proceq's Resipod (left) and Giatec surf™ (right)).

https://www.berraproducts.com.au/wp-content/uploads/2018/05/Surf%E2%84%A2-Data-Sheet.pdf

Moreover, different types of sensors have also been proposed by Milena (2018) to measure bulk resistivity of concrete. These sensors are installed and embedded in the fresh concrete and could provide measurements data in real-time.

On the other hand, in a published paper (Charmchi, 2018) that studied the relationship between concrete maturity and its electrical resistivity, some devices that used to measure electrical resistivity were compared including Giatec's RCON, German Instrument's Merlin, and Proceq's Resipod. in this paper, the resistivity development of eight different concrete mixtures curing in different environments were monitored by the above three resistivity meters related to sample maturity. The results show that Giatec RCON could provide relatively accurate results (±5%). The Giatec RCON is a non-destructive testing device to measure the bulk electrical resistivity of concrete which is fast (less than 5 seconds), accurate and allowing long-term continuous electrical resistivity measurements.

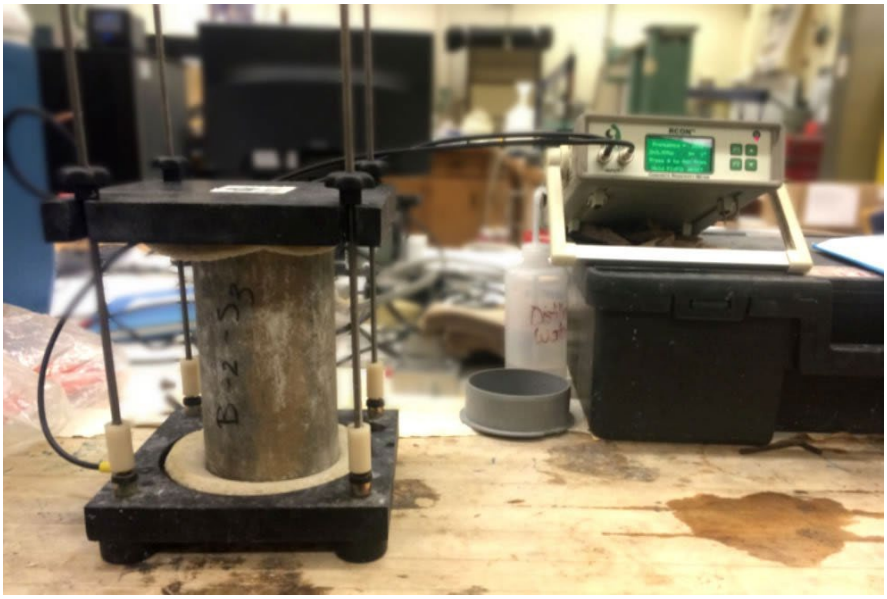

Figure 8: the Giatec RCON testing device.

https://medium.com/@Giatec/estimating-concrete-bulk-resistivity-via-the-maturity-method-b5588a4d185

Pore solution resistivity of concrete

The pore solution resistivity measurment is more challenging than measuring bulk resistivity because extraction of pore solution is a difficult process (Chang, 2018). In Chang's paper, some different methods used to determine pore solution resistivity were introduced. Besides, three methods were also introduced by Milena (2018) and Weiss (Weiss et al, 2017).

1) In some cases, a constant recommended value of 10 S/m (resistivity of 0.1 Ω·m) can be used ignoring the mixture design, degree of hydration, or material composition.

2) The electrical resistivity of pore solution can be determined by using a model by National Institute of Standards and Technology (NIST) to simulate the pore solution resistivity.

In this model, the needed input materials are mixture proportions, chemical compositions of cementitious materials and estimated degree of hydration. Based on this model, Bentz at NIST developed an online calculator to determine the pore solution resistivity. This calculator is simple to use although it has some limitations.

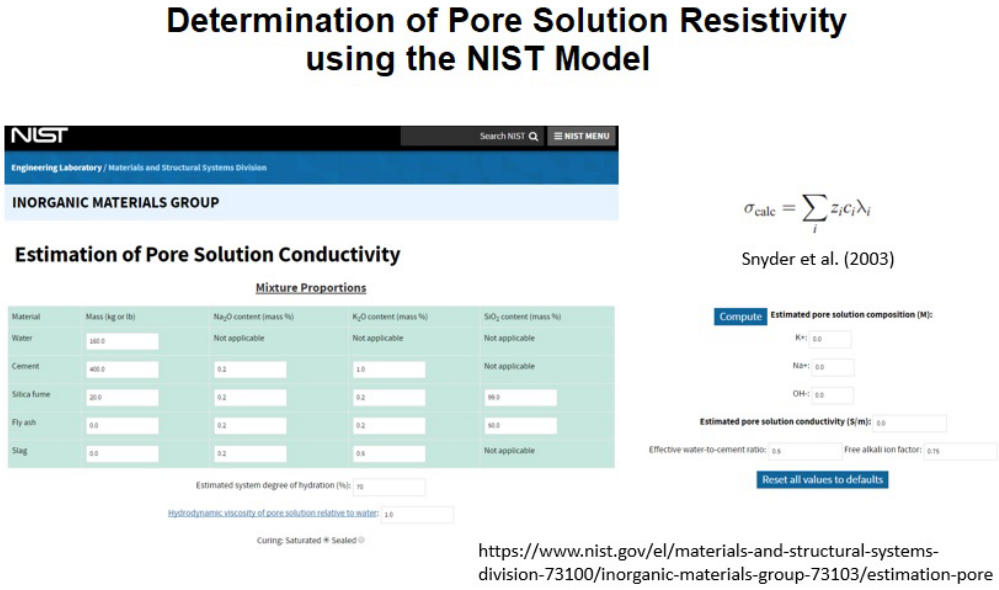

Figure 9: The model by NIST to calculate the pore solution resistivity (Bentz, 2007).

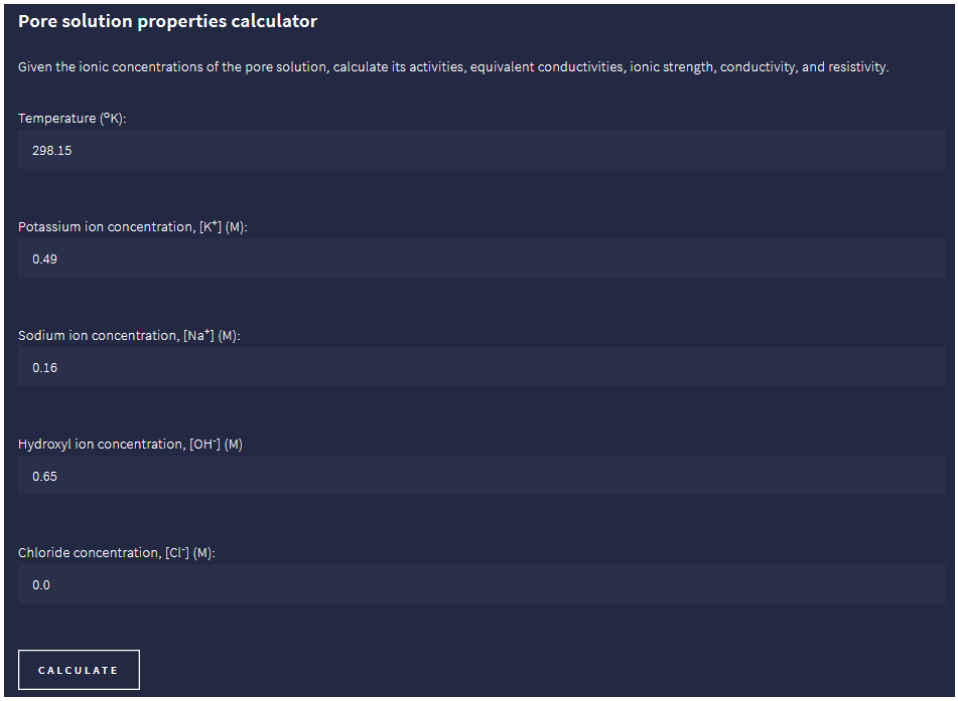

Figure 10: The online pore solution calculator (Bentz, 2007).

3) Pore solution expression method. The pore solution resistivity can also be determined directly and indirectly by extracting the pore solution from concrete.

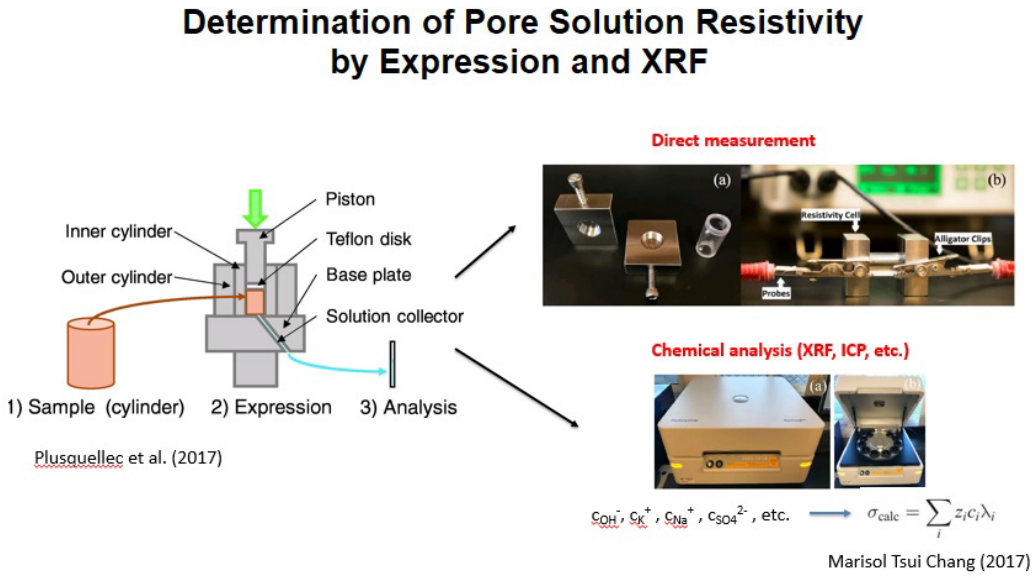

Figure 11: Determination of pore solution resistivity by expression and XRF (Chang, 2017).

The direct analysis uses a resistivity meter to measure the resistivity of the extracted pore solution, while the indirect analysis uses chemical analysis like X-ray fluorescence (XRF) or, inductively coupled plasma (ICP) to analyse the chemical composition of the extracted pore solution, which is called pore solution expression method.

2.4 Water Absorption and Initial Moisture Content

2.4.1 Background

The durability of concrete is greatly influenced due to the ingress of water into concrete. Generally, the deterioration mechanisms of concrete such as freezing and thawing, sulfate attack and reinforcement corrosion are closely related to water. Therefore, water absorption can be used to evaluate concrete quality and its resistance to deterioration.

The durability of concrete is largely related to its transport properties which means the transport resistance could measure the durability of concrete structure as an index. Water absorption is one of the most important and effective methods that have been studied many years used to measure transport mechanism (Mohammadi, 2013). Permeability, absorption and diffusion are the three

main modes of transport mechanisms in cementitious materials. In this part, a review of water absorption was performed.

2.4.2 Water Absorption Mechanism

Water absorption, or sorptivity, is defined as the water flow in unsaturated porous materials like concrete due to pressure difference caused by capillary and gravitational forces (M. Nokken and R. D. Hooton, 2002). The mechanism of water absorption has been studied by many researchers for a long time. During this time, some researchers like Washburn and Poiseuille proposed their own theoretical models regarding water absorption into a porous media. The Lucas-Washburn Equation (Washburn, 1921) describes the rate of flow in a horizontal pore based on some important assumptions, such as ignoring the air resistance. As the following equation shows:

$$\frac{dl}{dt} = \frac{r}{\eta}\frac{\gamma}{4l}cos\varphi \tag{5}$$

Where:

$\frac{dl}{dt}$: Rate of flow in a capillary (m/s).

r: Capillary radius (m).

η: Viscosity of the liquid (N·s/m^2).

γ: Surface tension of the liquid (N/m).

l: Length of pore already filled with the liquid (m).

φ: Contact angle (degrees).

Initially, the Hagen-Poiseuille equation is described as the following:

$$Q = \frac{\pi r^4}{8\eta}\frac{H}{l} \tag{6}$$

H is the head of pressure in the equation. In Nolan's research (Nolan, 1996), the head of pressure is divided into two parts: capillary pressure (H_c) and applied pressure head (H_a). The reason of using H_a is technical limitations in water absorption tests.

Moreover, a series of research was conducted. The research of Levitt (1971) states the description of H_c, and Hall (1981) found that *n* is almost equal to 0.5 for initial concrete water absorption in the experiments.

Finally, the following equation is obtained:

$$i = S \cdot t^{-0.5} \tag{7}$$

Where:

i: cumulative volume of absorbed water per unit of area (mm^3 /mm^2).

S: sorptivity (m/s$^{1/2}$).

t: time (s).

This equation is now widely used to for measurements of both in-situ and laboratory water absorption. It can be seen from the equation that the sorptivity value could be found by measuring the quantity of absorbed water and the calculating the square root of time.

2.4.3 Water Absorption and Moisture Content

Based on the results of some previous research, it was found that the concrete moisture content has a marked effect on water absorption. Several studies have been performed concentrating on the relationship between moisture content and water absorption measurement with different methods. This part briefly introduced these studies.

Figg (1973) studied the relationship between moisture content and water absorption of concrete with w/c ratio of 0.68, 0.78 and 0.88. The water absorption test was performed based on the Figg method. In this research, a linear relationship was found between absorption index and samples moisture content. In addition, it was also found that for higher w/c ratio concrete, the moisture content has a less effect on water absorption.

In 1997, the influence of moisture content on sorptivity was studied by DeSouza et al. (1997). This research studied four kinds of concrete mixtures under two different curing methods (moist curing and curing compound). The samples first were submerged in water for 14 days for saturation, and the initial saturated sorptivity index was confirmed to be zero. Then in order to obtain different moisture contents, the samples were dried in different ways. Before testing the sorptivity of the specimens, the mass after each drying step needs to be recorded. And finally, testing the sorptivity and recorded. The results exhibit in the following part and combine with the research of Nokken and Hooton (2002).

In the research performed by Nokken and Hooton (2002), it mainly studied the effect of concrete moisture content on water absorption. By using a method similar to the ASTM C1585 testing method, water absorption tests were conducted on three concrete mixtures that had been preconditioned to various initial moisture content. In their experiments, the sides of samples were sealed with electrical water and dried for 14 days before moisture conditioning. Then the specimens were exposed to water for 15 min-18 hours at 23 °C followed by placing them in sealed bags in a sealed container for four weeks to allow the samples to absorb water before testing the sorptivity, and finally, the sorptivity index of the samples was tested.

Based on the analysis on the data obtained from Nokken and Hooton's work, they found that there is a linear relationship existing between initial moisture content and sorptivity, as shown in Figure 12.

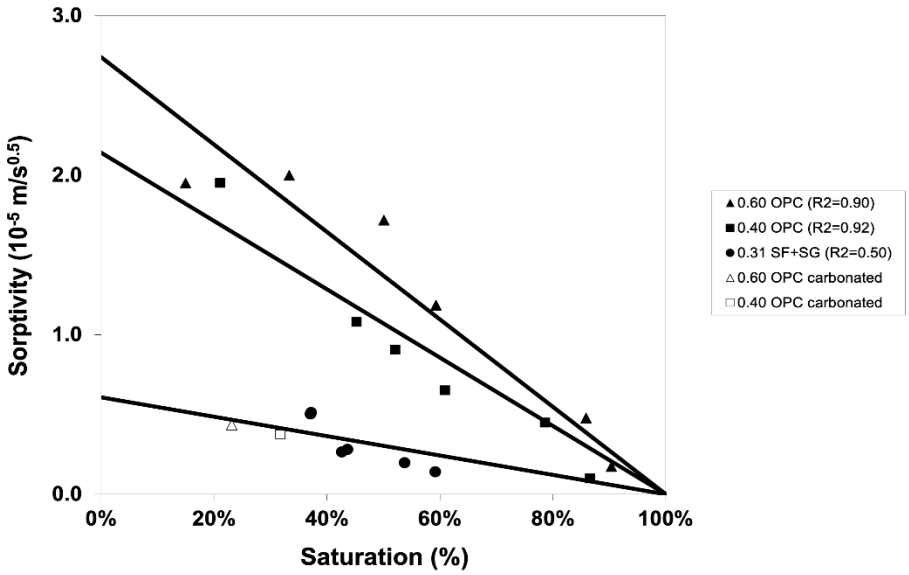

Figure 12: Effect of initial saturation on sorptivity (Nokken and Hooton, 2002).

From Figure 12, it can be found that the sorptivity decreases linearly as the level of initial degree of saturation increases. Besides, at the same level degree of saturation, the sorptivity will decrease with decreasing water-cement ratio for the mixtures, and this is the same for all values of initial saturation. Moreover, the greater the w/c ratio, the greater the downward trend of the sorptivity. This occurs may because pore size and connectivity increase with increasing w/c ratio.

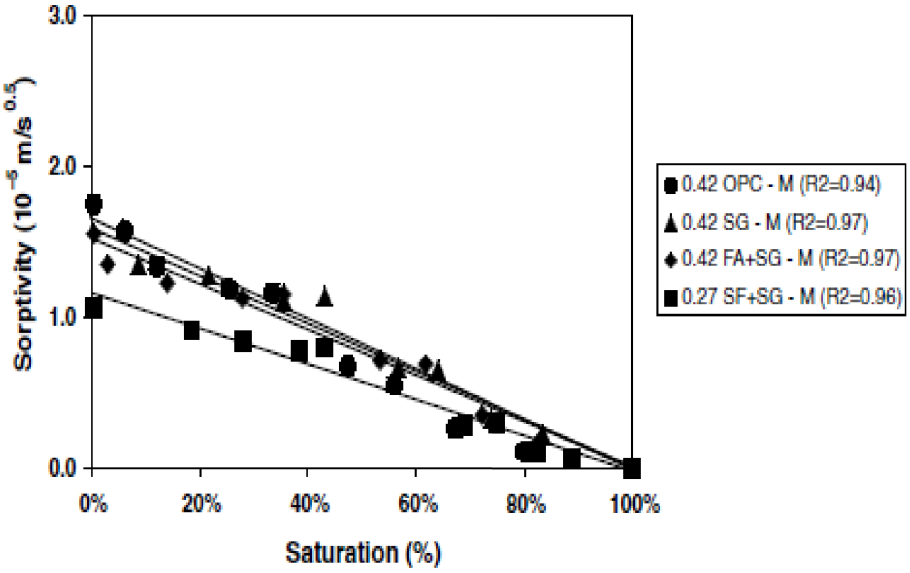

Figure 13: Sorptivity versus degree of saturation for moist cured mixtures (Nokken and Hooton, 2002).

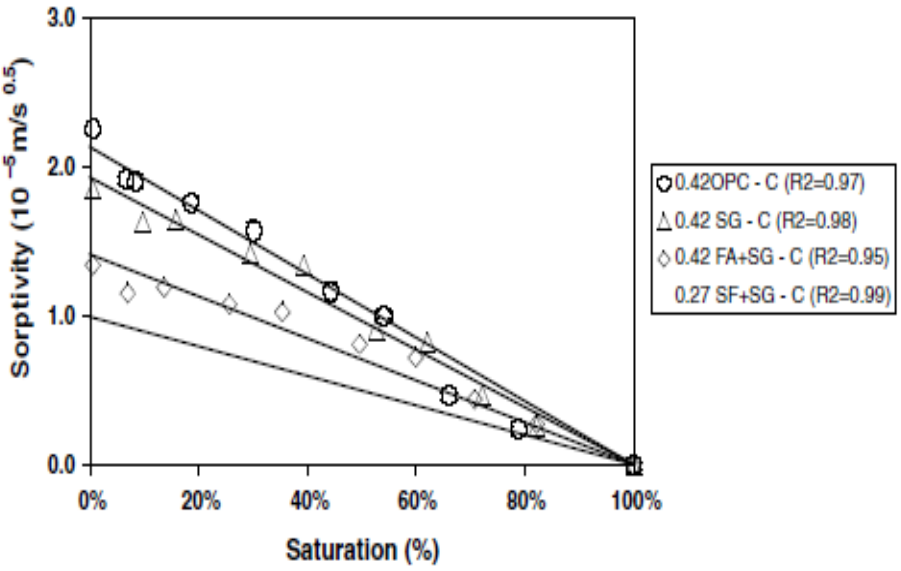

Figure 14: Sorptivity versus degree of saturation for curing compound mixtures (Nokken and Hooton, 2002).

In Nokken and Hooton's study, they also analyzed the data from the previous work performed by DeSouza et al. (1996, 1997) and combined with their results and found that the result of sorptivity show the same trend (Figure 13 and 14).

A study performed by Mohammadi and Nokken (2017) aimed to develop the in-situ water absorption method by laboratory study and field validation. The sorptivity measurements were performed at six different level moisture content.

The relationship between concrete saturation degree and sorptivity is shown in Figure 15. It is clear that a linear trend exists between the saturation degree and sorptivity index. For all mixtures, the sorptivity index increases with the decreasing of saturation degree. In addition, as the w/c ratio increases, the sorptivity index also increases at the same degree of saturation. This conclusion is the same with that from the research from Nokken and Hooton.

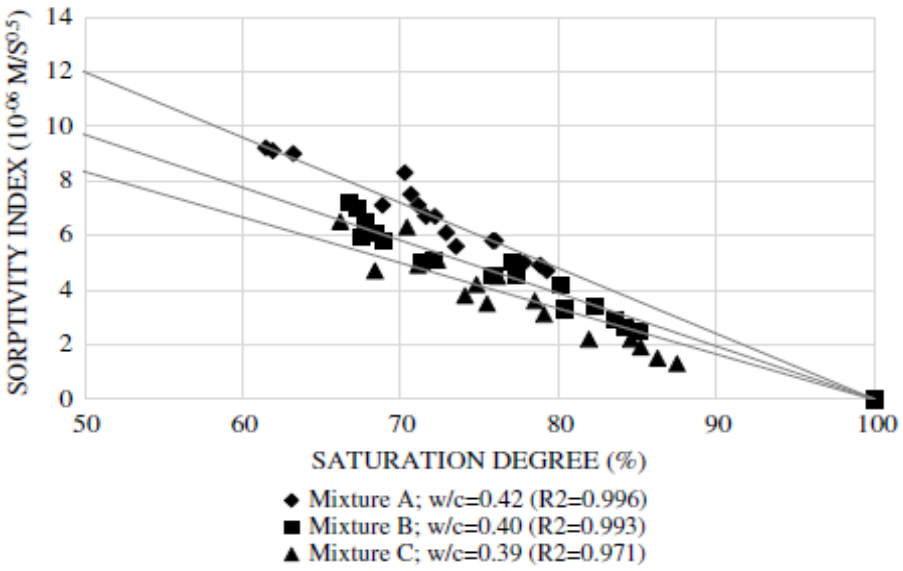

Figure 15: Relationship between concrete saturation degree and sorptivity for laboratory tests (Mohammadi and Nokken, 2017).

Figure 16 indicates the relationship between saturation degree and surface relative humidity (RH). There is also a strong linear relationship forming between the two results. Surface RH was found could be an accurate and practical indicator of concrete moisture content.

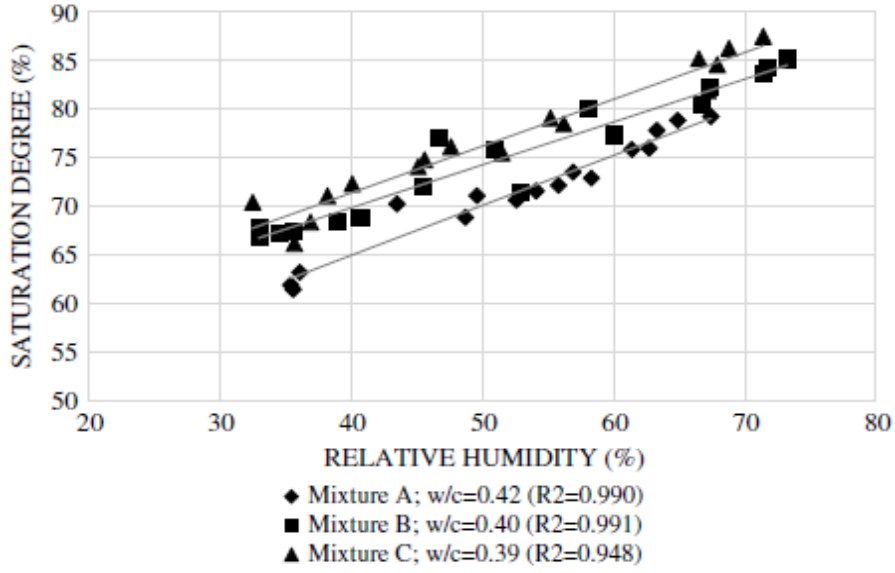

Figure 16: Relationship between saturation degree and relative humidity (Mohammadi and Nokken, 2017).

Moreover, although performing rapid nondestructive water absorption tests are simple at laboratory conditions. However, it is impossible to control the conditions like temperature or RH in-situ measurements. In this research, the outdoor and in situ measurements showed

acceptable correlation with laboratory results after using temperature correction which make the test reliable for quality control.

2.5 Electrical Probes for Determining Moisture Ingress

In this part, a brief introduction about electrical sensors was performed. The development of sensors system consists of integrated monitoring systems as an important part to assess cover-zone concrete (covecrete) performance and durability. It can be used to offer real-time data of the condition of covecrete (McCarter, Chrisp et al, 2005).

2.5.1 Cover-zone Concrete (covercrete) Electrode-array System

Figure 17 shows a sensor system developed by the study of McCarter (1995), which is used to obtain the spatial distribution of electrical conductivity within the cover-zone of concrete specimens (McCarter, Chrisp et al, 2005).

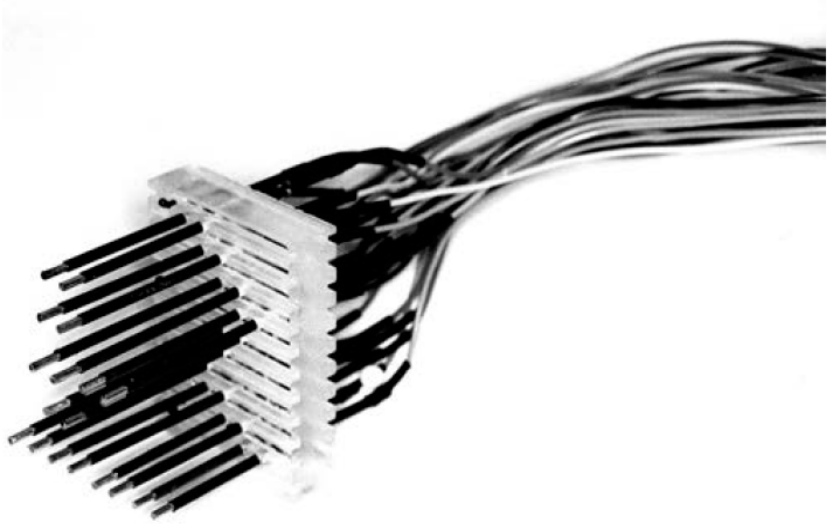

Figure 17: Electrode sensor (McCarter et al, 2005).

As the Figure 17 shows, the sensor includes 10 pairs of electrodes installed on a small plexiglass molder. Each electrode includes a stainless-steel needle (1.2 mm diameter) that exposes a 5 mm tip. The horizontal center distance of the pins is 5 mm in each electrode pair. The electrode pairs are then arranged vertically at 5 mm intervals so that electrical measurements can be made at 10 discrete points to a depth of 50 mm. The electrode pairs are not aligned in parallel in the horizontal and vertical directions and are offset from each other. In addition, four thermistors are installed on the sensor 10, 20, 30 and 40 mm from the exposed surface to obtain the temperature curve in this area.

2.5.2 Multi-ring Electrode Moisture Sensor

The geometry and layout of the electrodes in this system (see Figure 18) are very different from the cover-zone concrete (covercrete) electrode-array system. This sensor has been developed more than 10 years and many applications have been used. Multi-ring electrodes are widely used to determine the moisture distribution in concrete near the surface of a water-containing concrete (http://www.sensortec.de/sensoren-sensors/multiring-elektrode-multiring-electrode.html). The electrodes consist of eight 2.5mm thick stainless-steel rings (d = 20 mm, h = 5 mm) spaced 5 mm apart and a pt1000 temperature sensor. An insulation ring was placed between two adjacent steel rings. Through the measurement of the alternating current (AC) resistance between adjacent steel rings, the resistivity curve over the length of the multi-ring electrode can be determined. If the calibration curve of the concrete under consideration is known, it can be converted into a moisture curve. The number of stainless-steel rings, the distance between them and the geometry of the sensor can be adjusted according to the specific requirements of the structure.

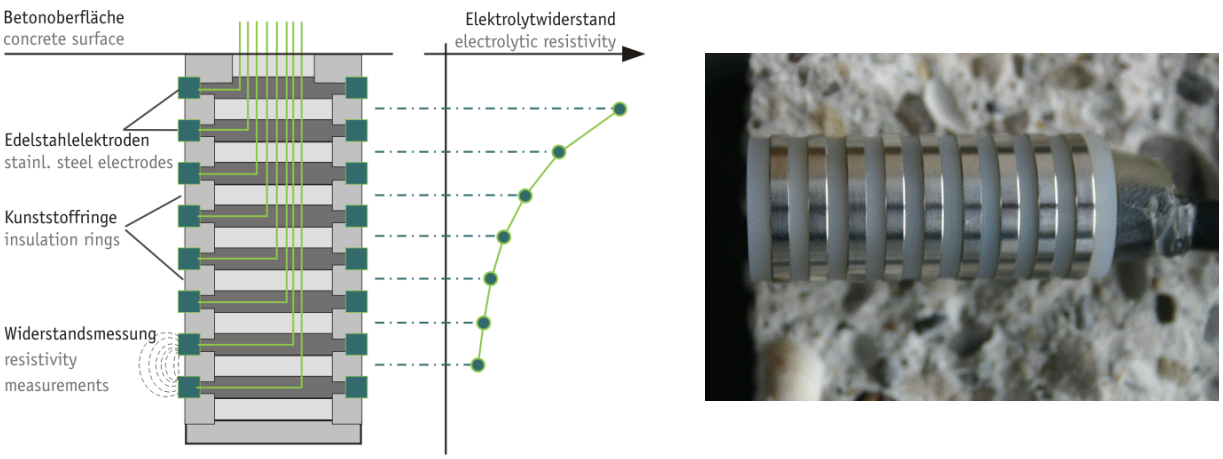

Figure 18: Multi-ring electrode (Brameshuber, 2003).

2.5.3 Multi-electrode Surface Resistivity Probe

The multi-electrode surface probe is used for depth investigation of cover concrete, by using the electrical resistivity tomography (ERT) to identify moisture and chloride gradients. The probe has been proven useful to analyse property gradients caused by chlorides and water ingress under controlled laboratory circumstances. It is capable of examining property gradients over depth (du Plooy et al, 2013). Figure 19 shows a 14-electrode surface probe.

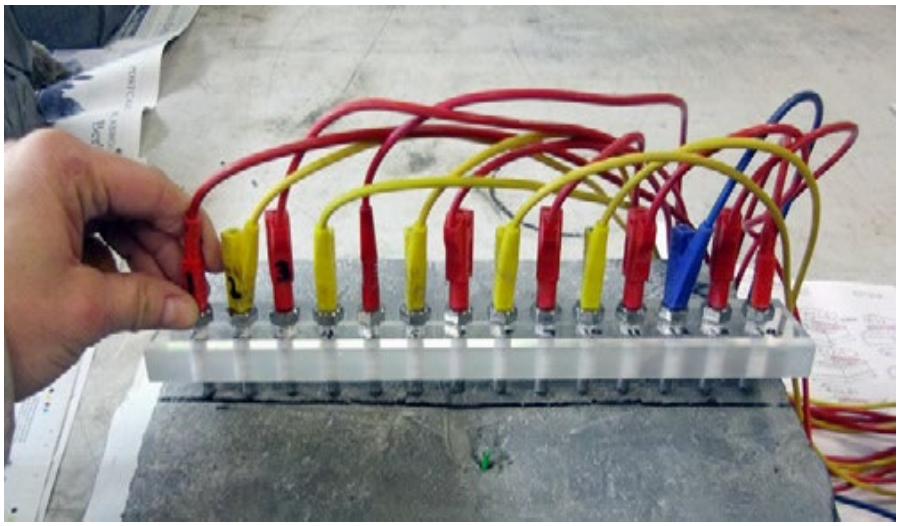

Figure 19: Multi-electrode resistivity probe (Du Plooy, 2013).

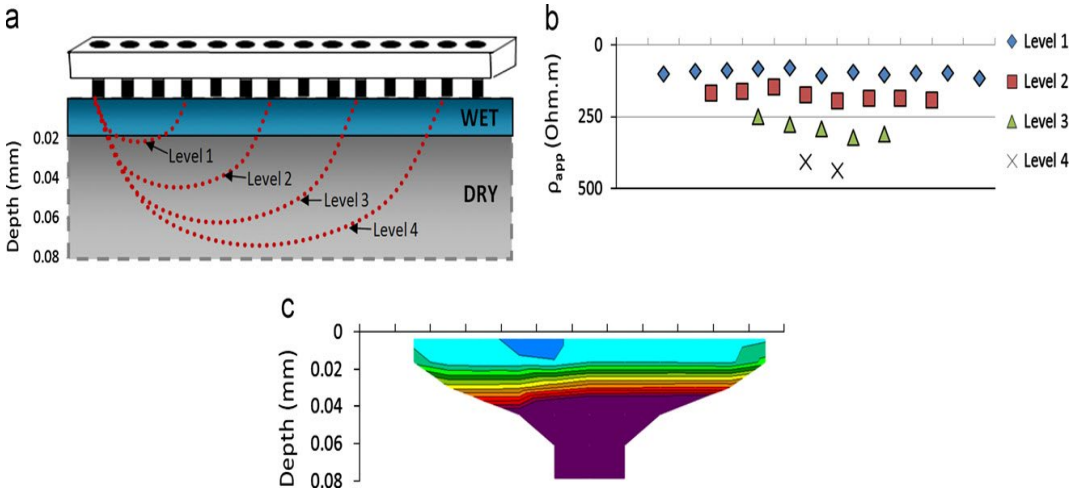

Figure 20: Steps from surface measurements with (a) multi-electrode probe measurements (b) to determine apparent resistivity and (c) inverted resistivity (Du Plooy, 2013).

The resistivities obtained from the multi-electrode probe are related to the degree of saturation by using the calibration curve. As the Figure 20 shows, after the surface potentials are measured (a), the geometric factor is applied to calculate the apparent resistivity for each of the measurement points (b). These apparent resistivities are then inverted to resolve the true resistivity values as a function of depth for a non-homogeneous medium (c) (Du Plooy, 2013.).

In the research of Badr, et al, 2019, the authors designed a type of multi-electrode sensor embedded in concrete structures to evaluate the resistivity over depth and moisture gradients. The sensor was designed as a printed circuit board (PCB), which resolved the issue of invasive cables, providing good geometric accuracy, and the sensor was embedded in the concrete structure, which overcome the limitation of the thickness for the other sensors. Figure 21 shows the geometry of the sensor.

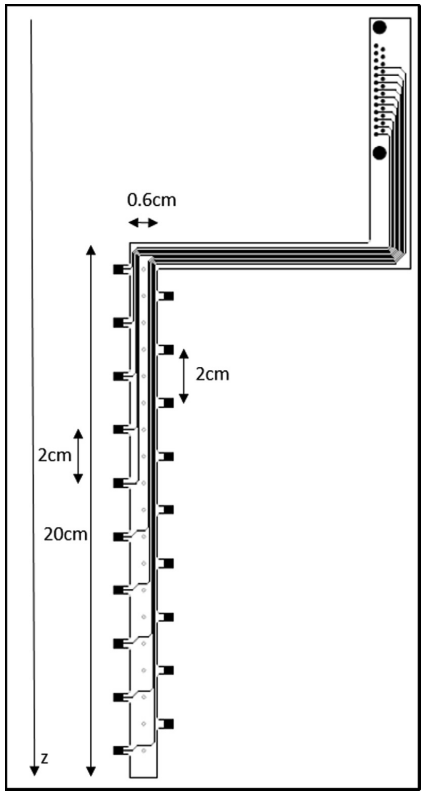

Figure 21: Schematic diagram of the ladder-shaped sensor (Badr, et al. 2019).

As for the material, the PCB is based on a Flame Retardant-4 (FR-4) material, a glass-reinforced epoxy laminate, and the electrodes are made of copper plated with a nickel-gold layer, which has a low electrical resistivity. This type of sensor is capable of providing measurements at the centimeter scale over the thickness of a concrete structure. It can keep good electrical contacts between the electrodes and the concrete with good precision. In addition, the sensor had been proven reliable by some researchers.

3 Methodology

The objective of this research is to investigate the combination of surface resistivity and water absorption as non-destructive tests to be used for quality control of concrete. As mentioned in the literature review, previous research by Sanchez Marquez and Nokken, (2014) and Mohammadi, Nokken and Mirvalad (2017) have shown that electrical resistivity and water absorption have the potential to be used as NDT tests for quality control of concrete.

The first part of this chapter will discuss the test methods used as they are common to both phases. Section 3.1 gives the test methods and Section 3.2 gives the general testing protocol. Details of each experimental phase with mixture designs are presented next. Phase one consisted of testing mature concrete cylinders. As cement hydration is well known to affect resistivity, the benefit of mature cylinders is that very little change in hydration is expected to occur during testing. Phase two consisted of testing mortar that had similar mixture design of two of the concrete mixtures from one.

The following two phases were completed to obtain some data of the surface resistivity (SR), bulk resistivity (BR).

> **Phase one**: Testing on concrete cylinders, see Section 3.3. This phase consisted of testing 3 concrete mixture designs with individual cylinders immersed in one of the 3 solutions. The mixture designs were selected to yield a range of concrete quality (permeability and resistivity). The first round of testing consisted of testing as-received sealed concrete cylinders. To test the effect of moisture state, a second round of testing was performed after drying the cylinders. The three concretes represented a range of permeability. The objectives of this phase were to determine the influence of time, immersion solution, mixture design and initial moisture state on resistivity.
>
> **Phase two**: Testing on mortar cylinders. This phase consisted of testing 2 mortar mixture designs with individual cylinders immersed in one of 2 solutions. In addition, some cylinders were cast with embedded wires to measure the resistivity with depth from the surface. The objectives of this phase were to investigate the influence of time, immersion solution and hydration on resistivity.

All phases were carried out in the laboratory conditions at Concordia University, and both phases utilized similar test methods as described in the next two sections followed by the details of the specific materials and procedures.

3.1 Test Methods

In this research, the surface resistivity (SR) and bulk resistivity (BR) of the concrete samples were tested through a commercial resistivity meter, Proceq Resipod (shown in Figure 22) with 38 mm (1.5 inch) spacing probes. All the experimental data were obtained by using this resistivity meter.

Figure 22: Resistivity meter Resipod.

https://www.globalgilson.com/resipod-concrete-resistivity-meter.

The Resipod works on the principle of a 4-probe Wenner system. It is an accurate instrument, fast and stable, able to provide reliable testing data. The included test strip was used to check performance of the instrument once a month to ensure that the instrument provides correct data that can be used for the research.

3.1.1 Measuring Surface Resistivity (SR)

Figure 23 shows how the Resipod works in the surface resistivity mode. The potential difference between the two inner probes is measured when a current is supplied to the two outer probes. Ions in the pore liquid transport the current. The result of the test is then displayed in kΩ-cm. The calculated resistivity is determined by the probe spacing. In this study, the probe spacing was fixed at 1.5 in. (38.1 mm) for all samples tested.

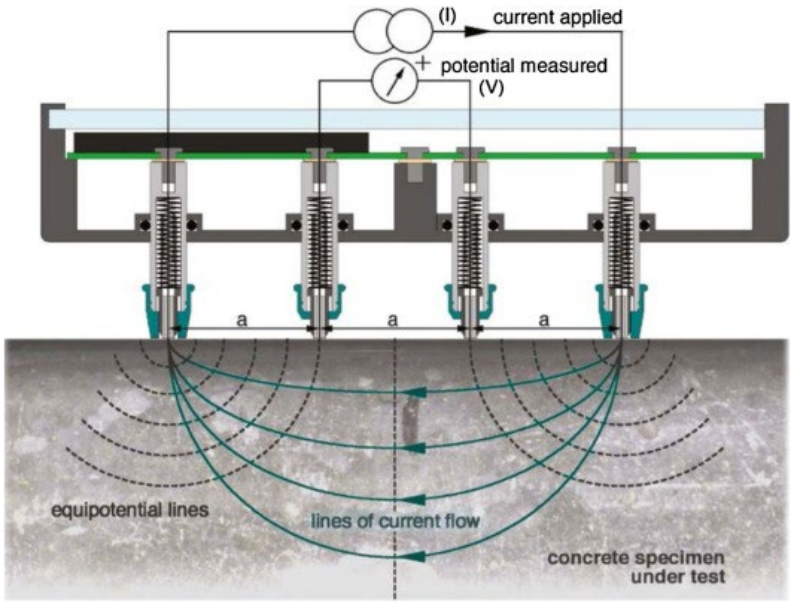

Figure 23: Schematic of surface resistivity meter (Proceq SA operating instructions, 2014).

Preparing the concrete surface is necessary before measuring. The testing protocol requires measurements along 4 longitudinal lines each located at 90 degrees from each other (see Figure 23). After determining the initial mass, 4 lines were marked and were used for each testing time. It is important to remove excess solution after taking the concrete samples out of solutions but not dry excessively. For this purpose, a rag that was saturated in the same solution as the concrete sample used to wipe the surface of the sample to make sure that the surface is in a saturated surface dry state.

As shown in Figure 24, the resistivity meter was placed on the concrete surface along the marking line. The instrument is pressed firmly down until the outer two rubber caps rest on the surface of the concrete sample. It is necessary to make sure that there is good connection between the probes and the concrete surface so that the measuring data is reliable. The instrument t gave the SR result directly when pressing the four probes against the sample. The calculations to convert the resulting voltage to surface resistivity are internal to the equipment (Resistivity $\rho = 2\pi aV/L$ [kΩ·cm]). One measurement is taken placing the resistivity meter along each line followed by a second measurement along the same line for a total of 8 measurements. After recording the 8 results, the concrete samples were returned back into the solution. These steps are repeated for each sample. However, the measured result does not account for the geometry of the cylinder. The internal conversion from voltage to resistivity assumes a semi-infinite geometry, but the boundaries conditions constrain the flow of current. As mentioned in the literature review, several researchers have suggested various corrections for geometry that

range from 1.8 to 1.9. In this research the measured resistivity was divided by 1.89 to obtain the actual resistivity.

Figure 24: Testing the surface resistivity.

3.1.2 Measuring Bulk Resistivity (BR)

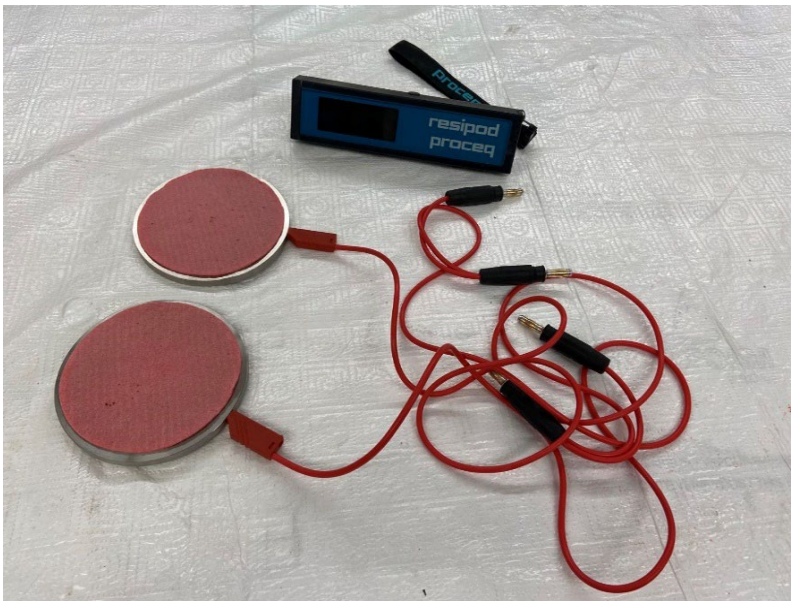

Figure 25: The cables, measurement plates and foam for testing BR.

The bulk resistivity was measured after completing the measurement of surface resistivity. This step should be finished within 5-10 minutes to minimize differences in sample saturation. After measuring the SR data, the Resipod was changed to the BR mode immediately (as shown in Figure 25).

In this mode, two measurement plates are connected with two cables that can be installed to the instrument. Before measuring, prepare the surface of the sample by wiping with a saturated rag as previously, then place it as Figure 26 shows. To ensure good electrical contact, a thin foam sponge (shown in pink in the figure) saturated with the testing solution was placed between each end of the cylinder and the plate. Once the specimen was in place, the instrument displayed the measured result. For each cylinder, two measurements were performed. A record of the data was taken before putting the sample back to the solution.

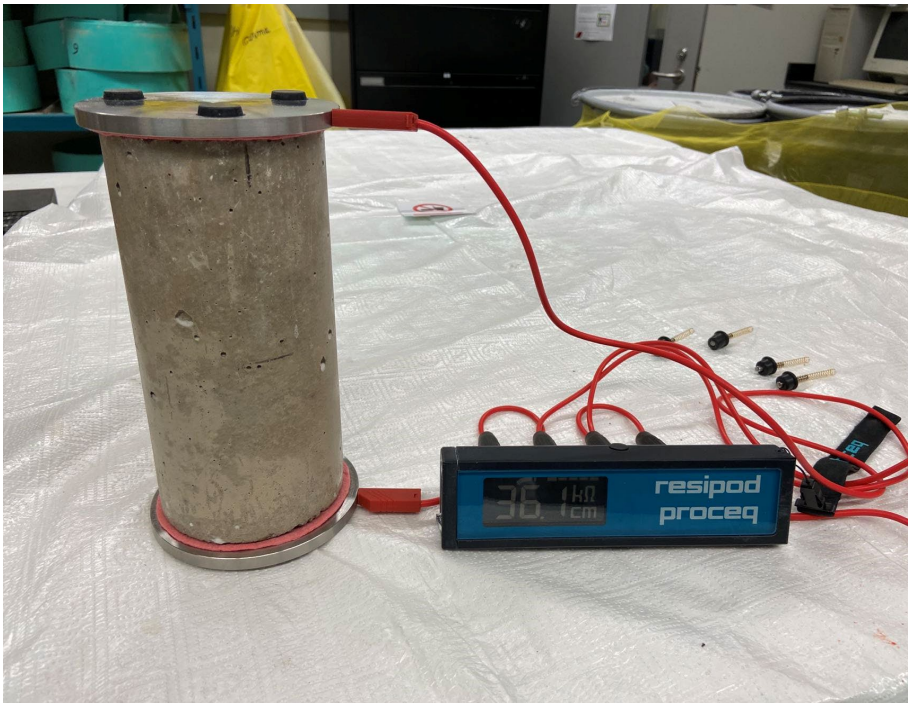

Figure 26: Measuring the BR of the samples.

Calculation of the bulk resistivity

Based on the equations of ASTM C1876 and the calculation method of bulk resistivity from the operating instructions, the calculation process is as follows:

Based on ASTM C1876, the bulk resistivity can be obtained from the following equation:

$$\rho = R \times \frac{A}{L} \tag{8}$$

Where:

ρ = Bulk resistivity,

R = electrical resistance of specimen, ohms,

A = specimen cross-sectional area, m^2,

L = average specimen length, m.

Since the sizes of the three specimens are 200 mm in nominal length and 100 mm in nominal diameter, the values of A and L can be obtained:

$$A = \pi \times (\frac{0.1}{2})^2 \text{ m}^2 \quad (9)$$

$$L = 0.2m \quad (10)$$

Therefore,

$$\frac{A}{L} = \frac{\pi \times (\frac{0.1}{2})^2}{0.2} = 0.0399\ m \quad (11)$$

Based on the operating instructions, the resistance of the cylinder is determined based on the results of the measured resistance and the two inserts:

$$R_{cylinder} = R_{measured} - R_{upper} - R_{lower} \quad (12)$$

Where:

$R_{measured}$ = The displayed resistance on the Resipod Device, kΩ·cm,

R_{upper} = The resistance of the upper foam, kΩ·cm,

R_{lower} = The resistance of the lower foam, kΩ·cm.

According to the results of testing:

$$R_{upper} = 1.6 \text{ k}\Omega\cdot\text{cm} \quad (13)$$

$$R_{lower} < 1 \text{ k}\Omega\cdot\text{cm}=0 \text{ k}\Omega\cdot\text{cm} \quad (14)$$

In addition, the resistance of cylinder, which is $R_{cylinder}$, is a number in kΩ·cm. Given that the device is designed for surface resistivity, this number should be divided by:

$$2\pi a \quad (15)$$

Therefore,

$$R_{cylinder(corrected)} = \frac{R_{cylinder}}{2\pi a} \quad (16)$$

Where:

a = the probe spacing, 3.8cm.

And the value of $2\pi a$ could be obtained:

$$2\pi a = 23.88cm \tag{17}$$

In conclusion, the following equation can be obtained:

$$\rho = R_{cylinder(corrected)} \times 0.0399 \tag{18}$$

Based on the above procedures, the bulk resistivity of the samples can be calculated.

3.2 Testing Protocol

The testing for the concrete and mortar phases consisted of the listed steps.

- Measure initial mass of the samples (scale accurate to 0.1g).
- Make markings for all the samples as per AASHTO T358. The cylinders were marked in four locations, as Figure 27 shows, each at 90 degrees, to show where the electrodes should be placed during the subsequent resistivity measurements.
- Measure surface resistivity. A total of 8 measurements is made of each cylinder at every testing time.
- Place each cylinder into the appropriate immersion solution (note the date and time).
- Remove cylinders at 1, 4, 8 hours and 1, 2, 3, 4, 5, 6, 7 days (at same time of day as initial immersion) and at 2, 3, and 4 weeks (at same time of initial immersion).
- At each subsequent test time, take the cylinders from the bucket, wipe with rag that saturated with same solution (dip rag into the bucket, as Figure 27 shows) and measure the saturated surface dry (SSD) mass.
- Immediately proceed with surface resistivity as per AASTHO T 358. On each of the 4 lines, two rounds of measurements were taken, which resulted 8 measurements in total per sample. Place back the samples into bucket briefly after recording the testing data.
- Change the Resipod device to the bulk resistivity mode and saturate sponges with the immersion solution. Within 5-10 minutes from the surface resistivity testing, measure the bulk resistivity (ASTM C1876). Upon removing the sample from the bucket and wiping SSD first, the sample was placed between the two foams inserts (Figure 26) and the BR measurement recorded, as the BR test method describes. A second measurement was obtained by rotating the cylinder 180 degrees and measuring BR again. Each cylinder was returned to the immersion solution until the next measurement.

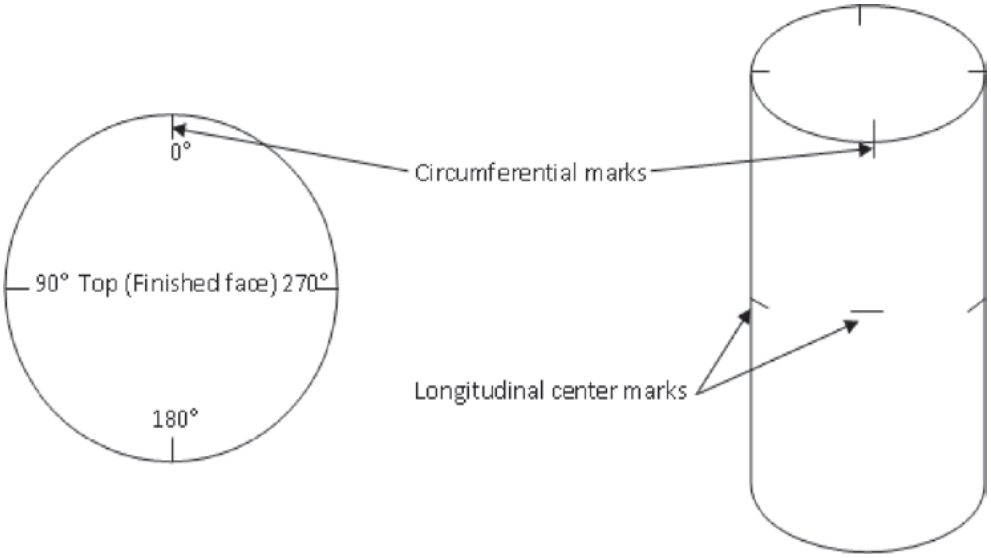

Figure 27: Marks of the locations and the saturated rag.

3.3 Phase One: Testing on Concrete Cylinders

Three concrete mixtures (mixture design shown in Table 1) were cast at St. Mary's cement plant in Toronto as part of an ASTM round robin testing program. The purpose of the testing program was to develop or improve precision and bias statements of several test methods including those

for surface and bulk resistivity. A total of 26 laboratories were involved in the program with testing scheduled for September 2020. Due to lab closures at that time, tests were initiated in January 2021 and April 2021 for this research. Three standard cylinders (10 x 20 cm) for each mixture design were shipped in a sealed bucket with each cylinder wrapped in fabric and plastic to prevent evaporation. The concrete samples were stored as received in lab conditions with a temperature of 23 (± 2°C) for about 11 months until the first tests occurred. All the samples were mature at the time of testing.

Table 1. Mixture design information of the concrete samples

	Mixture A	Mixture B	Mixture C
Description	High Permeability	Medium Permeability	Low permeability
Cast Date	Feb 13, 2020	Feb 12, 2020	Feb 12, 2020
Water to cementitious ratio (w/cm)	0.48	0.42	0.39
Total cementitious content, lb/yd^3 (kg/m^3)	540 (320)	598 (355)	655 (389)
Slag cement, percentage of total cementitious, %	0	25	25
Slump (mm)	175	170	150
Air content (%)	10.5	6.3	5.9
Concrete temperature (°C)	16.5	17.0	17.0
Ambient temperature (°C)	22.5	22.5	22.5
Maximum initial 24-hour curing temperature (°C)	25.0	23.0	23.0
Minimum initial 24-hour curing temperature (°C)	21.0	22.0	22.0

Table 1 shows the details of three different concrete mixtures that were tested in this research. The three mixture designs were selected to yield a range of concrete quality (permeability and resistivity). For permeability, the mixtures represent three different kinds of permeabilities: High Permeability (w/c=0.48), Medium Permeability (w/c=0.42) and Low Permeability (w/c=0.39). As shown in Table 1, Mixture B and Mixture C included the use of 25% slag. For the concrete mixtures that use slag, increasing of w/c means increasing permeability, research of Rupnow and Icenogle et al, (2011) has proven this conclusion.

The three solutions

In this research, three immersion solutions were investigated. Saturated limewater is commonly used for the curing of concrete cylinders for compressive strength testing. AASHTO T 358 (surface resistivity) requires immersion in limewater for a minimum of 21 days prior to testing. However, ASTM C1876 (bulk resistivity) utilizes a simulated pore solution to minimize the influence introduced by ionic concentration differences between the immersion solution and the internal pore solution of the samples. In order to examine the role of immersion solution further, an additional solution with doubled concentration of each hydroxide compound was used. Each solution and its chemical composition are detailed below.

Limewater (LW): 3g/L (13,500 g distilled water, 27 g Ca $(OH)_2$).

Simulated pore solution (SPS): (13,250 g deionized water, 102.6 g NaOH, 143.9 g KOH, and 27 g Ca $(OH)_2$).

Double simulated pore solution (DSPS): (13,250 g deionized water, 205.2 g NaOH, 287.8 g KOH, and 54 g Ca $(OH)_2$).

The first round of measurement for concrete cylinders

The three samples of each mixture and their corresponding immersion solution are shown in Table 2. Due to the limited number of samples, replicates were not feasible for all variables. For the first round of tests, replicates were tested in LW and DSPS solutions, but only a single cylinder of each mixture was tested in the SPS solution. For Mixture A, one sample was immersed in each of the three solutions; for Mixture B, one sample was placed in SPS, and the other two were immersed in DSPS (sample B and sample BR (R for replicate)); For Mixture C, one sample was placed in SPS and the other two were immersed in LW (sample C and sample CR (R for replicate)). In this first round, concrete cylinders were tested in the as received condition. Each cylinder was removed from the shipping bucket and unwrapped from the damp rags and plastic then tested according to the test protocol.

Table 2. Testing matrix for concrete samples

	Immersion Solution		
Mixture	LW	SPS	D-SPS
Mixture A (w/c=0.48)	Sample A (3PS3-11)	Sample A (3PS5-11)	Sample A (3PS1-12)
Mixture B (w/c=0.42)	none	Sample B (1PS1-12)	Sample B (1PS5-11). Sample BR (1PS3-11)
Mixture C (w/c=0.39)	Sample C (2PS1-12). Sample CR (2PS3-11)	Sample C (2PS5-11)	none

The second round of measurements for concrete cylinders

In order to investigate the influence of the initial moisture condition and moisture content on the electrical resistivity, a second round of measurements was conducted. After the first round of testing, the specimens were taken out of the immersion solutions and exposed to the lab air for about 6 weeks to dry at a temperature of 23 (± 2) °C. As mentioned previously, the second round of measurements on the samples were performed in April 2021. After drying, each sample was then placed in the same solutions as the first round. This allows the results of the two rounds of measurement to be compared. The mass of the cylinders was measured prior to placement in the solutions. Since it was not possible to measure the SR and BR of the samples in the dry state as there is insufficient moisture in the pore system to carry the electrical current, the first measurement on SR and BR was conducted after wetting the surface of the samples using a rag saturated in the receiving solution. In the second round of measurements, only the samples immersed in LW and SPS in the first round were tested.

For the second round of measurements, the test protocol and duration are the same as the first round. After 28 days of measuring, the samples were taken out of the solutions and placed into empty buckets.

3.4 Phase Two: Testing on Mortar Cylinders

In this section, two kinds of mortar mixtures were cast and investigated. One mixture included the use of blast furnace slag, the other did not. Some previous research mentioned that the use of SCMs will generate a more complex and dense pore structure inside the samples, the lower porosity and higher tortuosity leading to higher resistivity to the concrete samples. In addition, the difference in w/c ratio also influence the resistivity of the mortar samples. In this section, two mortar mixtures with different w/c ratio and the use of slag were investigated to study the influence on SR and BR. All the experimental samples were cast on July 20, 2021.

Table 3 shows the information of the two laboratory mixture designs and properties. For the two mixtures, the general use Portland-limestone (Type GUL) cement was used as the primary binder. The mortar samples also used the supplementary cementitious materials (SCMs) of blast furnace slag (S). Mortar A was made with w/c of 0.48 and Portland cement only, while Mortar C made with the w/c of 0.39 and 25% slag. There two mortar mixtures were intended to be similar to the high permeability (Mixture A) and low permeability (Mixture C) concrete mixtures from the first phase of the research to allow comparisons.

Table 3. Mixture design information of the mortar samples

	Mortar A	Mortar C
Cast Date	Jul 20, 2021	Jul 20, 2021
Water to cementitious ratio (w/cm)	0.48	0.39
Slag cement, percentage of total cementitious, %	0	25
Slump (mm)		
Air content (%)		
Concrete temperature (°C)	17.0	17.0
Ambient temperature (°C)	23.0	23.0
Maximum initial 24-hour curing temperature (°C)	25.0	25.0
Minimum initial 24-hour curing temperature (°C)	21.0	21.0

In the mortar phase, a total of 32 standard cylinders (10 x 20 cm) were cast in laboratory temperature conditions (23 (± 2) °C), 16 cylinders for each mortar mixture. All the samples were stored in the molds wrapped in plastic bags and placed in a box container with a small amount of water in the bottom after casting, and the container was covered and stored in the lab condition. Half of the cylinders were immersed at the age of 28 days from casting; the other half were tested at the age of 56 days to evaluate any differences in results due to additional hydration. At each testing age, 8 cylinders were tested. Six of these cylinders were tested for surface and bulk resistivity as per the testing protocol in Section 3.2. The remaining two cylinders were cast with wires to measure resistivity with depth as will be detailed in a subsequent section.

Measurements of the mortar samples at the age of 28 days

After curing in the cylinder molds for 28 days, six specimens of each mixture were removed from their molds and marked to indicate the positions to place the electrodes in the subsequent measurements, as Figure 27 shows.

Mass, SR and BR were measured using the Proceq Resipod meter for each cylinder before putting it into the LW or SPS solutions. For the six samples of each mixture, three of them were placed in limewater, and the other three were immersed in simulated pore solution. The testing protocol given in Section 3.2 was used up until 28 days of immersion transpired. In all cases, 8 measurements of SR and 2 measurements of BR for per sample were performed.

Measurements of the mortar samples at the age of 56 days

At age of 56 days, measurements to 12 additional samples of the two mortars were performed. Another 12 cylinders, six samples of each mortar, were removed from the molds and marked. One measurement of mass, SR and BR of the samples was conducted before putting into solution followed by 28 days testing as per the protocol. At end of testing, the cylinders were wrapped and placed in empty buckets.

3.5 Internal Resistivity Procedure

In order to investigate the penetration of solution, 4 cylinders of each mixture were cast with embedded wires (shown in Figure 28). Three pairs of wires were embedded, each pair at a different depth from the surface. The depths selected were 1cm, 3 cm and 5 cm from the surface. The spacing of these pairs was 50 mm from each other as well as 50 mm from the top and bottom ends. Initially, 8 gauges wires were used. However, it was found these were easily broken when demolding the cylinders at the age of 28 days. A second set of cylinders was cast with 14-gauge wires.

The Sensors were placed as following:

- Top: 1 cm depth.
- Middle: 3 cm depth.
- Bottom: 5 cm depth.

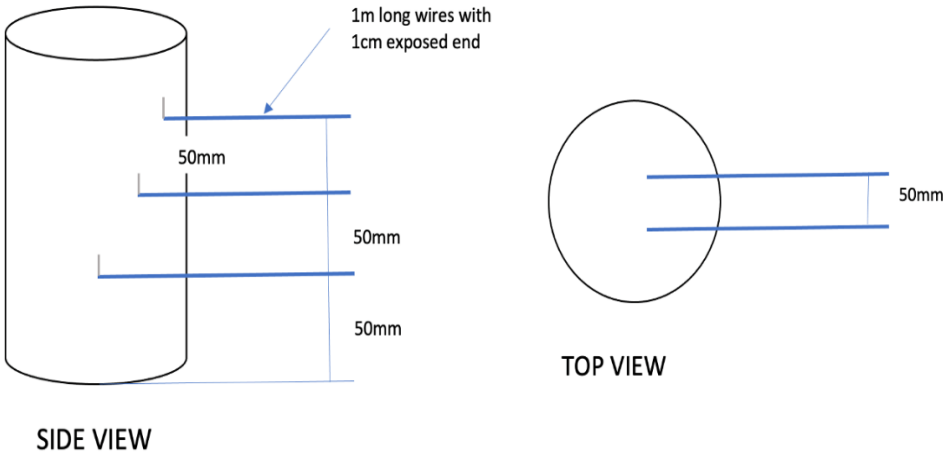

Figure 28: Schematic of embedded wires in cylinders.

After curing in the mold for 28 days, the cylinders were removed from the molds and placed in the LW and SPS solution. Based on the research of Dr. Rajabipour (2005), by measuring the resistivity of the mortar cylinders, the depth of wet front can be calculated by the following equation.

$$y_w = y_{elc} - Ad_{elc}\, In\left[\frac{\sigma_2 - \sigma_{meas}}{\sigma_{meas} - \sigma_1}\right] \quad (19)$$

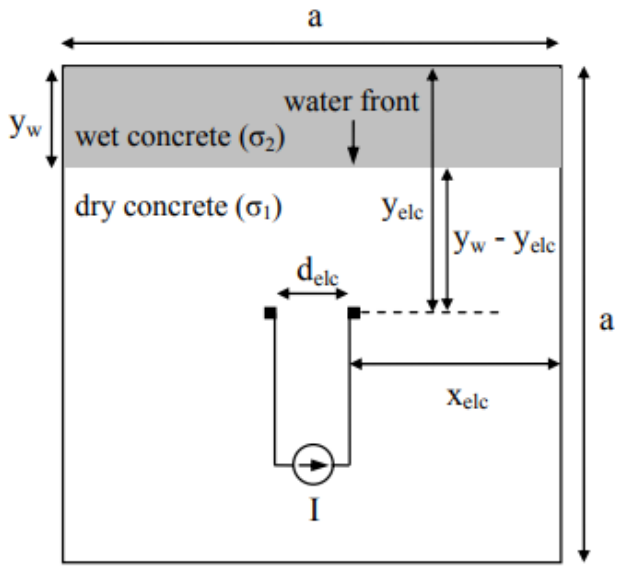

Figure 29. Specimen geometry for finite element analysis (Rajabipour, 2005).

As the Figure 29 shows, for the equation, y_w is the depth of the moisture front from the exposed surface, y_{elc} is the distance between the electrodes and the wetting surface, and d_{elc} is the distance between the two electrodes. σ_1 and σ_2 are the conductivity of dry concrete and wet concrete respectively, while σ_{meas} is the measured conductivity.

4 Results Analysis

This chapter analyzes the experimental results. The first part of the chapter will focus on the measurement results of three concrete mixtures. Subsequently, the results for the two mortar mixtures will be discussed. The experimental data was compared and analyzed in several aspects: a) to study how BR and SR change over time, b) the influence of mixture design on BR and SR in the same solution, c) the influence of different solutions on the BR and SR of each mixture and d) the ratio of SR and BR. All the presented SR and BR data in this chapter were corrected from the measurements displayed on Resipod. The SR results were adjusted using the correction geometry factor in the Methodology section. As mentioned previously, based on the research of Spragg et al. (2013a), for a standard cylinder size (10 x 20 cm), the value of correction coefficient (k) ranges from 1.8 to 1.9 when the probe spacing (a) is 38 mm. All the samples used in this research are standard cylinders (10 x 20cm). Therefore, the most commonly used correction factor of 1.89 is used in this research. The BR data was calculated based on the method shown in the Methodology section 3.1.2.

4.1 Analysis of the Concrete Samples

In this part, the corrected SR and BR data of the three concrete mixtures are presented and analysed. For the concrete samples, two rounds of 28-day measurements were taken in January 2021 and April 2021 respectively. The first round of measurements was conducted on the samples in the states as received. After the first round of measurement, the concrete samples were taken out of the immersion solutions and exposed to the lab conditions under the temperature of 23 (± 2°C) for 6 weeks in order to investigate the effect of the initial moisture condition. For the second round, each cylinder was immersed in the same solution as the first round. As the cylinders were cast in February 2020, the maturity of the specimens did not likely influence the measured results between the two rounds.

4.1.1 SR and BR Changes Over Time

4.1.1.1 The First Round of Measurements (Tests on Concrete Samples as Received)

As mentioned previously, there are three mixtures tested in phase one and three concrete cylinders for each mixture. The samples and their immersion solution can be seen in Table 2.

For this section, the samples that were immersed in simulated pore solution (SPS) are examined; the comparison of mixture designs and immersion solutions are given in subsequent sections.

Figure 30 shows the mass change, surface resistivity (SR) and bulk resistivity (BR) changes over time for Mixture A (w/c=0.48) in SPS. The x-axis is the square root of the time (hours) the sample was immersed in the solution. The results of SR presented in the figures are the average

of 8 measurements on one sample and the BR results are the average of 2 measurements on a single sample as explained in the Methodology section.

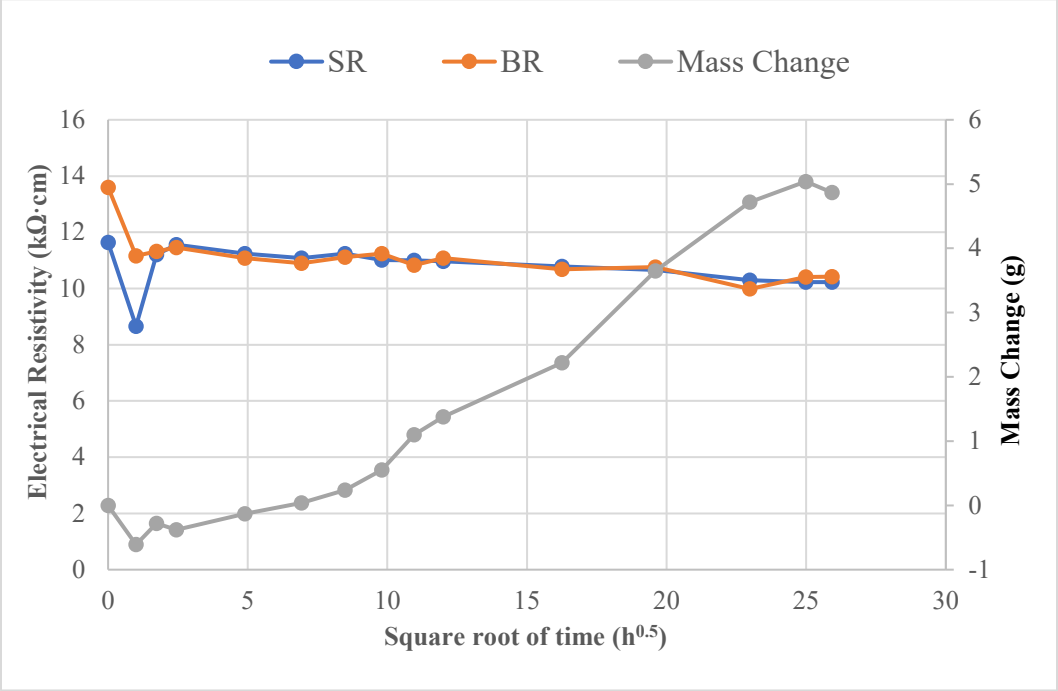

Figure 30: Mass, SR and BR change of Mixture A, (w/c=0.48).

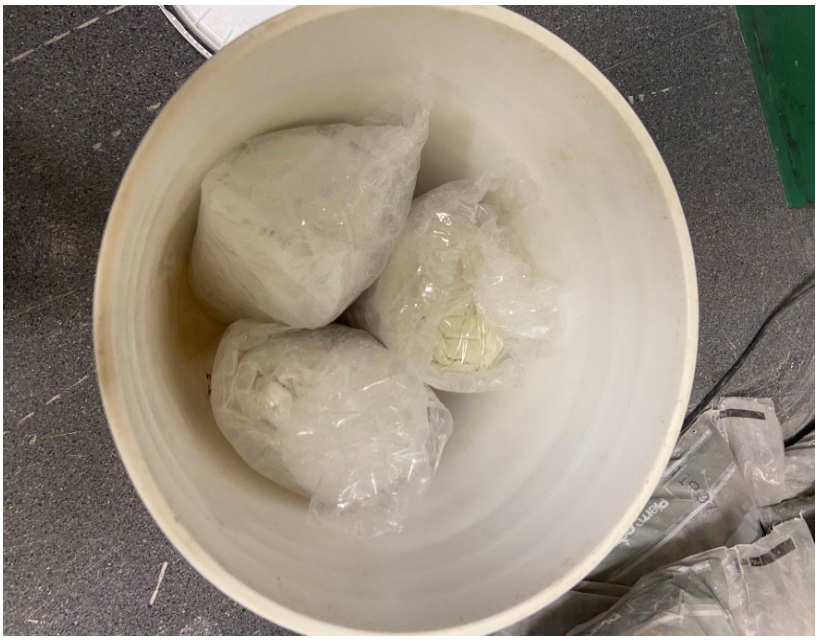

Figure 31: As received samples before the measurements.

It can be seen from Figure 30, there is only a 5 grams' mass increase that after 28 days of solution immersion. This result is expected since all samples as received were covered by saturated rags and wrapped in plastic films before the first round of measurement, as Figure 31 shows. Therefore, the sealed samples were nearly saturated at the beginning. Given the sealed conditions and the similarity of conductivity of the pore solution and the immersion solution (SPS), there was not a significant exchange of conductive ions. For this reason, the SR and BR do not show a clear changing tendency with time. In addition, it can be seen that the values of SR and BR are primarily ranging from 10 kΩ·cm to 12 kΩ·cm. A significant decrease of SR and BR in the second measurements were observed after the sample was placed into the solution for an hour. There was a clear rise in the subsequent third and fourth measurements, measured at 3 and 6 hours after the sample was immersed in the solution, respectively. The values of BR and SR then stabilized and decreased slowly until the end of the measurement. This anomalous result at one hour was seen several scenarios.

Figure 32: Mass, SR and BR change of Mixture B, (w/c=0.42).

Figure 32 shows the testing results of mass change through time and SR and BR change through time of Mixture B, (w/c=0.42). As seen in the Figure 31, there is only a difference of less than 2 grams in the mass change. The trend of SR and BR is similar to that of Mixture A, but the values are higher, ranging from 17 kΩ·cm to 21 kΩ·cm. (The influence of mixture design is discussed in a subsequent section). Moreover, there are obvious decreases and subsequent increases in the second and third measurement, tested at 1 hour and 3 hours after the sample was put into the solution, respectively. Afterwards, the results are nearly constant with time.

The mass change over time and SR and BR change over time of Mixture C, (w/c=0.39) are shown in Figure 33. In this case, about 1-gram change of mass illustrates that the sample was almost saturated before being put into SPS solution. However, compared with Mixtures A and B, the change of SR and BR of Mixture C is different over time. In the second measurement, the values of SR and BR didn't drop as significantly as Mixtures A and B, but instead showed an upward trend in the first few measurements and then the changes tended to be flat. The values of SR and BR are ranging from 30 kΩ·cm to 36 kΩ·cm.

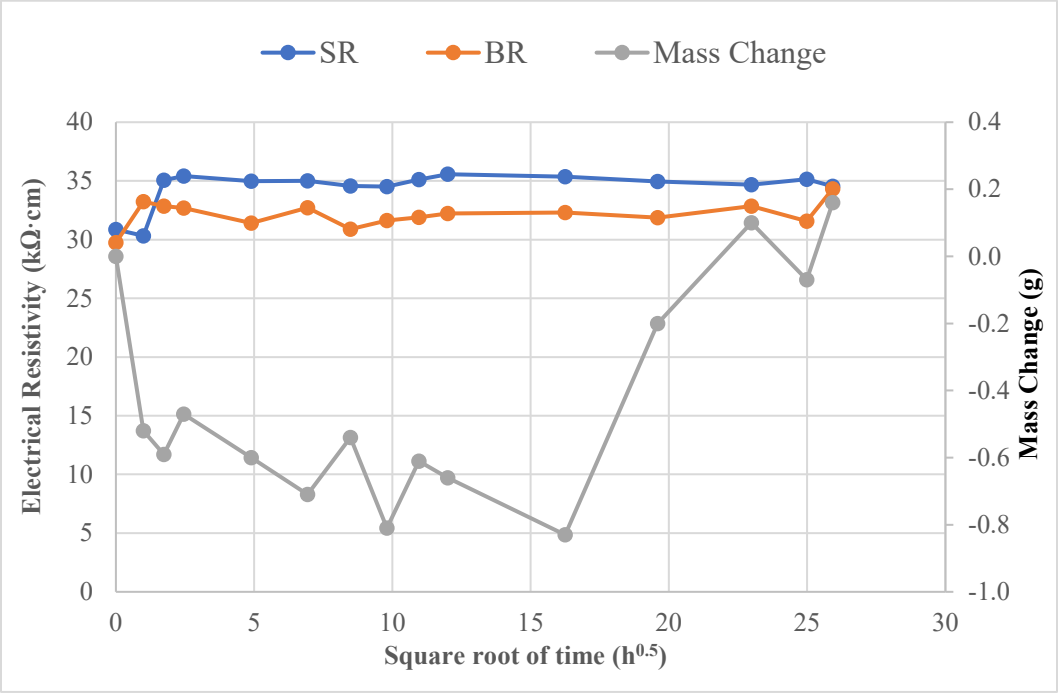

Figure 33: Mass, SR and BR change over time of Mixture C, (w/c=0.39).

In conclusion, in the first round of measurements, since all the samples were sealed and nearly saturated before starting the tests, the mass didn't increase much after 28 days of immersion in the solution, particularly for Mixture C, (w/c=0.39). For the changes in SR and BR, Mixture A and Mixture B show common tendencies. The values of SR and BR both decreased significantly in the second measurement (measured 1 hour after immersion in the solution), and then increased clearly in the next measurements (measured 3 and 6 hours after immersion in the solution).

As the measurements proceeded, though the changes are small, the gradual increase of mass means that a portion of the solution containing conductive ions entered the pore structure. This feature is commonly observed in secondary absorption (the absorption after capillary voids have been filled and the discontinuous air voids begin to be filled). This small increase in saturation is the reason why the values of BR and SR decreased slowly until the end of the measurement for some mixtures.

4.1.1.2 The Second Round of Measurements (Tests on Concrete Samples after Dried)

Before starting the second round of measurements, the concrete cylinders were stored exposed to the lab conditions for approximately 6 weeks, in order to dry the samples. One measurement of mass, SR and BR were taken before placing the samples into solution. All samples were placed in the same solution as the first round. In this section, the results of the second round of measurements were analysed for the SPS solution.

Figure 34 shows the results of second round measurements of mass change over time and SR and BR change over time of Mixture A. As mentioned previously, the results presented in the figures are the average of 8 measurements and the BR results are the average of 2 measurements on a single specimen.

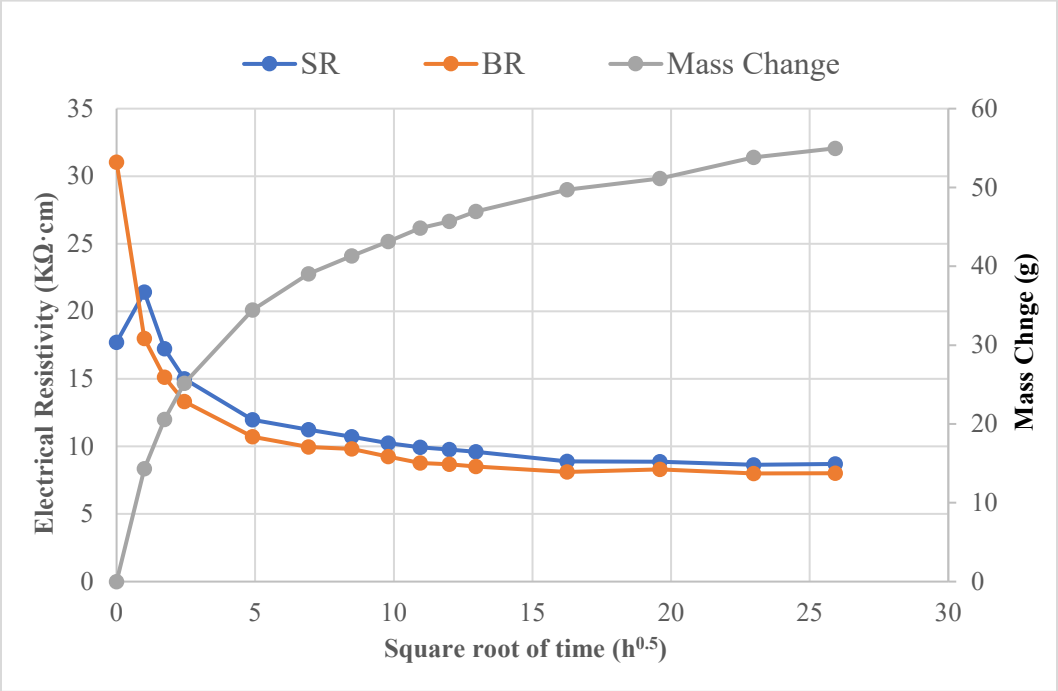

Figure 34: Mass, SR and BR change of Mixture A, (w/c=0.48), 2nd round (Tests on concrete samples after dried).

As shown in Figure 34, it is clear that mass of Mixture A, (w/c=0.48) gradually increased during the testing period, and the increase in mass was relatively rapid within 24 hours (~5, $h^{0.5}$) after immersion, and then the increase rate became slower. In most standard absorption testing, a clear linear relationship between mass gain and the square root of time is observed. However, for these tests, solution was absorbed into the sides, top and bottom of the cylinder giving different behaviour that the 1D absorption of the standard test. This behaviour is consistent with that observed by Qiao et al (2019). After 28 days of immersion, the mass of Mixture A increased by approximately 55 grams in total. Compared with the mass change of Mixture A in the first round (Figure 30), it can be observed that there is a significant increase of mass, which means a part of

the SPS solution entered the pore structure, resulting in a drop in the resistivity of Mixture A due to increased saturation. This is also corresponded with the change of SR and BR.

From Figure 34, it is observed that the SR and BR values declined relatively rapidly within 24 hours after the sample was immersed in the solution, and then the decreasing rate gradually slowed down until the end of the measurement. The bulk resistivity (BR) decreased by 22.67 kΩ·cm in total, 74% of the first measurement, while there was a reduction of 12.71 kΩ·cm in surface resistivity. The values of SR and BR of Mixture A in the last measurement are 8.71 kΩ·cm and 7.91 kΩ·cm, respectively.

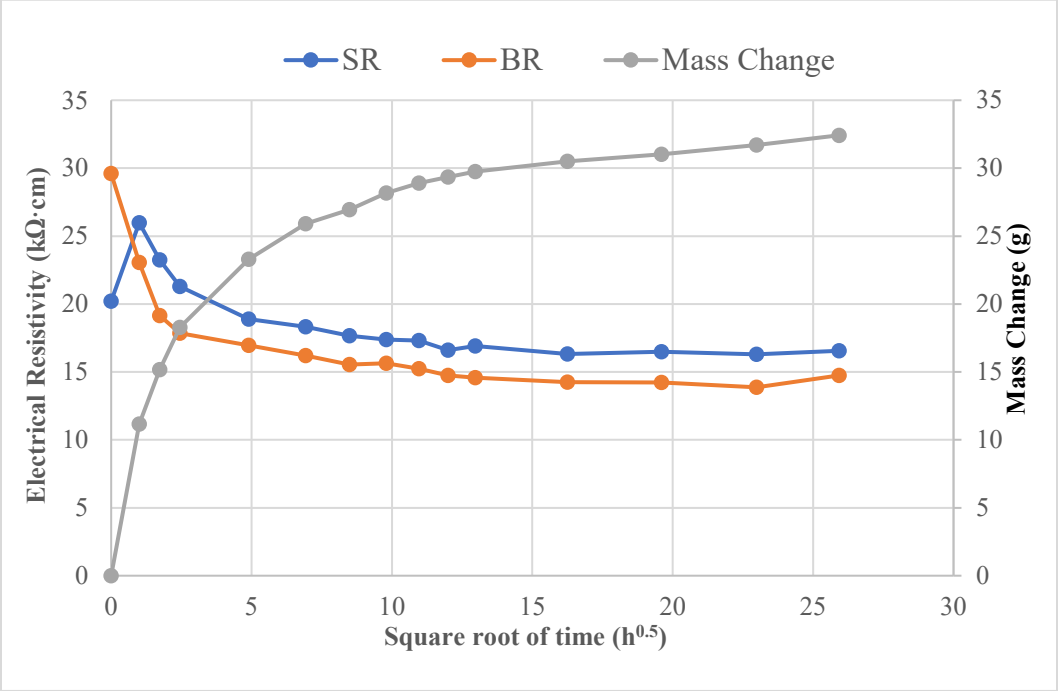

Figure 35: Mass, SR and BR change of Mixture B, (w/c=0.42), 2nd round (Tests on concrete samples after dried).

Figure 35 shows the test results of mass change and SR and BR change through time of Mixture B, (w/c=0.42). In this case, it can be seen comparing Figure 34 and Figure 35 that Mixture B shows the same trends as Mixture A. The change tendency of mass increase also represents that the rate at which the sample absorbed the solution was faster at first and then slower. There is 32.4 grams increase in the mass of Mixture B throughout the test period. The change of SR and BR show a very similar behavior with that of Mixture A. From Figure 35, a lesser decrease of SR and BR can be found. According to calculation of the values, there is a reduction of bulk resistivity (BR) up to 14.6 kΩ·cm in total, and a decrease of 9.43 kΩ·cm in surface resistivity (SR). The values of SR and BR of Mixture B in the last measurement are 16.55 kΩ·cm and 14.52 kΩ·cm, respectively.

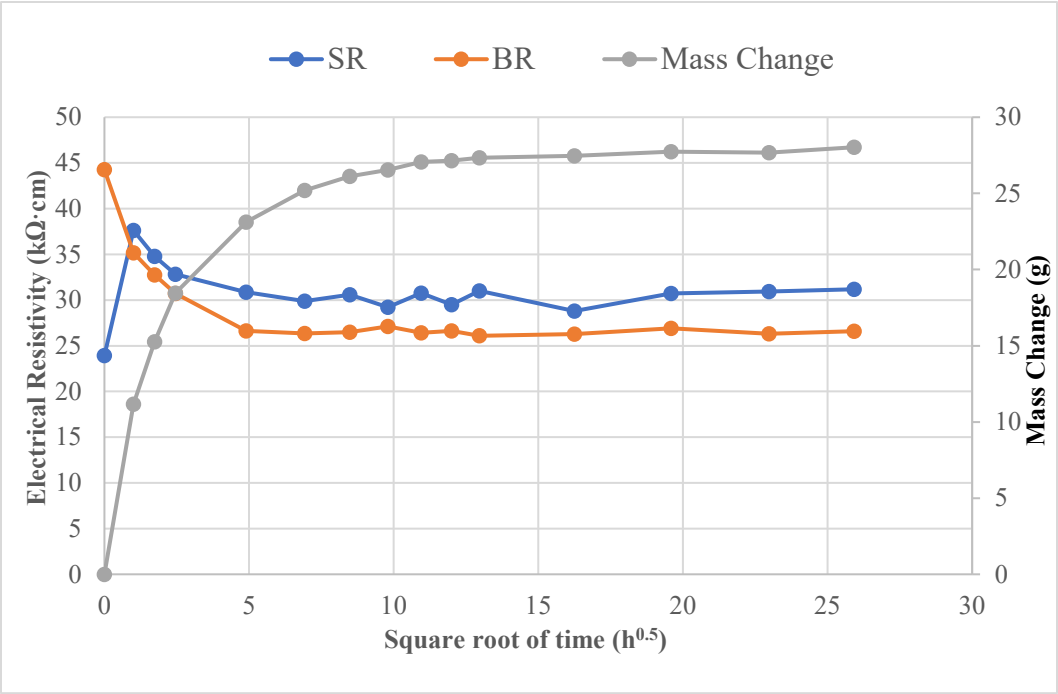

Figure 36: Mass, SR and BR change of Mixture C, (w/c=0.39), 2nd round (Tests on concrete samples after dried).

The mass change and SR and BR change of Mixture C, (w/c=0.39) in the second round are shown in Figure 36. A similar change tendency as Mixture A and B occurred for the mass of Mixture C. There was a 28-gram mass increase observed in Mixture C through the experiment. In addition, based on Figure 36 and the calculation of the data in Appendix 2, the bulk resistivity (BR) decreased by 17.4 kΩ·cm while the surface resistivity (SR) decreased by 8.8 kΩ·cm. The values of SR and BR of Mixture C in the last measurement are 31.18 kΩ·cm and 26.2 kΩ·cm, respectively.

In summary, from the results of the second round of measurements, the three samples showed common tendency in terms of mass change (Figure 34, 35 and 36), but differed in the amount of mass increased. The mass increases of the samples were significantly more rapid within 24 hours of immersion in the solution, and the rate of mass increase gradually slowed down over the next 27 days. Among the 3 concrete samples, sample A has the largest increase in mass, while B and C have relatively less. This is partly because Mixture A has the largest water-cement ratio (0.48), compared to B (0.42) and C (0.39). The water to cement ratio largely controls both porosity and drying capacity of the samples. Mixture A is expected to have high porosity and more drying, so the increased absorption is expected. On the other hand, Mixture B and C have more complex and dense pore structures (with SCMs added to the concrete), resulting in poorer water

absorption capacity. The Mixture A without SCMs is less complicated allowing more immersion solution to enter the concrete.

As for SR and BR, the three concrete samples also showed basically the same trends, corresponding to the change in the mass change of the samples. The rapidly declining SR and BR proved the study of Azara et al, (2017) that the electrical resistivity measurements are highly influenced by the moisture content of concrete, which when the moisture content is increased, the resistivity is reduced significantly. As the solution entered the pore structure of the concrete samples, the SR and BR values gradually decreased. From the data, the SR values and BR values of sample A are the most reduced, and the reduction of values of sample B and C are not much different. It is observed that there is another common situation occurred in the three figures: the first measurements of SR values of the three samples (measured at the beginning of the tests (time = 0), before placing the samples into the solution) are all smaller than the second measurements (measured after the sample was placed into the solution for an hour).

4.1.1.3 Comparison the Results of the First and Second Round of Measurements

For the mass change, it can be clearly seen that there is a significant difference in the results of the first and second rounds of measurements. In the first round of experiments, the three samples were saturated at the beginning, so there was no apparent mass change. The second round of experiments was performed when the samples had been dried by lab air for 6 weeks. After immersion in the solution, the mass change is more obvious. In addition, it can be observed that in both rounds of measurements, the final mass of all samples in the second round of experiments are lower than the values in the first round of experiments. Mixture A lost about 12 grams of mass (Figure 30 and Figure 34) and Mixture B and C lost about 6 grams of mass (Figure 32, 35 and Figure 33, 36). This is mainly because the initial states of the samples were different in the two rounds of measurements. In the first round of measurements, the samples were nearly saturated at the beginning, and became saturated after 28 days of immersion. While in the second round, the samples were dry before testing, and after 28 days of immersion, they still did not reach a fully saturated state. From Figure 34, Figure 35 and Figure 36, it can be seen that at the end of the experiment, the mass of the samples still continued to increase slowly.

For SR and BR, the values became relatively stable between 24 hours (5 $h^{0.5}$) and 6 days (12 $h^{0.5}$) of immersion in the solution as can be seen in Table 4 and Figure 34 to 36. Due to the highly saturated state, in the first round of experiments, SR and BR did not change much, while in the second round of experiments, the changes were more obvious and monotonically decreasing. In the standard methods for SR (AASHTO T358) and BR (ASTM C1876), both standards require moist curing prior to immersion for a minimum of 28 days. This moist curing environment would make standard tests most similar to the first round of tests performed in this research. As can be seen in Table 4, the SR and BR results at 24 hours are within 5% of the results at 6 days and within 10% of the results at 21 days. For this reason, Sanchez Marquez and Nokken (2014) recommended one day of immersion to significantly decrease the time of testing. The standard tests require 21 days immersion for SR and 6 days for BR. For concrete tested as soon as permissible after casting, 49 days for SR and 34 days for BR, there would be considerable

cement hydration between the time of immersion and the standard testing age leading to a significant increase in resistivity during the testing period. For the cylinders examined in this research hydration has reached a near-ultimate state and changes in resistivity are due to saturation (or as will be discussed later an immersion solution whose resistivity is different that the concrete's pore solution).

In the second round of experiments, the final values of SR and BR are lower than the values of the first round. There are at least two possible reasons for the decrease. Firstly, as the cylinders were dried for approximately 6 weeks, there is a considerable moisture gradient in the sample at the start of the second round of testing. This moisture gradient leads to absorption primarily through surface tension. It is possible, that the immersion solution more easily permeated pores that were not filled during the first round. Secondly, as the sample dried water evaporated from the concrete's pores leaving behind the salts of the immersion solution. With immersion during the second round, these salts dissolve into solution effectively increasing the ionic concentration within the concrete thus lowering the resistivity of the pore solution and the overall resistivity of the concrete.

Table 4. Part of the measured data of SR and BR for the three samples

		First Round (As received) (kΩ·cm)				Second round (dried for 28 days) (kΩ·cm)			
		Initial	24 hours	6 days	21 days	Initial	24 hours	6 days	21 days
Mixture A	SR	11.64	11.24	10.97	10.29	17.71	11.98	9.77	8.64
	BR	13.60	11.09	10.92	9.98	31.04	10.73	8.67	8.00
Mixture B	SR	19.24	19.50	19.03	18.97	20.22	18.89	16.61	16.30
	BR	21.84	17.83	18.14	17.65	29.60	16.95	14.74	13.87
Mixture C	SR	30.85	34.99	34.68	34.54	23.93	30.88	29.50	30.94
	BR	29.74	31.41	32.87	33.80	44.26	26.64	26.63	26.31

4.1.2 Influence of Mixture Design

In this section, the influence of mixture design on surface resistivity (SR) and bulk resistivity (BR) was investigated. As shown in Table 1(shown in Chapter 3, Methodology), three types of concrete mixtures were used in phase one: Mixture A, w/c = 0.48; Mixture B, w/c = 0.42 with 25% slag and Mixture C, w/c = 0.39 with 25% slag. This part studied how the three mixtures influence SR and BR of the samples submerged in simulated pore solution (SPS).

Figure 37 and Figure 38 show the change of surface resistivity (SR) and bulk resistivity (BR) over time of the three mixture samples in the two rounds of measurements. It is obvious that in both figures, SR and BR values of Mixture A are the lowest, followed by Mixture B, and the SR and BR of Mixture C are largest. In addition, since the samples are nearly saturated at the beginning of the first round of measurements, the values of BR and SR didn't change much with time as mentioned in the previous section.

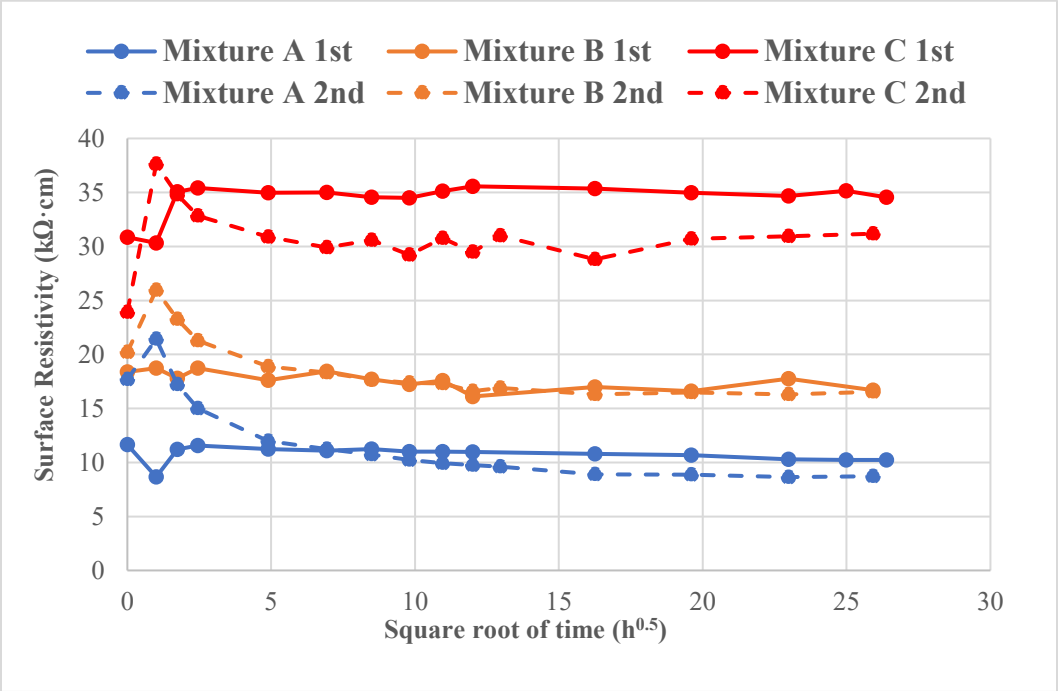

Figure 37: The surface resistivity (SR) changes over time of the three concrete mixtures in the two rounds of measurements.

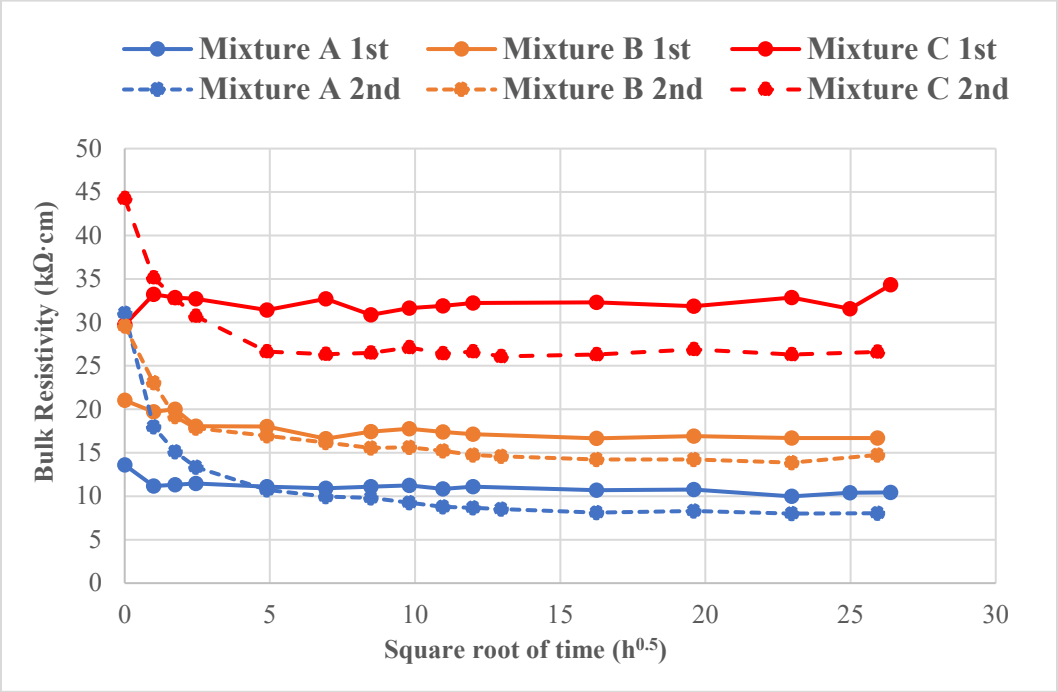

Figure 38: The bulk resistivity (BR) changes over time of the three concrete mixtures in the two rounds of measurements.

In addition, it can be observed from the two Figure 37 and Figure 38 that SR and BR of the three samples show very similar tendencies over time in the second round of measurements. In the second round of measurements, the relationship of SR and BR between the three samples is the same as that of the first round of measurements. Moreover, it can be found that in the two rounds of measurement, whether it is SR or BR, the measurement values of the second round are lower than the values of the first round as mentioned in the previous section.

In summary, from Figure 37 and Figure 38, it can be seen that the electrical resistivity relationship between the three samples is: Mixture A, (w/c=0.48) < Mixture B, (w/c=0.42) < Mixture C, (w/c=0.39). On one hand, the difference in water to cement ratio is one factor. As mentioned in section 2.1 in Literature Review, increasing of water to cement ratio means increasing permeability and decreasing resistivity. According to the research results performed by Noort et. al, (2016), for different concrete compositions with varied w/c ratio, the electrical resistivity of the concrete increased as the w/c ratio decreased. The study of Rupnow (2012) also proved that for all mixtures, an increase in the w/c ratio leads to a decrease in surface resistivity, showing a more permeable concrete. In this research, Mixture A has the largest w/c ratio among the three mixtures (0.48), so its surface resistivity is lowest, while mixture C's surface resistivity

is highest with the lowest w/c ratio (0.39). This result agrees with the conclusions of published research.

Additionally, there are supplementary cementitious materials (SCMs), specially 25% slag, included in Mixture B and C. The SCMs will generate a more complex and refined pore network, leading to increasing resistivity, as noted in the research of Sanchez (2015). Azara et al (2017) stated, "Due to a reduction in capillary porosity and hydroxyl ions (OH^-), the inclusion of reactive additional cementitious materials such as blast furnace slag and fly ash results in lower permeability and higher electrical resistivity". Therefore, even at the same w/c ratio, the mixtures with SCMs show higher surface resistivity. Compared with Mixture A, Mixtures B and C not only included with SCMs, but also have lower w/c ratio, resulting in higher SR. Based on the research of Rupnow and Icenogle et al (2011) and Sanchez et al (2015), in the short time after the concrete with the same slag content is cast (within 60 days), there was not an observation of decrease on resistivity as the w/c ratio increased. This is mainly due to the different degree of slag reaction within the concrete in the short term. However, in this study, the concrete samples used were casted for nearly one year, the slag in the concrete has been fully hydrated. Therefore, for Mixtures B and C, the degree of slag hydration is the same. For mixture C, the lowest w/c ratio among the three mixtures gave it the largest resistivity, while the addition of SCMs made its resistivity even larger.

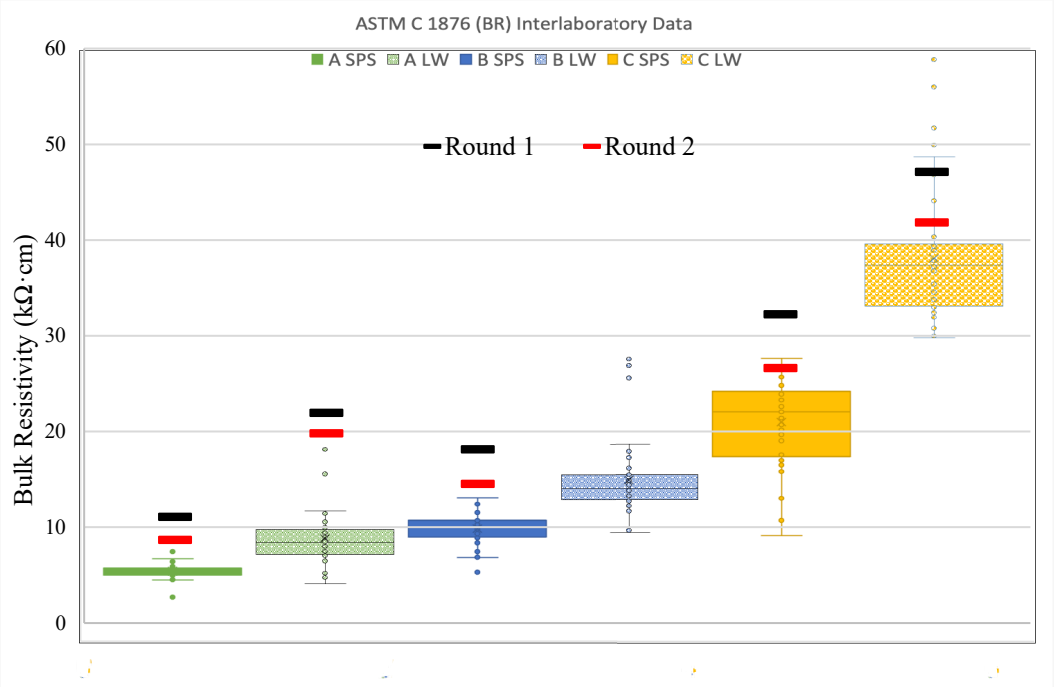

Figure 39: Comparison BR of this research with the results of interlaboratory study (ILS) data.

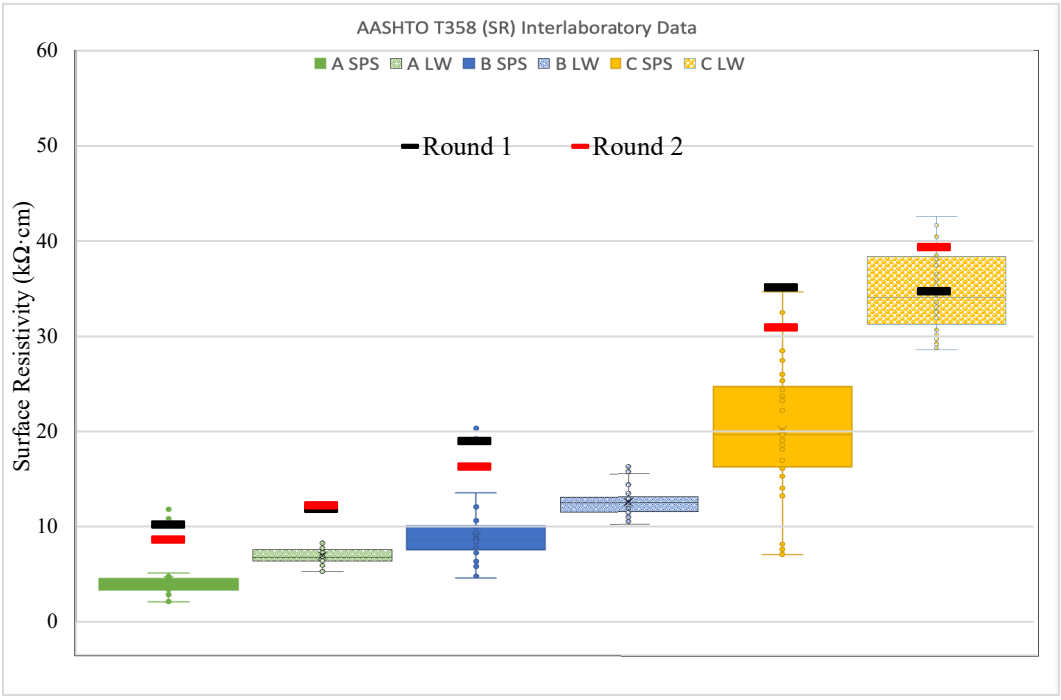

Figure 40: Comparison SR of this research with the results of interlaboratory study (ILS) data.

As mentioned in the Methodology section, a limited number of cylinders were available for testing. For the SPS solution, only a single cylinder was tested for each concrete mixture. Figure 39 shows the comparison of the results of BR data and Figure 40 shows the results of SR. The black dashes are the measured results of the first round in both figures, and red dashes are the results of the second round. The presented BR results are the measurement data for the sixth day, and the SR results are the measurement data for the 21st day as per the relevant standards.

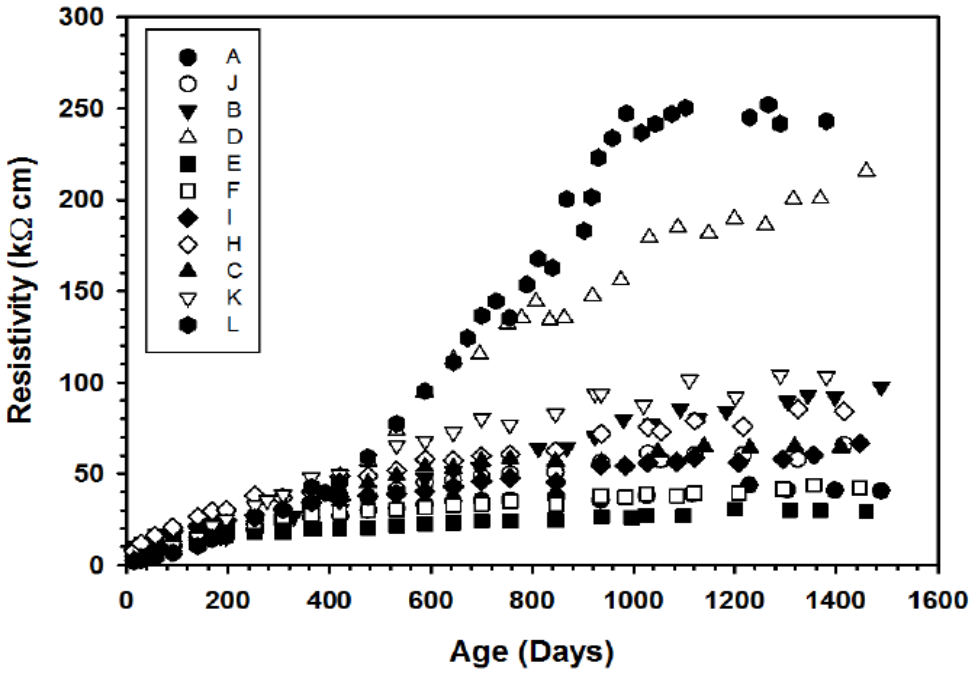

Figure 41: The evolution of electrical resistivity by Liu and Presuel (2015).

It is observed that the data of the research are generally higher than that of ILS study average for the SPS immersion (the LW will be discussed later). In some cases, the results of this research were with the range of the ILS study (within the "whiskers"), while in other cases, they would be considered outliners for the ILS population. The observed increase is partly because the samples tested in this research were measured at a later age. The ILS data were obtained from the tests performed in September 2020, while the data of this study were measured in January 2021 and April 2021, respectively. Based on the research of Liu and Presuel (2015), although the electrical resistivity of most mixtures tended to reach a relatively stable value at the age of about 300 days, the resistivity will still increase slowly over a long period of time (1500 days). In the case of this research, the cylinders are approximately 450 days old at the end of the second round of tests. Overall, the results from this research were 30-40% higher on than the ILS average (the standard deviation for the ILS study was as much as +/- 26% variation).

4.1.3 Influence of Different Solutions

In this section, the influence of different immersion solutions on surface resistivity (SR) and bulk resistivity (BR) was investigated. As mentioned previously, there are 3 different solutions used in phase one (section 3.1): Limewater (LW), Simulated pore solution (SPS) and Double simulated pore solution (DSPS). Based on the results of the two rounds of measurements, this part studied how the immersion solutions influence the SR and BR of the three mixtures.

As Table 5 shows, in this research three immersion solutions were used. The measured immersion solution conductivity was 0.83 S/m for limewater, 7.03 S/m for simulated pore solution and 13.16 S/m for the double-strength pore solution.

The simulated pore solution as specified by ASTM C 1879 (the standards for BR) is designed to be in the range of most concrete. Bui and Weiss (2014) give the range of concrete pore solutions as 0.0060 to 0.0380 kOhm·cm. As limewater is a common storage solution for laboratory curing and well at the standard solution for AASHTO T358 (the standard for SR), this solution was also investigated. The measured resistivity of limewater was 8.77 times greater than that of the simulated pore solution. An additional low resistivity solution was produced by doubling the amounts of chemicals of the simulated pore solution. This double-strength pore solution (DSPS) was 0.535 times the resistivity of the simulated pore solution.

In addition, the conductivity of pore solution of the three mixtures is estimated as 12.08 S/m, 6.81 S/m and 9.33 S/m for Mixtures A, B and C, respectively by using the National Institute of Standards and Technology (NIST) online tool, which is a technique to determine the conductivity of the pore solution through the concentration of different ionic species (Snyder et al. 2003). The technique was programmed into a free web application by Bentz (2007) that can be found at the following website: concrete.nist.gov/~bentz/poresolncalc.html. To determine the estimated pore solution conductivity of each mixture, the chemical composition and other details from the mixture design were input with the default hydration of 0.70 and under sealed conditions. It can be observed that the resistivity of Mixture B and the SPS immersion solution are very similar. The resistivity of the pore solutions for Mixtures A and C lie between SPS and DSPS.

Table 5. Electrical properties of immersion solutions and pore solutions

Immersion solutions (measured)	Conductivity (S/m)	Resistivity (kOhm·cm)
Limewater	0.83	0.1245
Simulated pore solution	7.03	0.0142
Double simulated pore solution	13.16	0.0076
Pore solutions (estimated)		
Mixture A (w/c=0.48)	12.08	0.0083
Mixture B (w/c=0.42)	6.81	0.0149
Mixture C (w/c=0.39)	9.33	0.0107

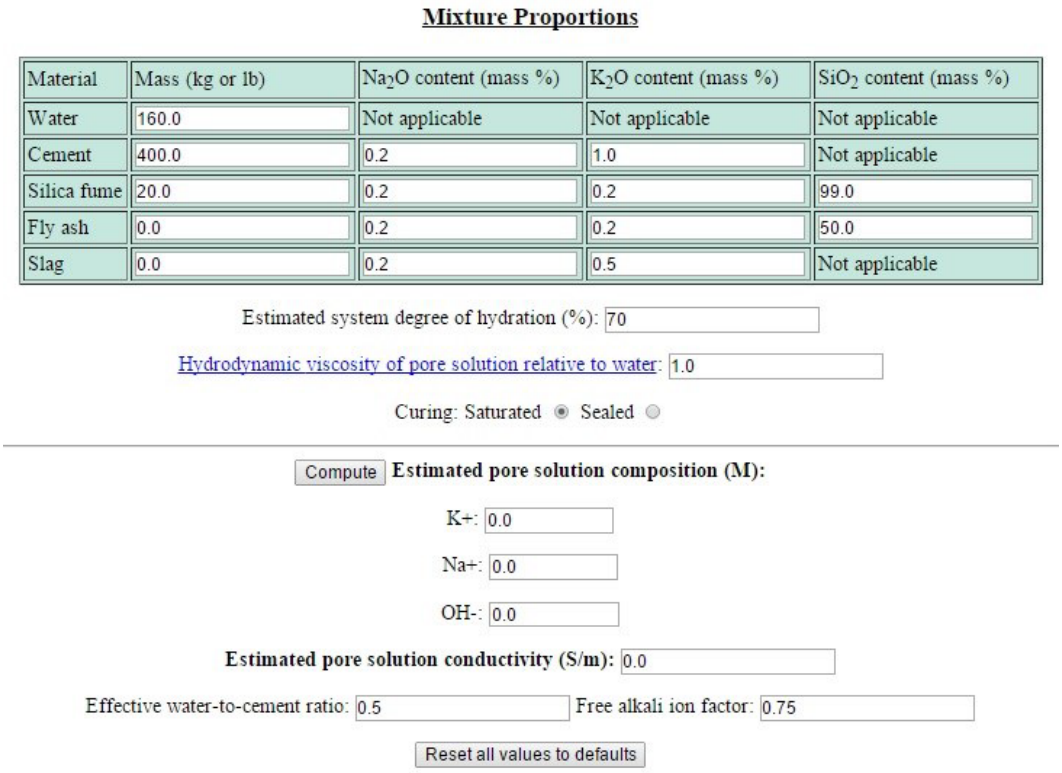

Mixture Proportions

Material	Mass (kg or lb)	Na_2O content (mass %)	K_2O content (mass %)	SiO_2 content (mass %)
Water	160.0	Not applicable	Not applicable	Not applicable
Cement	400.0	0.2	1.0	Not applicable
Silica fume	20.0	0.2	0.2	99.0
Fly ash	0.0	0.2	0.2	50.0
Slag	0.0	0.2	0.5	Not applicable

Figure 42: Screenshot of the web application (Bentz, 2007).

The measured results show that the highest measured resistivity was for the limewater (LW), followed by the simulated pore solution (SPS) and finally the double-strength pore solution (DSPS). In order to compare the influence of the solutions, the limewater and double-strength pore solution were compared to the simulated pore solution.

4.1.3.1 The First Round of Measurements

As Table 2 in Methodology shows, the three specimens of Mixture A were immersed in the three solutions; two samples of Mixture B were placed in DSPS, one in SPS; two of Mixture C were put into LW, one in SPS. In the first round of measurements, the samples were nearly saturated at the beginning. This part studied how the solutions influence SR and BR.

4.1.3.1.1 The Influence of Limewater on SR and BR

There were three samples in limewater, one of which was Mixture A (w/c=0.48), the other two were Mixture C (w/c=0.39). In addition, one sample of each of these two mixtures was placed in the SPS. In this part, the influence of limewater was investigated by analysing the change tendency with time for SR and BR and comparing the ratio of SR and BR of the two mixtures in LW relative to SPS.

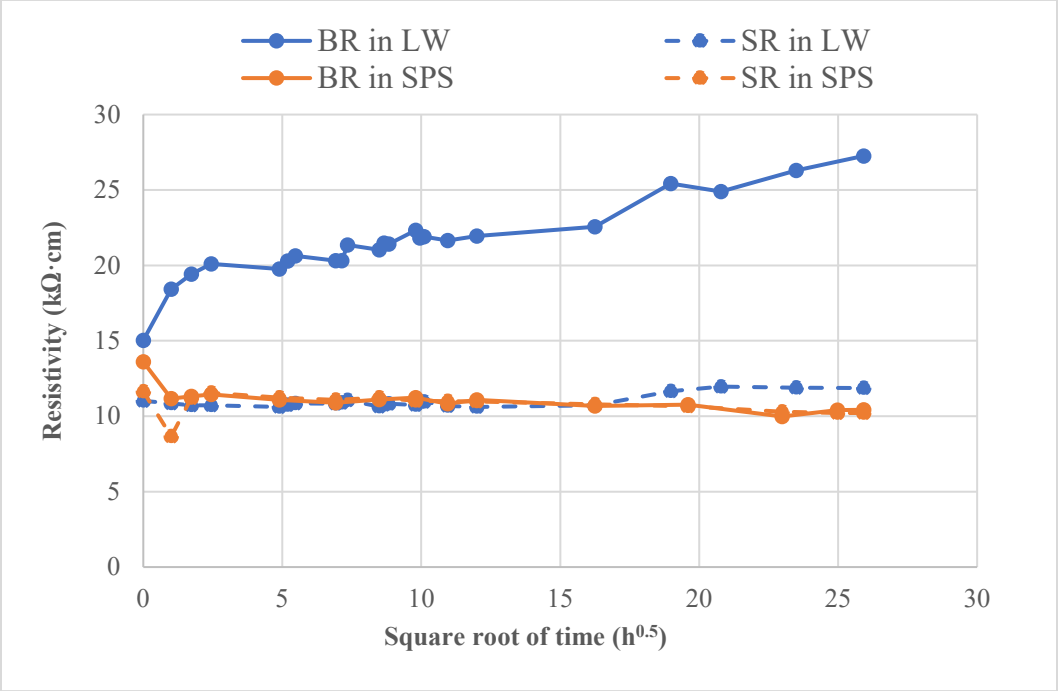

Figure 43: SR and BR change of Mixture A samples in LW and SPS.

Figure 43 shows the change with time for SR and BR of the two Mixture A samples immersed in LW and SPS. It can be observed that limewater has a marked influence on BR. The bulk resistivity of the sample in limewater kept a continuous increase throughout the experiment and is significantly higher than SR in the same solution and resistivity for both resistivity tests of the sample in SPS. In addition, it can be found that there is a slight increase of SR of the sample in LW at approximately 14 days. Overall, the values of SR in LW are similar with that of the sample in SPS. The values of SR and BR for the sample in SPS can be seen to be very similar. This situation can also be seen from the samples of mixture C, as Figure 44 shows.

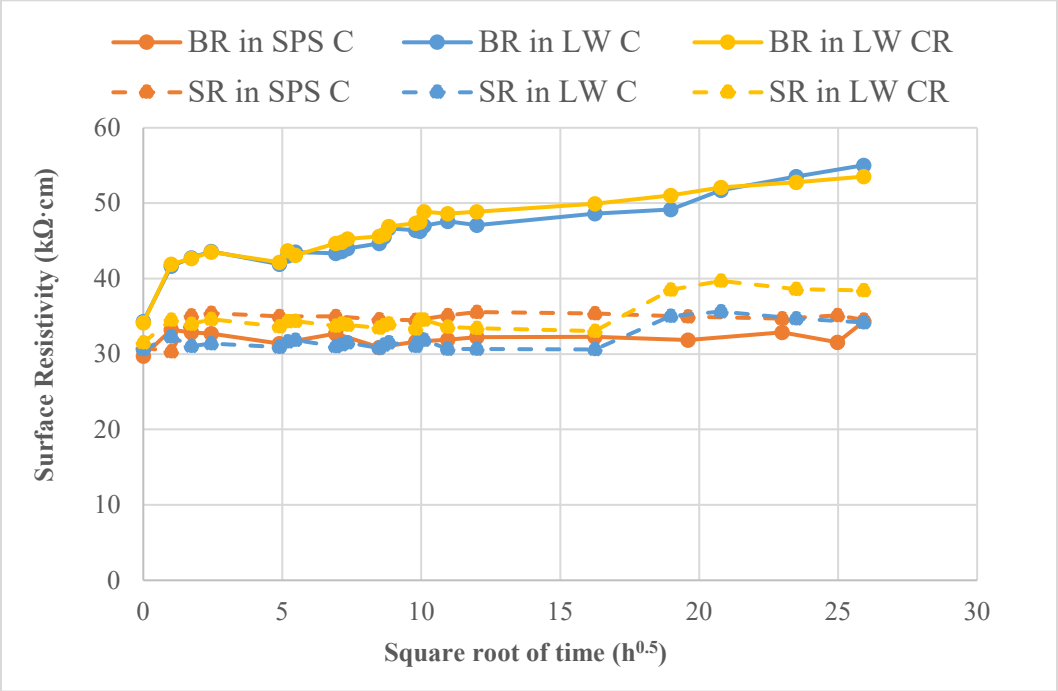

Figure 44: SR and BR change of Mixture C samples in LW and SPS.

As Figure 44 shows, for the two samples of mixture C submerged in limewater (sample C and the replicate sample CR), it is obvious that the bulk resistivity of the two samples had a continued increase and have higher resistivity compared with BR of the sample in SPS. Moreover, for surface resistivity (Figure 44), the two samples in LW showed similar change tendencies, a small increase at ~14 days. While the SR and BR of the sample in SPS remain relatively stable.

Since the samples were nearly saturated before the first round and all mature (~ 11 months old), it is reasonable to conclude that the SR and BR would not change much with time due to additional cement hydration or slag reaction; the only expected changes are the differences in immersion solution. For the first round, the samples tested in LW increased in resistivity with time significantly more than samples immersed in SPS. The increased resistivity with time is expected since LW is about 10 times higher resistivity than the concrete's pore solution. Over time, the immersion solution penetrates further into the depth of the cylinder and mixes with the concrete pore solution leading to a move resistive liquid phase. However, the surface resistivity in LW did not experience such a marked increase. It is possible that the differences in the path of the electrons between BR and SR are partly responsible for these results. As mentioned previously, for the samples of the two mixtures in SPS, the values of SR and BR are similar to each other and remain relatively stable.

Figure 45 and Figure 46 show the comparison of LW resistivity relative to SPS solution for Mixture A and Mixture C, respectively. It can be found that for both mixtures, the ratio of

surface resistivity (SR) for the limewater compared to the SPS samples does not change much with time, staying near 1.0 at all times other than the anomalous reading at one hour. However, for BR of the two Mixtures A and C, it is clear that the ratio of bulk resistivity maintains a steady, increase during the testing process. As mentioned earlier, the resistivity of limewater is 8.77 times that of the simulated pore solution. The final measured bulk resistivity of Mixture A was about 2.5 times that of the sample immersed in SPS, while this number is 1.6 times for Mixture C. From these results, it is clear that the pore solution is a blend of the initial pore solution and the immersion solution. Given sufficient time, it would be expected that LW would replace the initial pore solution and the ratio would be closer to 8.77.

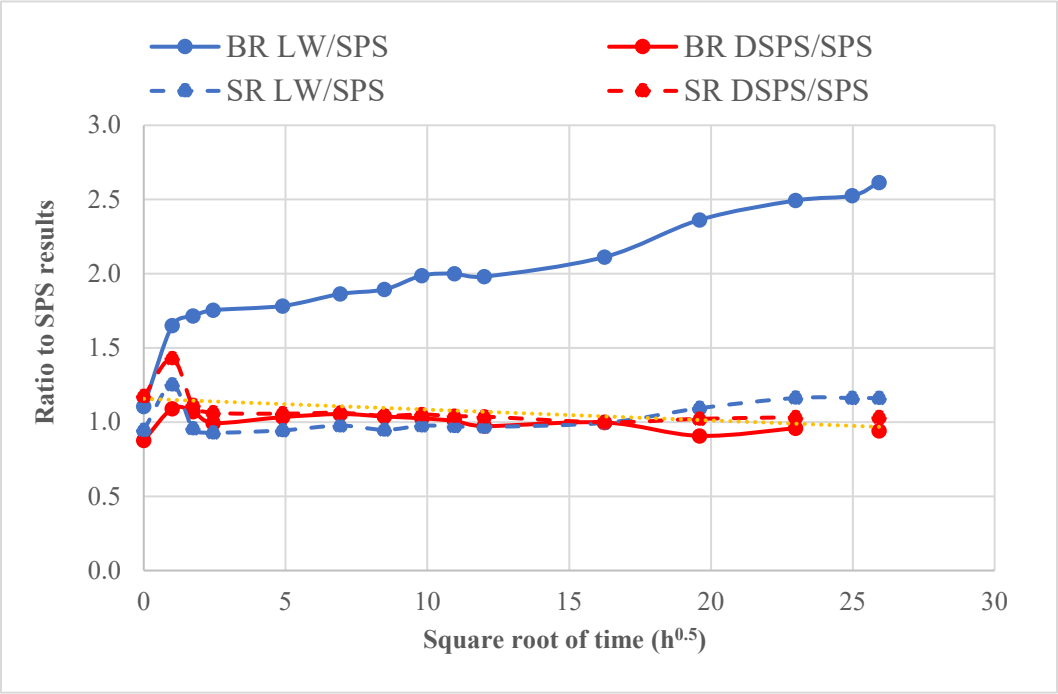

Figure 45: Comparison of resistivity relative to SPS solution — Mixture A.

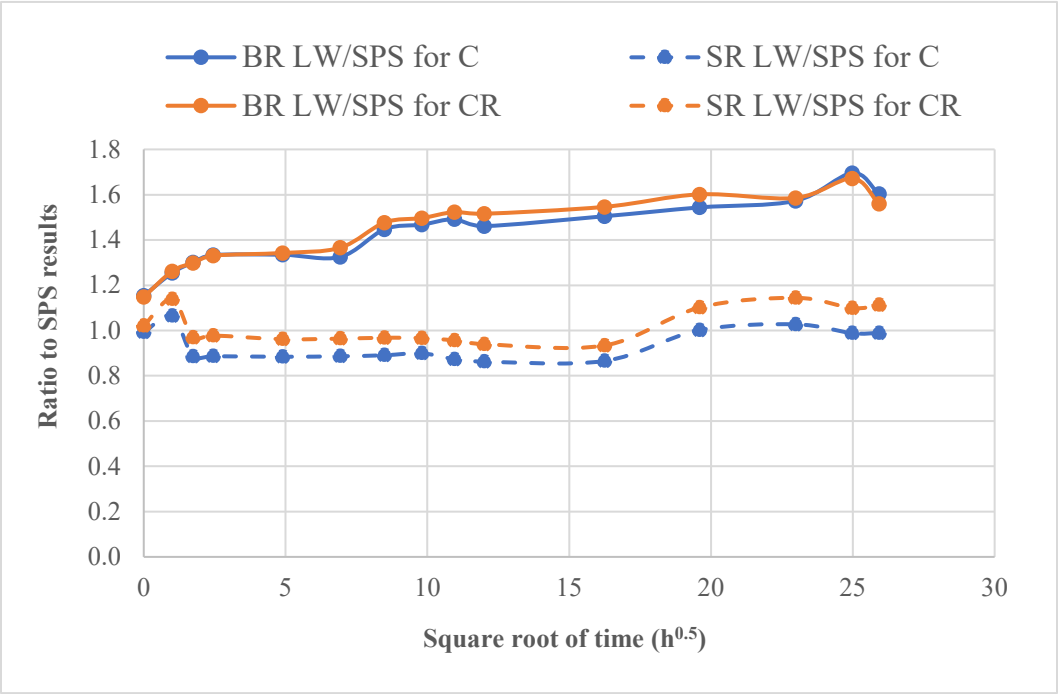

Figure 46: Comparison of resistivity relative to SPS solution — Mixture C.

4.1.3.1.2 The Influence of Double-strength Pore Solution on SR and BR

There were three samples immersed in double-strength pore solution (DSPS), one of which was Mixture A (w/c=0.48), the other two were Mixture B (w/c=0.42). In addition, one sample of each of these two mixtures was placed in the SPS. In this part, the influence of DSPS was investigated by analysing the change tendency for SR and BR and comparing the ratio of SR and BR of the two mixtures in DSPS relative to SPS.

Figure 47 shows the SR and BR change with time for the two samples of Mixture A submerged in SPS and DSPS. It can be seen that there is no obvious difference in resistivity of the two samples in either test. The four lines of SR and BR almost overlap each other, which means the DSPS does not have an obvious influence on SR and BR of the samples.

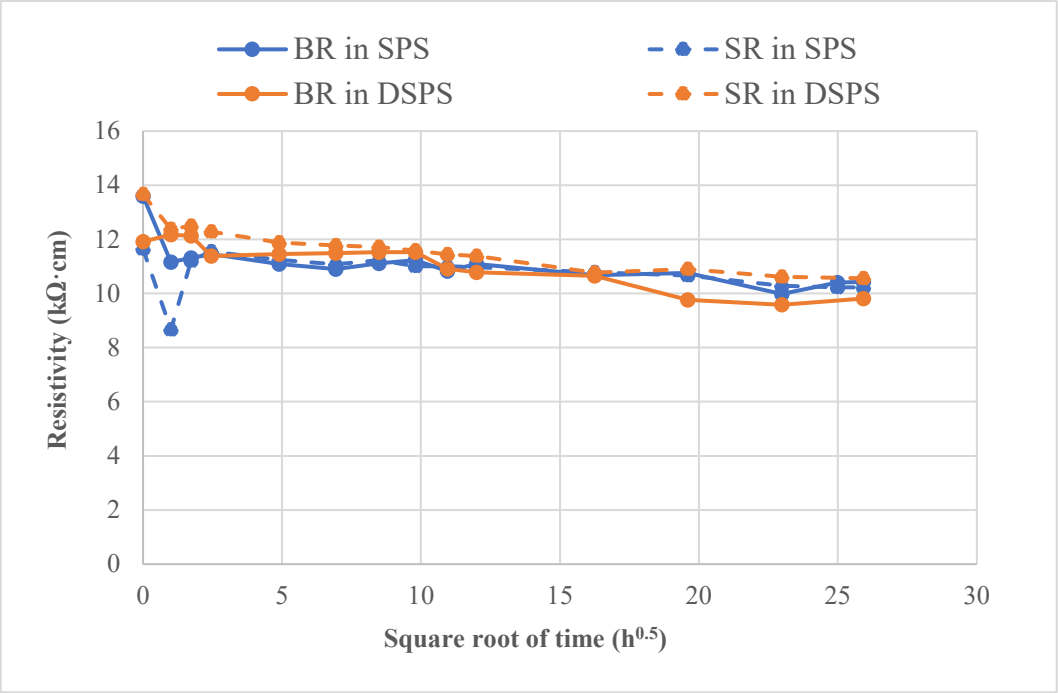

Figure 47: SR and BR change of mixture A samples in SPS and DSPS.

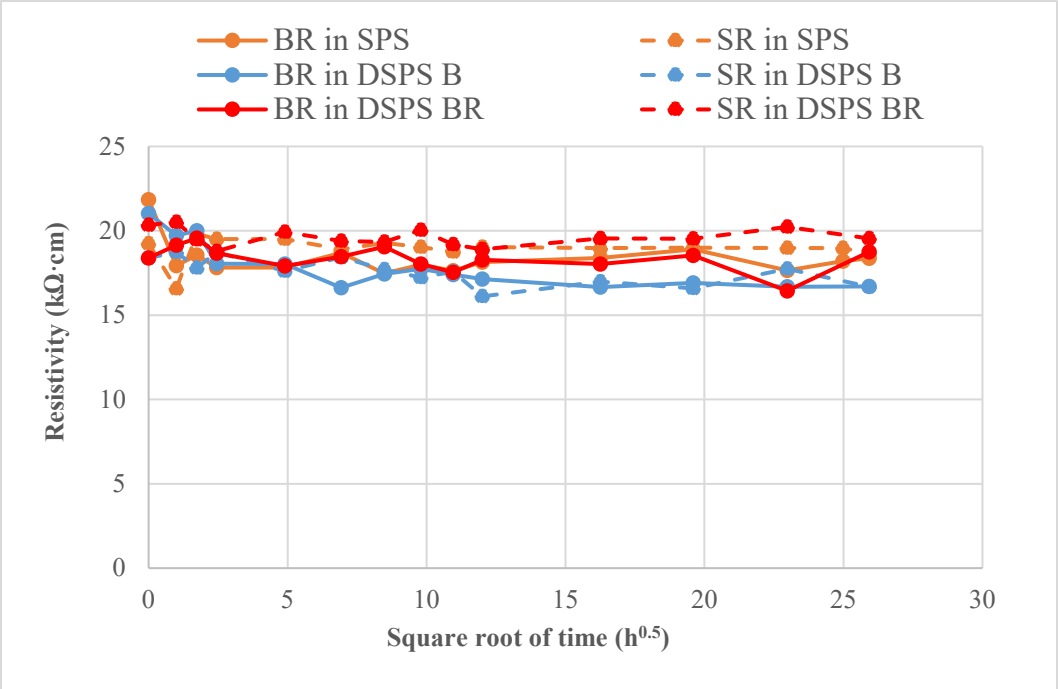

Figure 48: SR and BR change of mixture B samples in SPS and DSPS.

Figure 48 shows the resistivity change for the three samples of Mixture B. As the figure shows, two samples were immersed in DSPS and one in SPS, all the resistivity values are ranging between 15 kΩ·cm and 20 kΩ·cm. From the figure, it's hard to see how the resistivity values of the sample in SPS are different from the values of the samples in DSPS, which also indicates that DSPS does not influence the SR and BR much. The resistivity between the SPS and DSPS is much smaller than that of LW and SPS. As mentioned earlier, the resistivity of DSPS is about half of SPS which should lead to a noticeable decrease in the resistivity of the samples immersed in DSPS. For Mixture A, the estimated pore solution lies between that of SPS and DSPS, so it is not unexpected that the results of testing in the two solutions are so similar. For the case of Mixture B, the estimated resistivity of the pore solution is very close to that of SPS. Although one of the replicate samples has a slightly higher ratio of SPS/DPS, the overall influence of DSPS is negligible.

Based on Figure 47 and Figure 48, the almost overlapped changing lines illustrate that the values of SR and BR for the samples immersed in SPS and DSPS are similar, which can be concluded that the DSPS has very little effect on SR and BR of the samples compared with samples in SPS. This is also apparent in the ratio of resistivity relative to SPS solution (the ratio is close to 1), as Figure 49 shows.

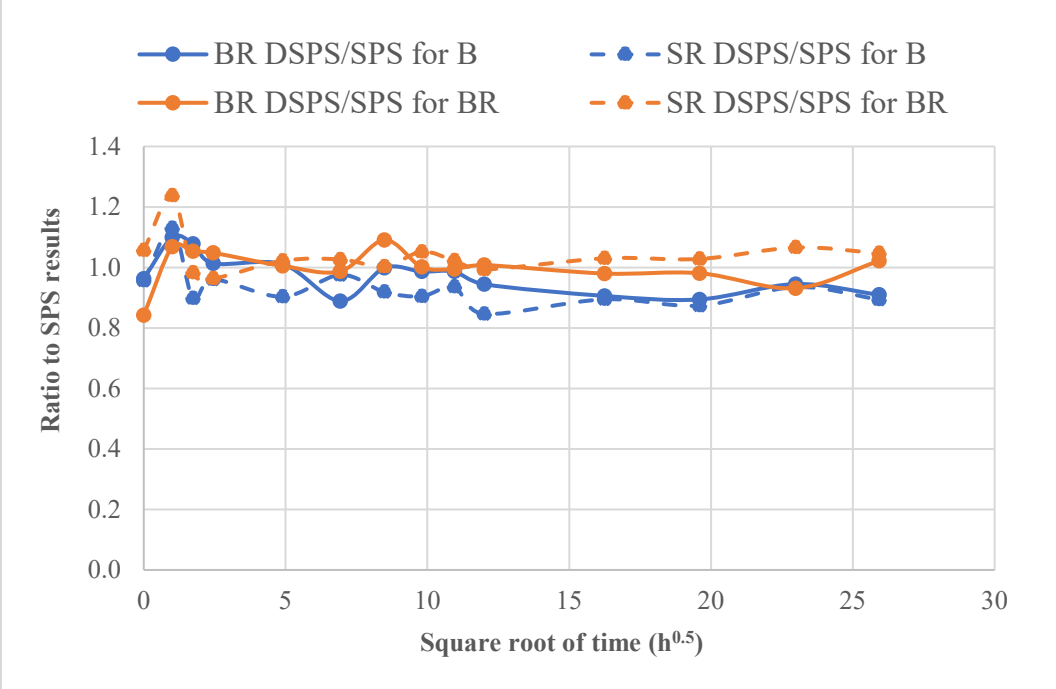

Figure 49: Comparison of resistivity relative to SPS solution — Mixture B.

4.1.3.2 The Second Round of Measurements

The samples were dried for approximately 6 weeks before the second round of measurements. In this part of the experiments, only the samples in LW and SPS were dried and measured. Therefore, this part studied how limewater influences the SR and BR of the samples after drying.

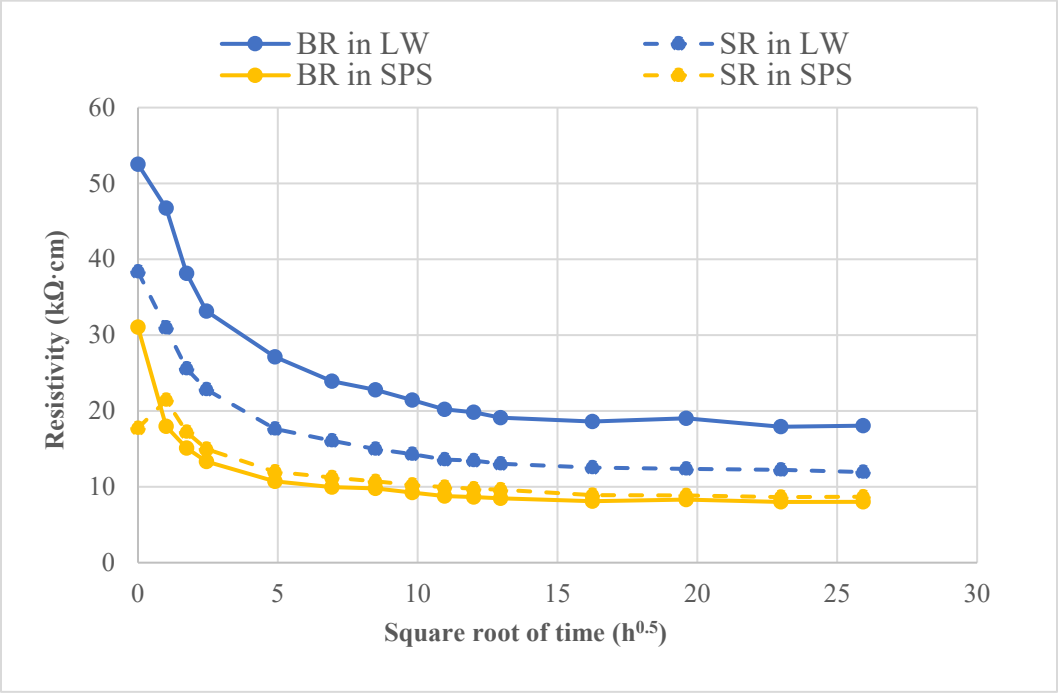

Figure 50: SR and BR change of mixture A samples in LW and SPS—2nd round (Tests on concrete samples after dried).

Figure 50 shows the SR and BR change with time for the two samples of Mixture A immersed in LW and SPS. In the second round of measurements, the primary influence on SR and BR is saturation as the samples were dry at beginning. The resistivity decreased as the solution entered the pores of the samples. Therefore, the resistivity curve showed a downward trend throughout the experiment for both samples as discussed in previous section. From the figure, it can be seen that for the sample in LW, BR is significantly higher than SR, while for the sample in SPS, the values of SR and BR are similar. Moreover, by comparing SR and BR of samples in the two solutions, it can be found that the resistivity of the sample in LW is higher than that of the sample in SPS, especially the BR, which is almost 10 kΩ·cm higher at the end. The samples of mixture C submerged in LW and SPS also show similar situation, as the Figure 51 shows.

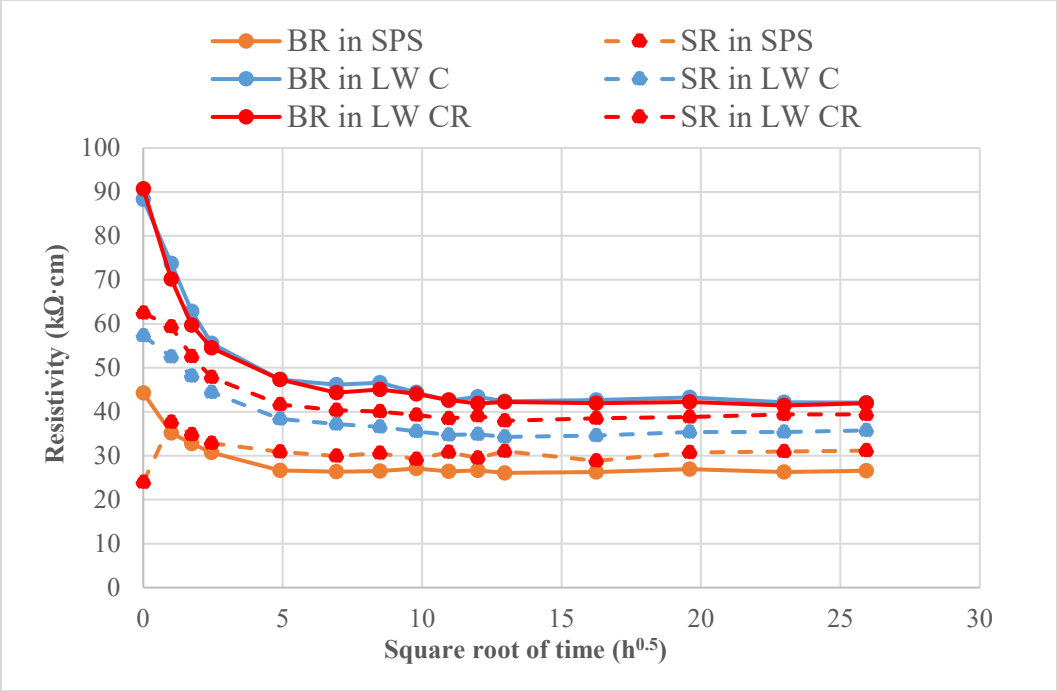

Figure 51: SR and BR change of mixture C samples in LW and SPS—2nd round (Tests on concrete samples after dried).

It is observed from Figure 51 that for the sample in SPS, there is a small difference between SR and BR, with SR slightly higher than BR for Mixture C. For the two samples in LW, the BR values are very similar and slightly higher than the SR values. There is a slight difference in the SR values of the two LW samples. Comparing the sample in SPS with the two samples in LW, it is obvious that the SR and BR values of both samples in LW are higher than those of the sample in SPS, especially BR, which is about 15 kΩ·cm higher at the end. According to Figure 50 and Figure 51, it can be seen that the LW has a significant influence on the resistivity of concrete samples in the second round of measurements.

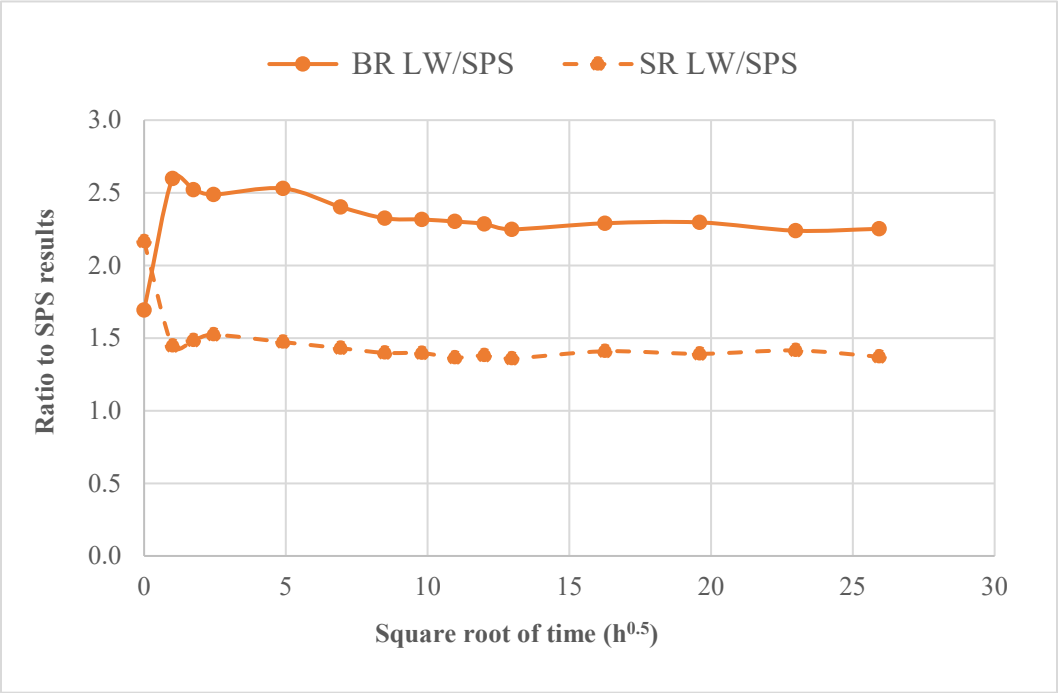

Figure 52: Comparison of resistivity relative to SPS solution –Mixture A, 2nd round.

Figure 52 shows the comparison of resistivity of the sample in LW relative to SPS solution of Mixture A. From the figure, it can be seen that comparing SR and BR in SPS with LW, the values of the ratio of both SR and BR are higher than 1, which means the LW does influence the resistivity of concrete (increase the resistivity, precisely). The ratio of BR is higher than SR means that the LW has a greater impact on BR (because of the longer path of the current). In comparison to the results from the first round for Mixture A, the ratio of LW/SPS was higher for BR than SR for both rounds. However, in the second round, the ratio at one hour was 2.52 decreasing gradually over time to 2.25. In the first round, the ratio for the same scenario increased at a higher rate and ended with a ratio of 2.61 at the end of testing. The ratio of the samples of Mixture C also show this situation, as Figure 53 shows. The BR test is much more sensitive to the change of solution than the SR test.

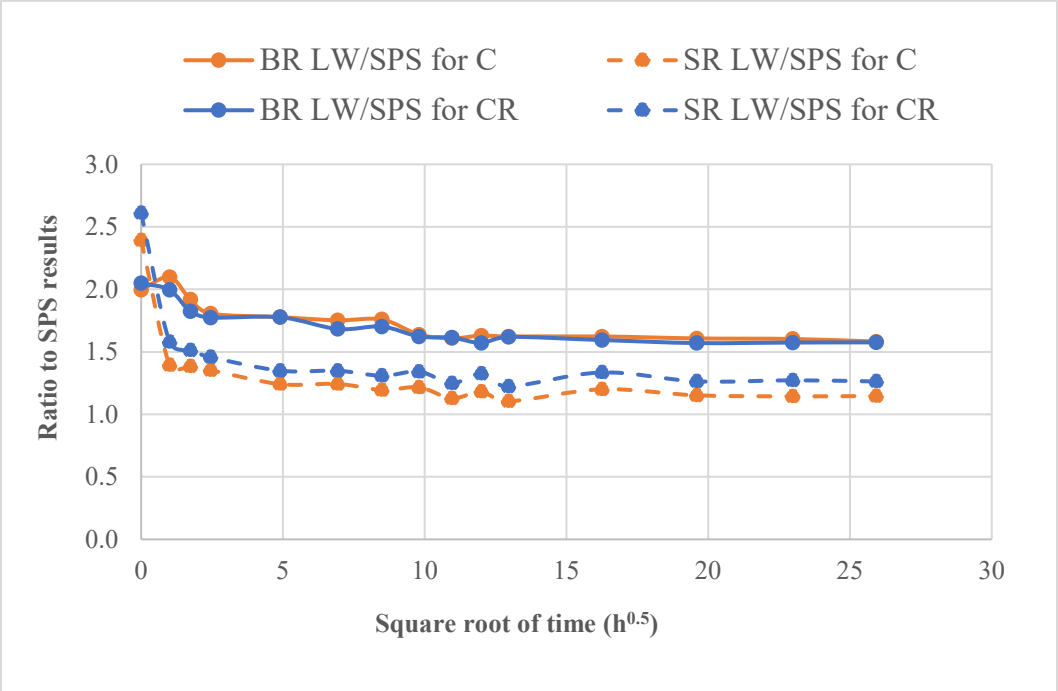

Figure 53: Comparison of resistivity relative to SPS solution –Mixture C, 2nd round.

Since the samples were previously submerged in the same solution as the second round of measurements, the concrete's pores in the second measurement round have a pore solution that is more similar to the immersion solution (from the first round) than the original pore solution. As the limewater samples then dried for 28 days, the outer depth of the cylinder contained residual chemicals left from the drying process. Subsequently, the immersion solution mixes with these residual chemicals as the samples became saturated. In addition, the internal pore solution and immersion solution gradually reaches equilibrium over time by diffusion.

It is interesting to note that the AASTHO T 358 (SR) test gives a factor of 1.1 to correct for specimens cured in limewater rather than moist curing in a chamber (or the reciprocal, 0.91 for limewater to moist room). This factor originates from an empirical relationship found by Kessler et al. (2005) that the surface resistivity of moist-cured specimens was 1.0973 times that of those cured in limewater as shown in Figure 54. The reference is not specific, but it is assumed that the cylinders were tested for surface resistivity directly on removal from the curing condition. In this research, the ratio of resistivities measured in limewater to simulated pore solution are between 1 and 1.5. As stated earlier, it is expected that given identical concrete cylinders that limewater immersion would lead to higher resistivity due to the differences in resistivity of the solutions. In the case of the published references, the opposite effect is observed. It is postulated that the differences observed in the original published research may be due to the changes to the concrete's pore structure during curing rather than the effect of the solution.

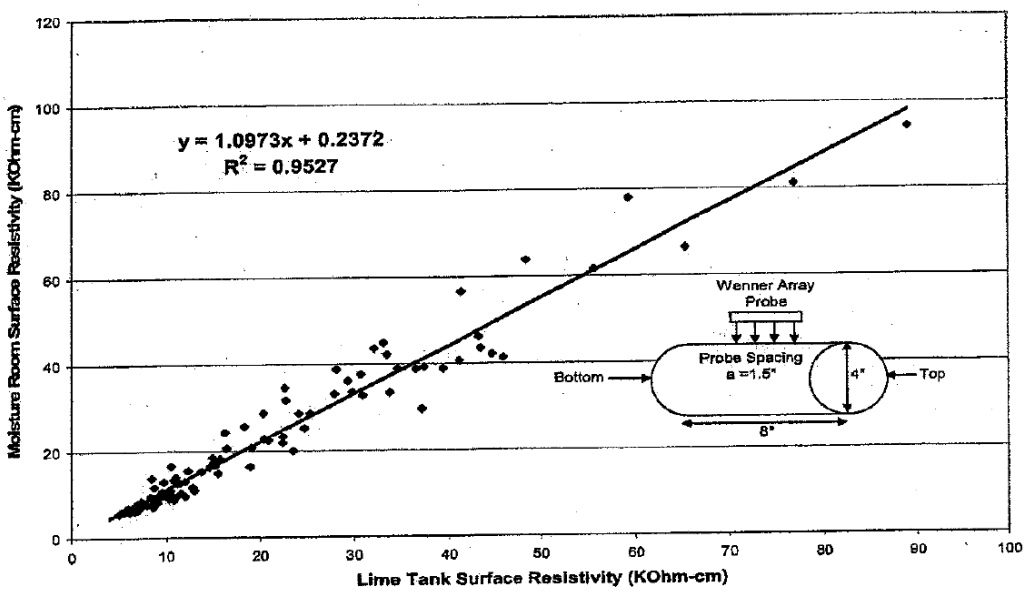

Figure 54: The relationship of SR for samples cured in LW and moisture room (Kessler et al, 2005).

In conclusion, based on the analysis of the results of the two rounds of measurements, it can be concluded that that LW has a significant effect on the resistivity of concrete samples compared to SPS, and it can be seen that the influence is greater on BR. From the results, DSPS has little effect on the resistivity of concrete samples.

4.1.4 SR to BR Ratio

In this section, the ratio between SR and BR was investigated. Since the values of SR were adjusted using the correction geometry factor and the values of BR were processed, ideally the ratio of SR/BR should be 1.0. This part studied the SR/BR ratio of the samples in different solutions and compared with the results of Interlaboratory data.

4.1.4.1 The SR/BR Ratio of LW and SPS

The SR/BR ratio of limewater

Figure 55 and Figure 56 are the ratio of SR/BR of LW for the two rounds of measurements. It can be seen that in both rounds of LW immersion that all the values of the ratio are less than 1.0, which also illustrates that LW not only affects the resistivity of concrete samples, but also affects SR and BR to different degrees. For the first round, the ratio of SR/BR showed a slow decreasing trend throughout the experiment, which is the result of the gradual increase in BR of the samples in LW. The samples were saturated before being immersed in the solutions. As the immersion solution gradually entered the pores of the samples, the original pore solution was changed, and the concentration of conductive ions in the pore changes, accordingly, thus affecting the resistivity of the samples. For the second round, it can be seen that after the initial several measurements, the ratio became relatively stable. After the first round of measurements, the pore solutions of the samples had been changed by the immersion during testing, compared with their original pore solutions. With drying for 6 weeks, the conductive ions remained inside of the specimen. In the second round of experiments, the samples were immersed in the same solution as the first round, resulting in a faster equilibration. From both figures, it can be seen that Mixture A had a much lower SR/BR ratio. Mixture A has the lowest water to cement ratio and therefore the highest permeability. In this mixture, the transport of ions and the exchange of fluids occurs more quickly, so the changes due to solution come about faster.

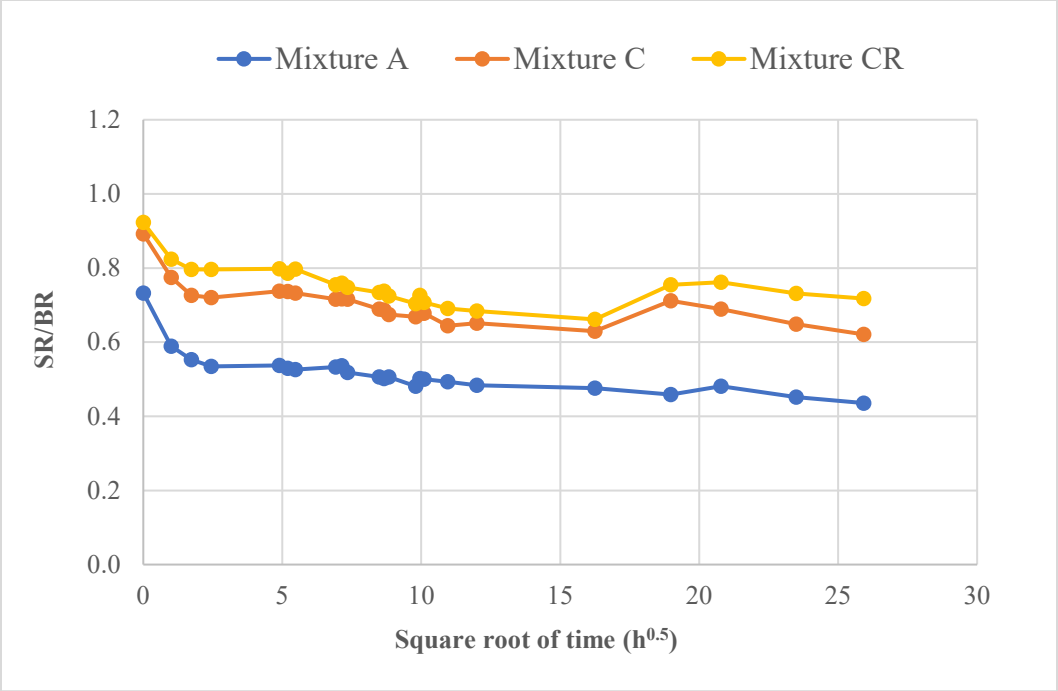

Figure 55: The SR/BR ratio of the three samples in LW—1st round (Tests on concrete samples as received).

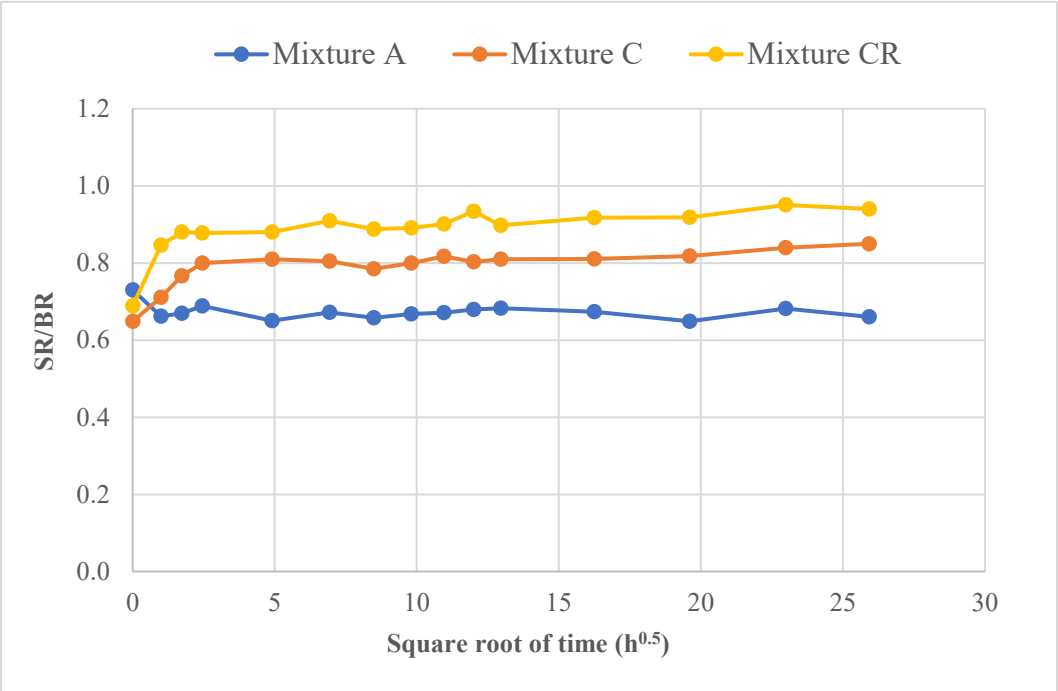

Figure 56: The SR/BR ratio of the three samples in LW—2nd round (Tests on concrete samples after dried).

The SR/BR ratio of SPS

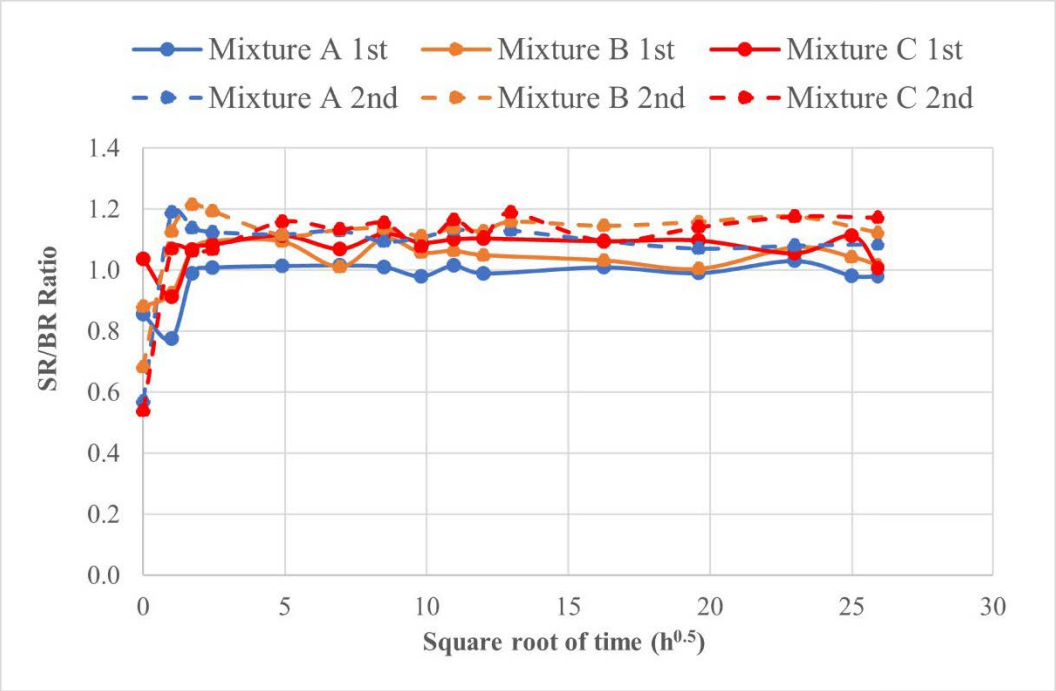

Figure 57: The SR/BR ratio of the three samples in SPS—2 rounds.

Figure 57 shows the ratio of SR/BR of samples in SPS for the two rounds of measurements. It can be seen that except for the first few measurements, most of the values are in the interval of 1.0 to 1.2, within ±25%. In addition, the ratio above 1.0 means higher values for SR.

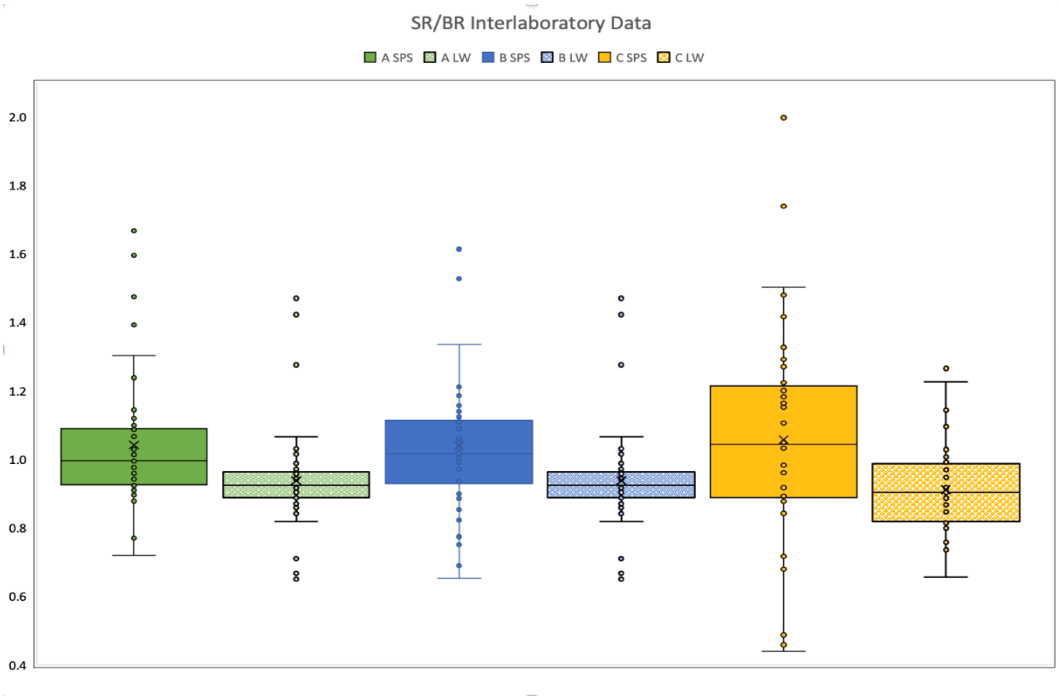

Figure 58: The results of SR/BR ratio of ILS data.

Figure 58 shows the results of SR/BR ratio of ILS data. It is observed that there is high variability in the ratio. For the samples in LW, it appears that the majority of values for SR/BR ratio are below 1.0 with an overall average of 0.92. In this study, the ratios are lower, with ~0.5 for Mixture A and ~0.7 for Mixture C. For the samples in SPS, the ratio of ILS data is mostly ranging from 0.9 to 1.2 (with an overall average of 1.05). In this case, the ILS results agree with the data of the research.

4.1.4.2 COMSOL Modelling

As can be seen schematically in Figure 59, the path of the electrons in the surface resistivity and bulk resistivity tests differ. In the surface resistivity test (shown on the left), an electrical current is applied on the two outer probes, while the voltage is determined by measurements on the two inner probes. The electrons follow hemispherical path through the sample. In contrast, for the bulk resistivity test, the electrons move along the length of the cylinder as shown in the right. When the cylinder consists of two layers of differing resistivities (shown as the grey areas on the figures), this presents are more complex path for the electrons. In order to better understand the influence of a layered resistivity, some further analysis of the bulk and surface resistivity was undertaken using COMSOL version 5.5, a multi-physics modelling software.

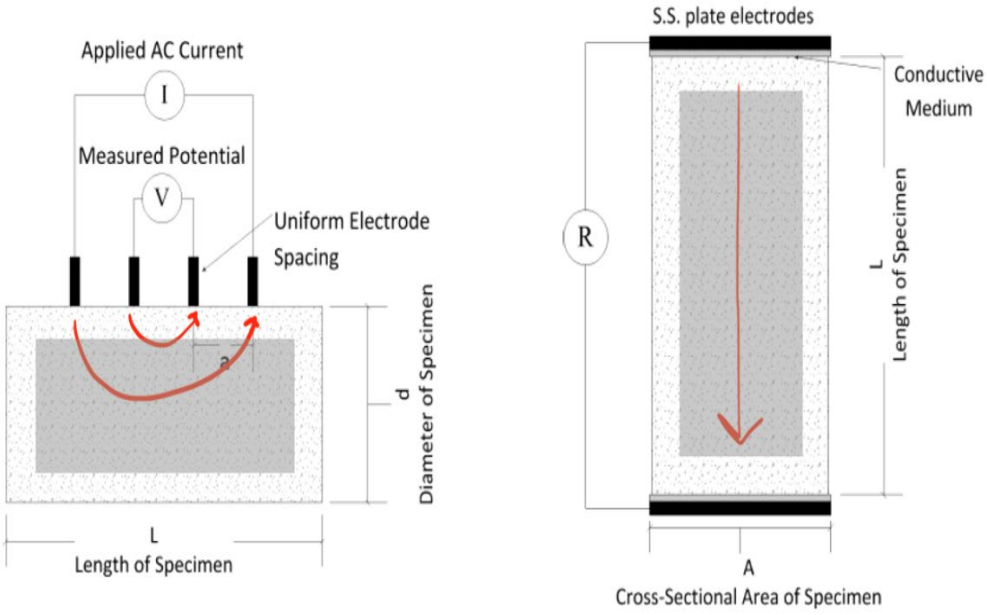

Figure 59: Schematic representation of surface and bulk resistivity tests (Layssi, 2015).

Figure 60 shows the geometry used for the model. The concrete cylinder was modelled as two axis-symmetric cylinders of differing sizes. The other cylinder represents the actual cylinder with diameter of 100 mm and length of 200 mm. Initially, the cylinder consists of a single resistivity. As the solution penetrates into the cylinder from all sides, the penetration depth, d, represents another resistivity. The modelling was done with the parameter (d) ranging from 0 to 50 mm. As such the inner cylinder with the original resistivity decreases in size as d increases.

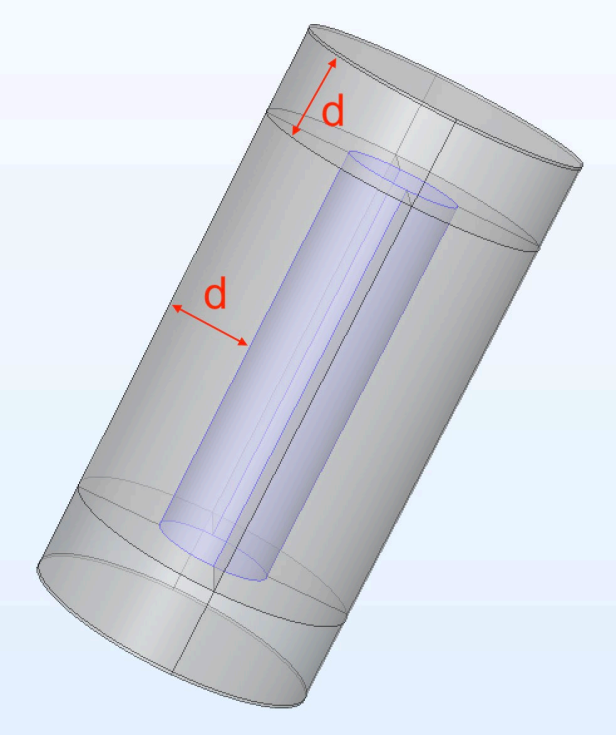

Figure 60: Model used for COMSOL analyses.

For the COMSOL modelling the cylinders immersed in SPS for the 2nd round were used. In this case, the inner cylinder represents the dried state, and the outer shell represents the depth of penetration of the SPS solution. For purposes of the model, the measured experimental data prior to immersion was used for the resistivity of the inner cylinder (or in the case where d = 0, the dried cylinder prior to immersion). For the outer shell, the resistivity was set to an average value of the measure surface and bulk resistivity at the end of testing (when d = 50 mm). It is acknowledged that this is a simplified layered model with a marked distinction of resistivity. Although the cylinder was dried for 6 weeks, it is probably unlikely it is at a uniform moisture state throughout the depth. As well, upon immersion, the varied sizes of pores create a non-uniform wetting front and not a sharp distinction. However, even with these limitations, the modelling was carried out to see results of the simulation compared to the measured results.

Table 6. Resistivities for the layered model

Immersion solutions (measured)	Outer shell (kOhm·cm)	Inner cylinder (kOhm·cm)
Mixture A (w/c=0.48)	8.3	30.0
Mixture B (w/c=0.42)	15.5	30.0
Mixture C (w/c=0.39)	28.7	43.5

Given that the experimental data was measured over time and the model output gave the resistivity with depth, a conversion for time to depth was needed. For this purpose, the nick point concept as outlined in Qiao et al (2019) was used. The nick point defines the demarcation between initial and secondary absorption. The period of initial absorption concludes with the filling of the capillary pores; during secondary absorption air voids are filled. shows the mass gain for the three concrete mixtures immersed in SPS for the second round of testing (after 6 weeks of drying). The mass gain for all mixtures exhibited strong non-linear behaviour followed by a notable linear behaviour. The nick point was defined at the boundary between the non-linear and linear portions and is different for each mixture. (For each mixture, the nick points also corresponded to 82 to 83% of the total absorption). For the conversion, the nick point was set to d = 50 mm (0.05 m) and each square root of time point was converted as a ratio of this relationship (e.g., for Mixture A, 10.95 $h^{0.5}$ = 0.05 m).

Figure 62, Figure 63 and Figure 64 show the results predicted by the COMSOL model compared to the experimentally measured data. For all mixtures, the general shape of the predicted behaviour matches that of the experimental results with a rapid decreased followed by a slower drop. The rapid decrease occurs up to the point where d = 0.02 to 0.03 m. This indicates that as the immersion solution reaches half the radius, the composite resistivity is less affected by the drier core. As can be observed, in all cases for both experimental and predicted values, the SR exceeds the BR results. However, differences between the two resistivity tests are much more pronounced in the experimental data. It can also be noted that the differences between SR and BR increase with the decreased permeability of the concrete. Mixture A has the highest w/c and therefore the high permeability of the sample seems to yield more similar results between the two tests.

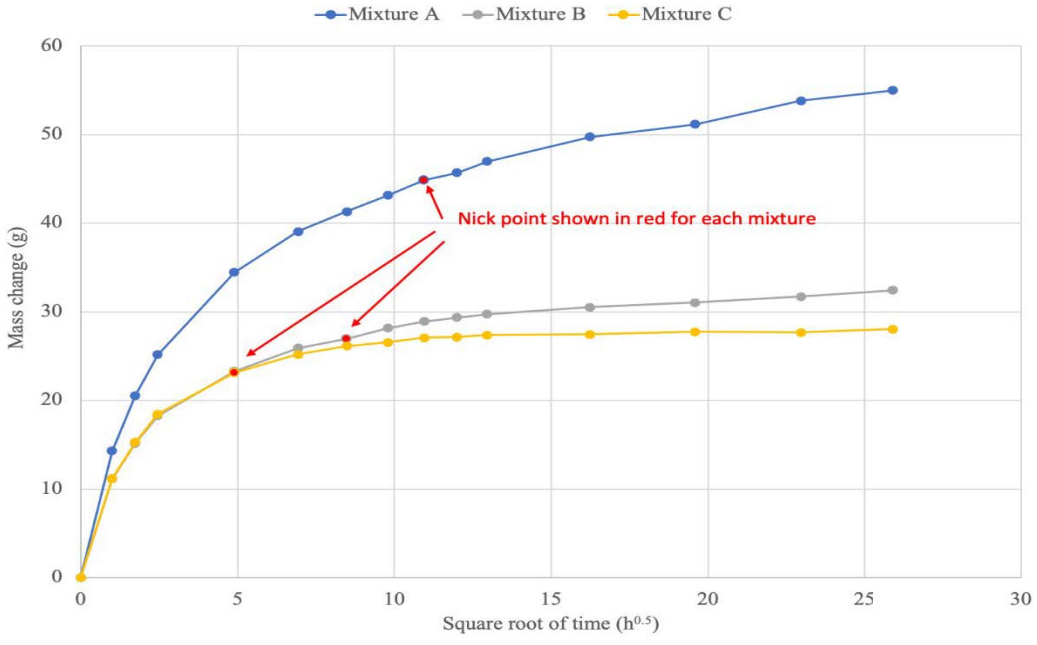

Figure 61: Mass gain for SPS immersion of 2nd round tests.

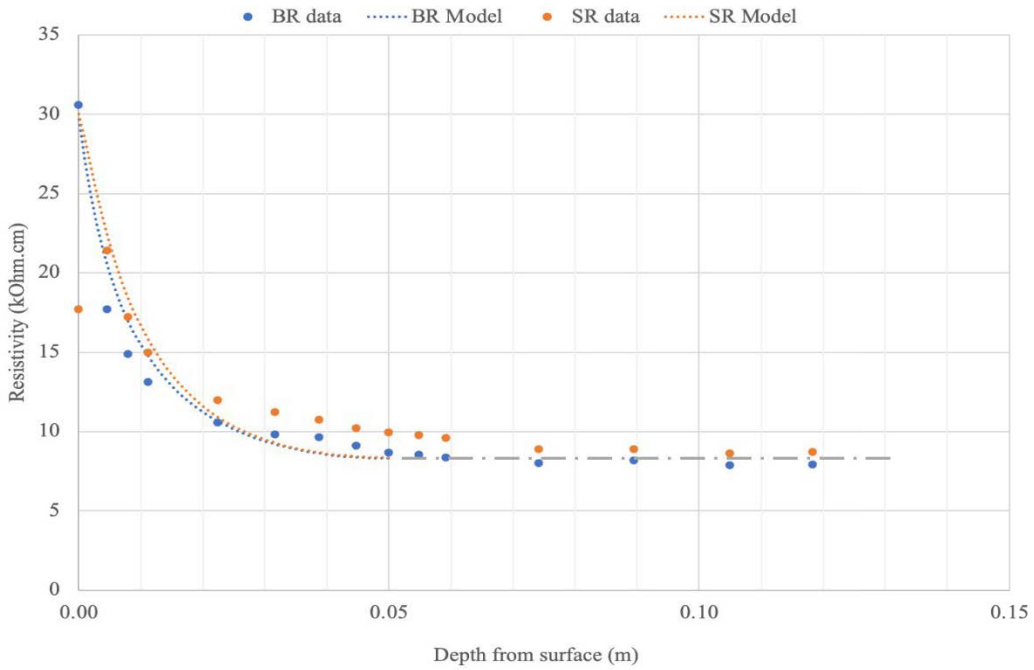

Figure 62: Experimental and predicted resistivity for Mixture A.

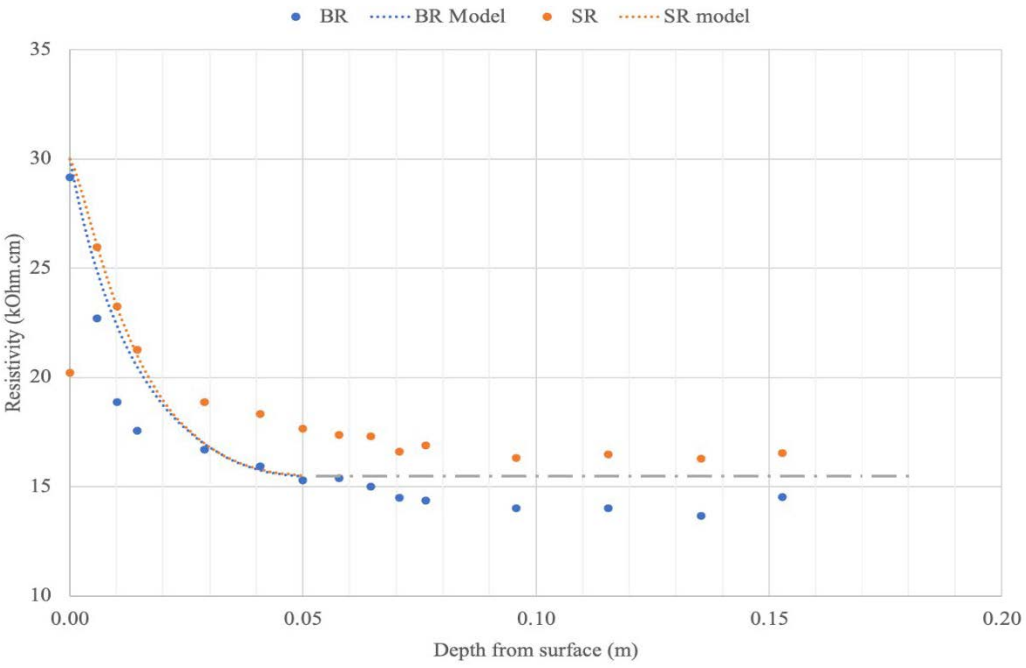

Figure 63: Experimental and predicted resistivity for Mixture B.

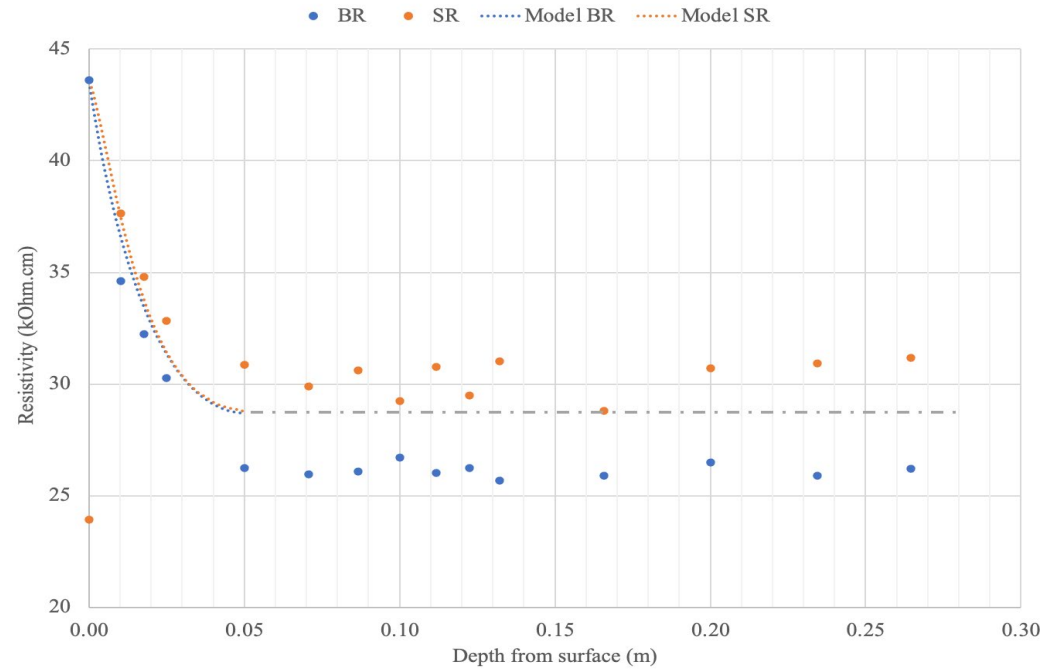

Figure 64: Experimental and predicted resistivity for Mixture C.

Figure 65 shows the ratio of surface to bulk resistivity for the experimental results and those predicted by COMSOL. As can be seen, the predictions result in a clear increase in a ratio as the w/c increases. The predicted maximum occurs when the depth of penetration roughly equals 10% of the radius (~ 5 mm or 0.005 m) for all mixtures. As the depth of penetration increases, the relationship between the two tests tends towards unity. However, the observed ratio has no clear relation to the depth of penetration (or time). As mentioned previously, the two layered model is a simplification of the physical behaviour as the resistivity is not constant within the sample either before or during testing. However, the model was useful to give some insight into the observed results.

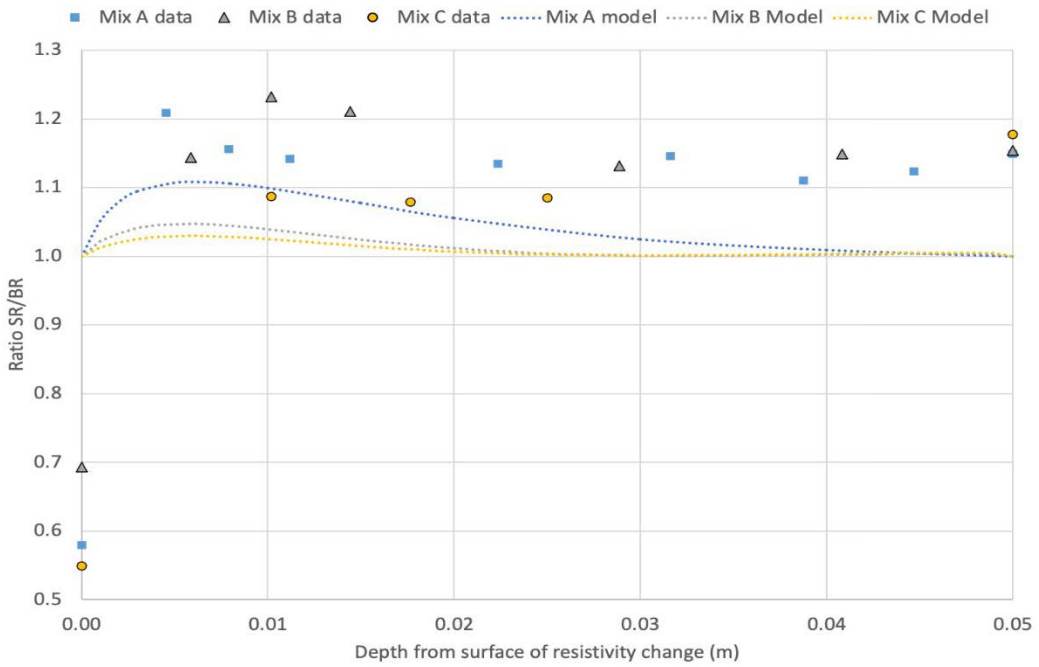

Figure 65: Experimental and predicted SR/BR ratio.

4.2 Analysis of the Mortar Samples

For this part, the results of the mortar samples at two different ages (28 and 56 days) were investigated. As mentioned previously, all the electrical resistivity results presented, including the results of SR and BR, are corrected by using the geometry factor of 1.89 and the calculation process in Section 3.1.2.

For the mortar samples, two rounds of 28-day measurements were performed, one at each age. For the surface and bulk resistivity, there were 12 samples in total for each round and 6 for each mortar mixture. Of the six cylinders, three cylinders were immersed in limewater and three in simulated pore solution for each mortar. The final presented results are the average values of the three samples.

4.2.1 SR and BR Change Over Time

4.2.1.1 SR and BR Change Over Time at the age of 28 days

As mentioned before, SR and BR changes were measured for 2 mortars immersed in LW and SPS in phases two, Mortar A (w/c=0.48) and Mortar C (w/c=0.39). This section studies the results of the samples immersed in LW and SPS at the age of 28 days.

Figure 66 shows the SR and BR change over time for Mortar A and Mortar C tested starting at the age of 28 days. It can be seen that the first two measurements of the two mortars are variable as was seen in the concrete phase. Some samples showed a downward trend (Mortar C-BR in SPS (up to 15 $h^{0.5}$), Mortar A-BR in SPS), while some samples showed an upward trend (Mortar C, particularly after 15 $h^{0.5}$). This may be due to the different initial saturation states of the samples before immersing into the solutions; the low water to cementing material ratio of Mortar C may have caused some self-desiccation. In addition, for the samples of Mortar A, it can be found that the resistivity in LW and SPS show similar tendency, decreasing slightly with time throughout the test for both SR and BR and remain relatively stable. The resistivity of the samples in LW are higher than that of the samples in SPS as was seen in the concrete phase.

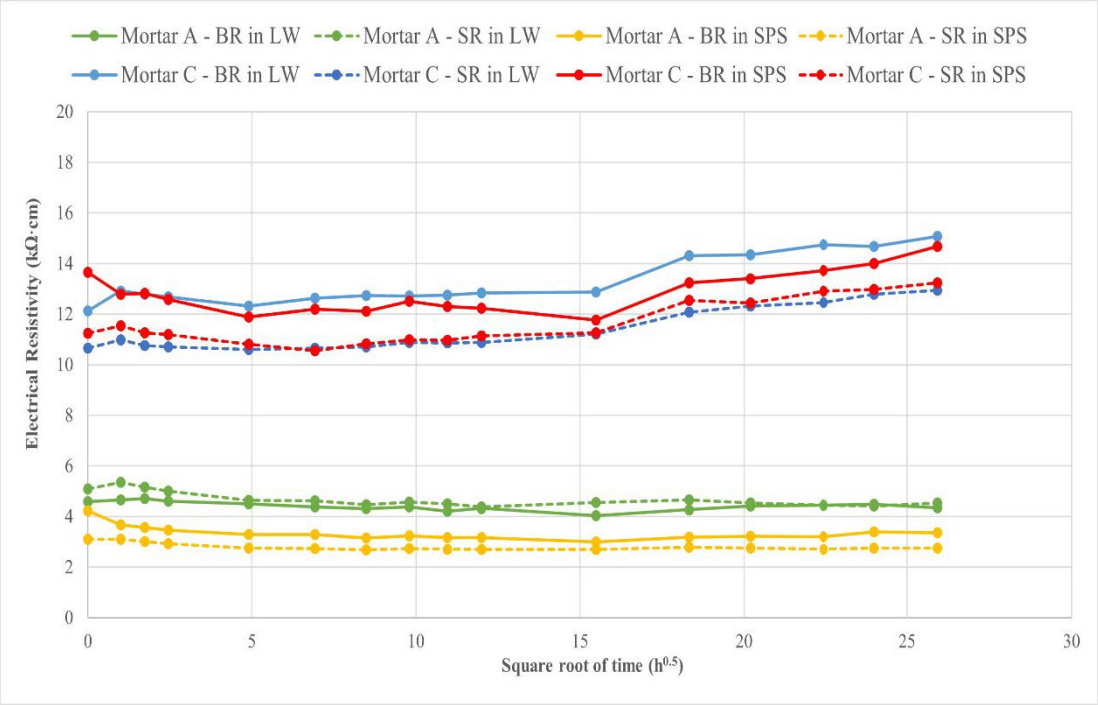

Figure 66: SR and BR change of the two mortars tested at the age of 28 days.

It is observed for both resistivity of the samples of Mortar C in both solutions, there was insignificant changes between the 1 hour and 10-day (15.5 $h^{0.5}$) measurements. In the subsequent measurements between 10 and 28 days, there was an increasing trend occurred which might

indicate increased hydration inside the cylinders. Since Mortar C included the use of 25% slag, there was a longer hydration process.

In conclusion, for the samples measured at the age of 28 days, there is no significant change observed for Mortar A. This is mainly because Mortar A contained only Portland cement and achived a high degree of hydration at the age of 28 days, while for Mortar C containing the use of 25% slag, increases in resistivity with time can be found. As mentioned in the literature review, resistivity is supposed to increse as the hydration proceeds. Therefore, the observed increase in resistivity for Mortar C may caused by the sustained react of slag.

4.2.1.2 SR and BR change over time at the age of 56 days

At the age of 56 days, 12 additional cylinders were removed from the molds and the resistivity was measured for 28 days. Figure 67 shows the SR and BR change with time for Mortar A and Mortar C at the age of 56 days. It is observed that for both mortars, there was an obvious decrease in resistivity within the first 24 hours (4.95 $h^{0.5}$). This is mainly due to the increase of moisture content of the samples during this time. For Mortar A, after the first 24 hours, the resistivity decreased very slightly with time throughout the test, reaching a very steady state. In addition, the resistivities of the samples in the two solutions are very similar.

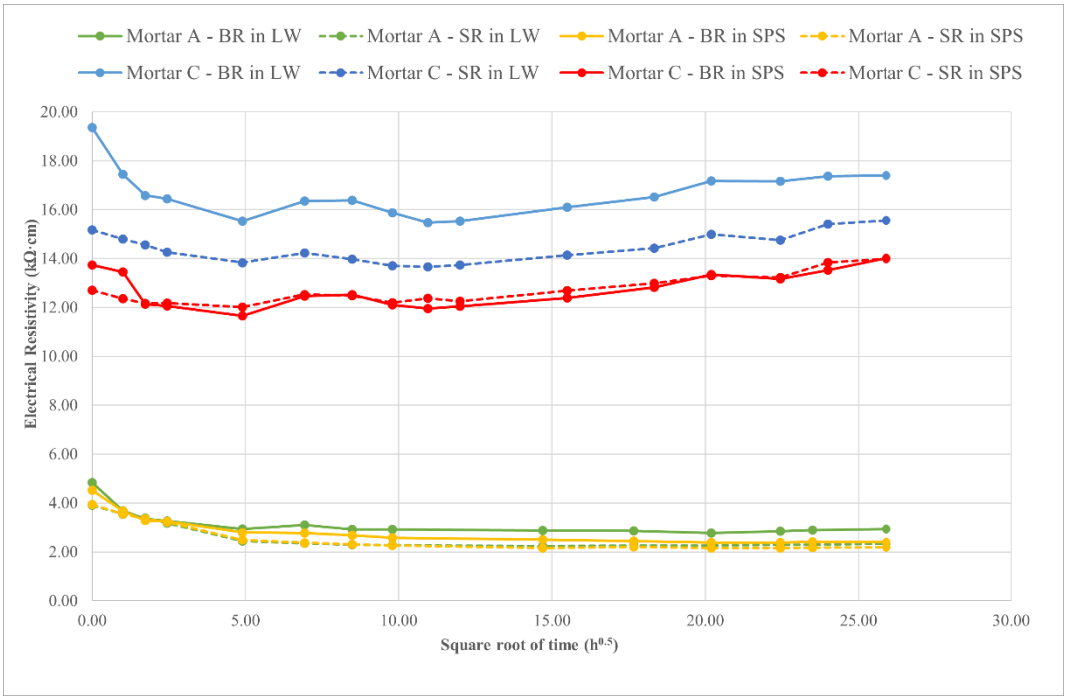

Figure 67: SR and BR change of the two mortars tested at the age of 56 days.

For Mortar C, the decrease in resistivity in the first 24 hours is the same with Mortar A. The resistivity changes between the 1 day and 10 days (4.95 $h^{0.5}$ to 15.5 $h^{0.5}$) can be found very low, and then followed by a slight increasing trend in the rest of the measurements, which illustrates that the hydration process may be still ongoing. Moreover, it is also can be observed that the resistivity for the samples in LW is higher than that of the samples in SPS.

In summary, from the results shown in the two figures, it can be concluded that for Mortar A containing only Portland cement, the slight change in resistivity shows that the cylinders had reached a considerable high degree of hydration at the age of 28 days after casting. In addition, it is observed that the values of SR and BR became stable after immersing the cylinders in the solutions for 24 hours. For Mortar C containing slag, the SR and BR had a slight increase in the experiment which indicates that the hydration process of cylinders continued for a long time.

4.2.2 Influence of Mixture Design

As mentioned before, two types of mortars were used in phase two: Mortar A, w/c = 0.48; Mortar C, w/c = 0.39 with 25% slag. This part investigated how the two mixture designs influence SR and BR of the samples.

As shown in Figure 66, at the age of 28 days, it can be clearly seen that the resistivity for Mortar C was 3 to 4 times higher than Mortar A. One of the reasons is that the w/c ratio of Mortar is higher than Mortar C. As mentioned in the concrete part, as well as previously published research, increasing of the water to cement ratio causes increasing permeability and decreasing resistivity. Another reason is that there is slag included in Mortar C. The use of slag caused a more complex and refined pore network than Mortar A, as described in the concrete part, resulting in increasing resistivity. Therefore, the lower w/c ratio and use of slag of Mortar C gives it higher resistivity than Mortar A.

At the age of 56 days, as shown in Figure 67, it is observed that the behavior of SR and BR change is similar to the change at the age of 28 days. The resistivity for Mortar C was about 5 to 6 times higher than Mortar A. Apart from the above two reasons, the cylinders of Mortar C at the age of 56 days had a higher degree of hydration than the cylinders at the age of 28 days, resulting in higher resistivity, corresponding to the research of Sanchez et al (2015). Therefore, compared with the results at the age of 28 days, the cylinders of Mortar C tested at the age of 56 days were higher in resistivity. However, for Mortar A, it shows a different situation. The results of resistivity at the age of 56 days are lower than that at the age of 28 days, but the differences between the two ages is not large. As shown in the interlaboratory study in the concrete section, the resistivity can vary up to +/- 25% within a population. The small differences in Mortar A between 28 and 56 days may be due to this variability.

4.2.3 Influence of Solutions

The influence of the two solutions was investigated in this part. In phase two, two different solutions were used: limewater and simulated pore solution.

At the age of 28 days, for Mortar A, it can be seen from Figure 66 that the BR of the cylinders in SPS was a little higher than SR, but nearly the same for the LW solution. In addition, the resistivity (SR and BR) of the cylinders in LW was higher than that of the cylinders in SPS. For the concrete tests, it was observed from Figure 43 that BR of Mixture A (w/c=0.48) in LW gave significantly higher resistivity than SR in LW as well as higher than both tests in SPS. Another difference is that the values of SR in LW are similar with the resistivity of the sample in SPS for the concrete tests, while in the mortar tests, the SR in LW was higher than SR and BR of the cylinders in SPS.

While for Mortar C, the BR was higher than SR for both LW and SPS solutions, and SR for the two solutions were similar. Compared with the concrete tests, as shown in Figure 44, the similarities are the BR in LW was higher than SR and the resistivity in SPS. However, LW has a greater effect on the BR of concrete samples. For SPS, the SR for concrete samples was higher than BR, while the samples for Mortar C showed the opposite situation.

At the age of 56 days, for Mortar A, it is observed from Figure 67 that there is no significant difference of SR and BR in the results of the cylinders in both LW and SPS. In this case, the effects of LW and SPS on the resistivity of the cylinders are not significantly different. The main reason is that the resistivity of the Mortar A cylinders is very low to show obvious differences between the two solutions.

For Mortar C, it can be seen that the BR was higher than the SR for LW, while for SPS, the values of SR and BR were very similar. In addition, the SR and BR of the cylinders in LW were higher than the samples in SPS. In this case, it is obvious that the influence of LW on SR and BR are more significant than SPS. For LW, the effect on BR is more apparent than SR, but not obvious for SPS.

In conclusion, it can be found that LW is more influential on the resistivity of the two mortars than SPS even if it is not so apparent for the Mortar A samples. Given that LW is about 10 times higher resistivity than the mortar's pore solution, this result is expected. In addition, for Mortar C, LW had a greater effect on BR than SR.

4.2.4 Compared the Mortar Results with Concrete Results

Figure 68 shows the comparison between surface resistivity in SPS for concrete and mortar samples. It can be observed that the resistivity is about 3 times higher for concrete for the 0.39 slag mixture (Concrete C) and 4 times higher in the 0.48 mixture (Concrete A) compared to the companion mortar. There are two influences that can explain the differences.

Firstly, as mentioned previously, it is well established that the resistivity increases with hydration, the concrete samples were tested approximately 11 months old after casting while the mortar was tested at the age of 28 days. At the age of 28 days, the mortars samples had not reached fully hydration, especially for the Mortar C samples with slag. According to Figure 66 and Figure 67, although it can be seen that Mortar A samples had reached a high degree of hydration, it is predicted that with the further increase of the degree of hydration, the resistivity will increase significantly, while Mortar C requires longer hydration time due to the use of slag.

Secondly, concrete contains a large coarse aggregate while mortar contains sand only. The large impermeable aggregate creates a longer pathway for electrons, leading to higher resistivity.

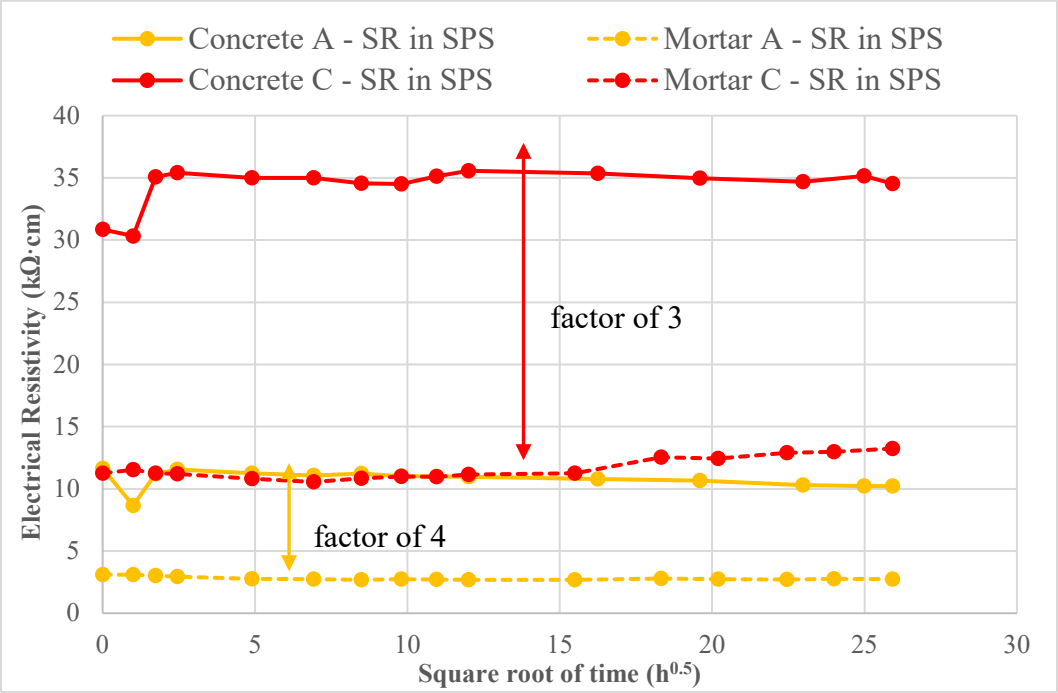

Figure 68: Comparison of surface resistivity in SPS for concrete and mortar.

4.2.5 Results of Internal Sensors

In this part, in order to investigate the penetration depth of the solution with time inside the mortar samples, 8 mortar cylinders in total (four of each mortar mixture) were made with wires embedded at 1, 3 and 5 centimeters. As described in the Methodology part, each depth has a pair of parallel wires with 5 cm apart. The measurements were carried out for 5-7 days as the resistance was stable in most cases at this time.

The Sensors were placed as following:

- Top: 1 cm depth.
- Middle: 3 cm depth.
- Bottom: 5 cm depth.

Unfortunately, due to the low resistivity of the mortar cylinders, and some top sensor wires (the wires embedded at 1cm) were damaged during the process of removing the molds, some testing results were missing, and some are not good as expected. The following shown figures are only part of the testing results. In addition, at the beginning of measurements (at time=0, prior to immersion), one test was carried out in order to obtain the dry conductivity of the samples which was shown in the figures at time zero.

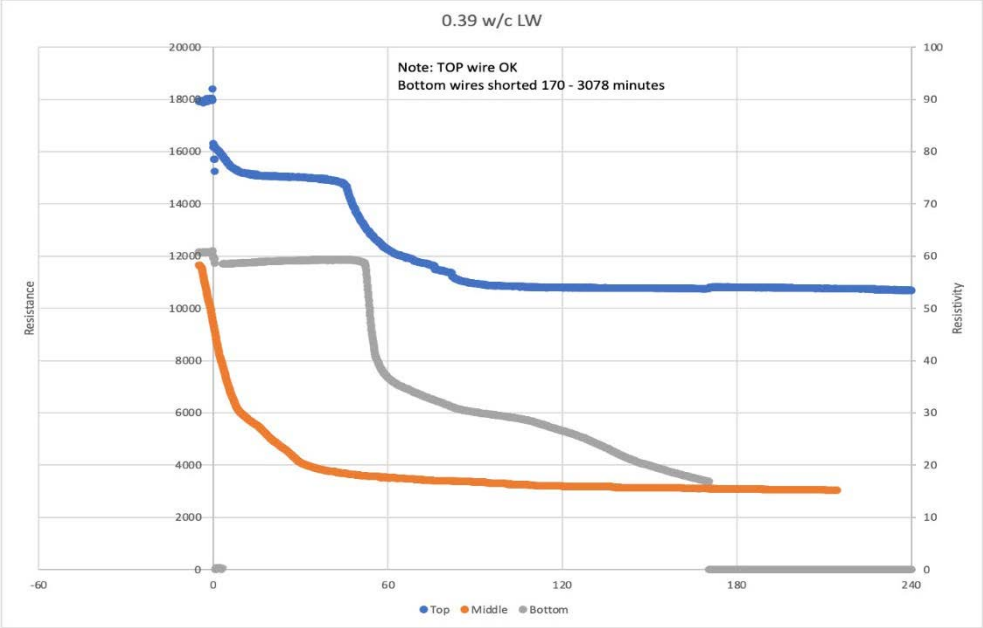

Figure 69: The testing results of mortar cylinders with 0.39 w/c in LW (up to 240 minutes).

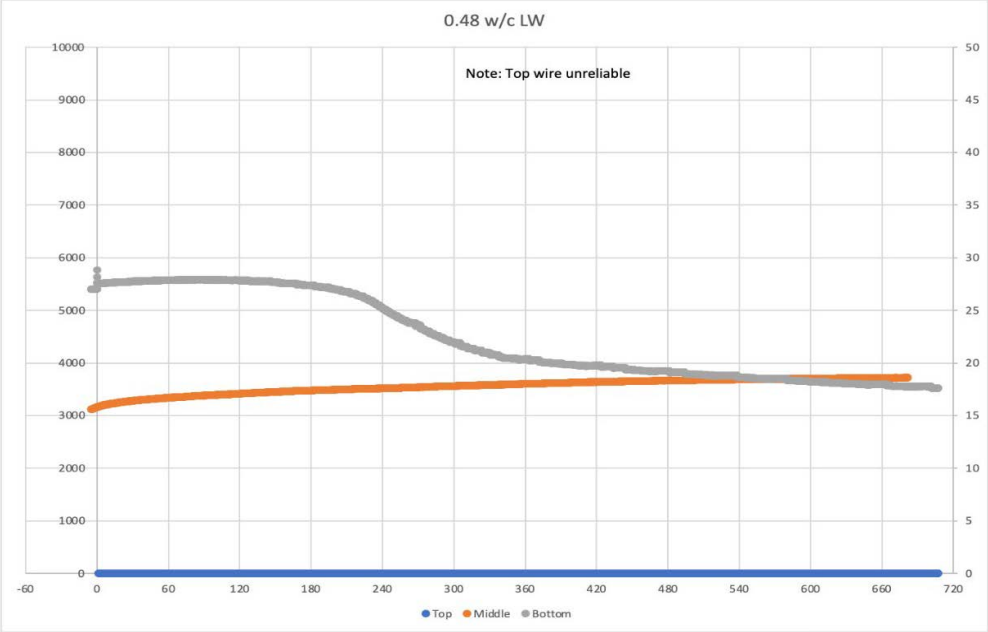

Figure 70: The testing results of mortar cylinders with 0.48 w/c in LW (up to 720 minutes).

The time for the solution to reach the sensor was determined by the inflection point of the curve or the method of Rajabipour (the average of the stable values before and after the steep change). Figure 69 shows the testing results of mortar specimens with 0.39 w/c immersed in LW. In the case, it is observed that the solution reached the sensor within one hour for all sensor locations.

Figure 70 shows the results of mortar specimens with 0.48 w/c immersed in LW. Due to the top sensor was damaged when removed the mold, there is no change for the top sensor (blue curve). For the middle sensor, it can be seen that there is no infection point for this curve (orange curve), which means the middle sensor was also damaged. For the bottom sensor, the solution reached the bottom between 240 and 360 minutes (4-5 hours).

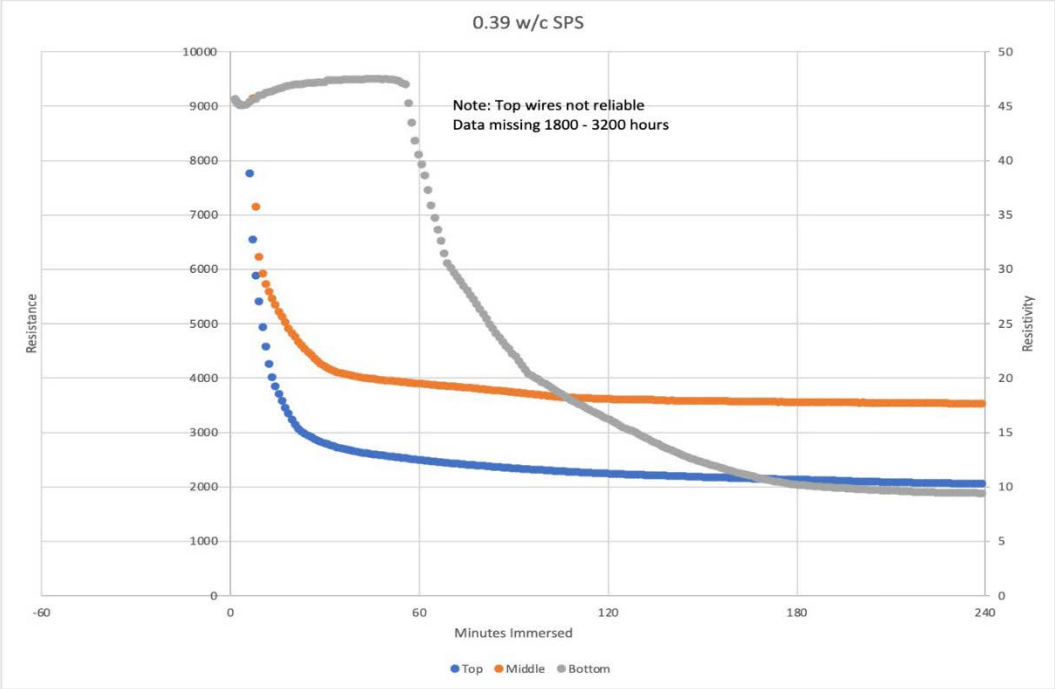

Figure 71: The testing results of mortar cylinders with 0.39 w/c in SPS (up to 240 minutes).

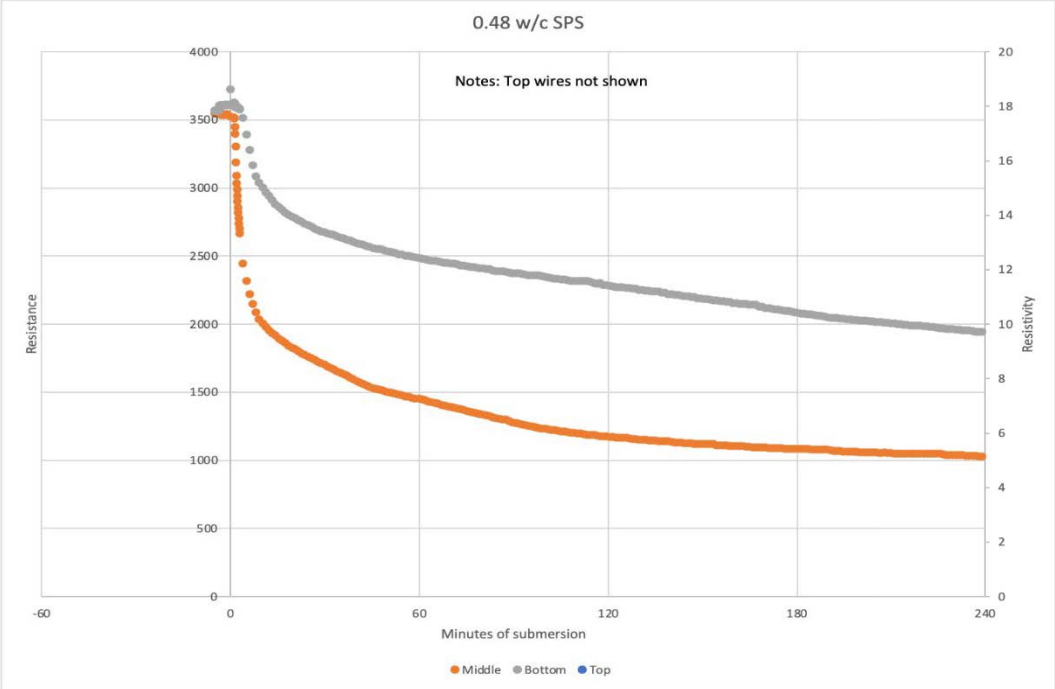

Figure 72: The testing results of mortar cylinders with 0.48 w/c in SPS (up to 240 minutes).

Figure 71 and Figure 72 show the results of mortar specimens with 0.39 w/c and 0.48 w/c immersed in SPS. It can be found that in the case of mortar with 0.39 w/c in SPS, although the top sensor was loose, the data seems reasonable. The solution reached the top and middle sensors within an hour and the bottom sensor between 1-2 hours. While in the case of mortar specimens with 0.48 w/c in SPS, the top sensor is not reliable. The solution reached the sensor within an hour for the middle and bottom sensors.

In this part, although some data was unreliable and some data was missing due to the damage of the sensors, from the rest data, it can be concluded that the tests on the surface and bulk resistivity show very low resistivity suggesting a very permeable material. Compared the results with SR and BR of the specimens in the lab, it can be found that there are minimal differences in SR and BR measurements for the entire submersion time indicating a few possibilities. 1) the sample-maintained moisture while in the cylinder. 2) the porous nature allows for quick ingress of solution. In addition, the resistivity measured by the internal sensors (after 1 or more days) was in the same range as the SR and BR measurements.

5 Summary, Conclusions and Recommendations

This project studied the electrical resistivity changes with time of concrete and mortar cylinders that were immersed in different solutions to investigate various influences that may affect the standard tests. The surface resistivity, bulk resistivity and mass change of three mixture designs of concrete at the age of about one year old were tested at two different initial moisture states for an immersion duration of 28 days. The first round of measurements of the concrete cylinders were performed with the samples at initial sealed saturation state, while the second round of measurements were carried out with the laboratory dried samples. For the mortar cylinders, samples with two mixture designs were made and tested at the age of 28 days and 56 days, and both rounds of measurements lasted 28 days. Further, the penetration of the solution was investigated by monitoring the saturation at varying depths.

Based on the testing performed in this study, the following conclusions are made:

1. The SR and BR are influenced by the immersion solutions. The concrete samples tested in limewater were found to have higher in resistivity than simulated pore solution since limewater is about 8.77 times higher resistivity than SPS. However, it seems that the double strength pore solution showed very little influence on resistivity. In all cases, the internal pore solution composition was unknown as the initial concrete pore solution and the immersion combined. The difference in resistivity cannot be purely attributed to the immersion solution.
2. In the second round of testing concrete, it was shown that SR and BR decreased rapidly within 24 hours after immersion in the solution, and the rate of decrease gradually slowed down over the next 27 days. Even in an unsaturated condition, the standard immersion duration might be longer than necessary.
3. For the concrete mixtures with different w/c and combinations of SCMs, the mixture with the highest w/cm and no SCMs had the lowest resistivity. For the two mixtures with 25% slag, a small decrease of w/cm from 0.42 to 0.39 resulted in a nearly two-fold increase in resistivity indicating the pore system is highly segmented and discontinuous in the 0.39 slag concrete.
4. It was shown that for the concrete cylinders immersed from the initial sealed state, that the SR and BR results at 24 hours are within 5% of the results at 6 days and within 10% of the results at 21 days. This indicates that the immersion duration for the standardized tests is overly conservative and could be reduced.

In addition, in this study, the following points were also found: 1) It was found that for standard concrete cylinders (10 × 20cm), the electrical resistance of the concrete is highly influenced by the moisture content as evidenced by the differences in the two rounds of testing. The change trend of SR and BR are opposite to that of the mass since increasing saturation is known to reduce resistivity. 2) It was found that limewater has an obvious influence on the resistivity of the concrete and mortar samples, and the influence of limewater on bulk resistivity is more

obvious than that on surface resistivity. 3) For samples immersion in LW, the ratio of surface to bulk resistivity was less than 1. However, for SPS, the ratio was higher than 1, which was verified with COMSOL modelling. The two standardized tests use different solutions, care should be used in comparing standard tests. 4) For the mortar cylinders, the electrical resistivity tested at the age of 56 days is higher than that of 28 days due to higher hydration, particularly for the mixture containing slag. 5) It was found that the resistivity of mortar cylinders was significantly lower than the companion concrete with a similar mixture design. Although part of this difference may be due to the increased maturity for the concrete, the lack of coarse aggregate in the mortar was responsible for its more permeable structure. 6) For the study on penetration of solutions, unfortunately, the internal sensors did not provide a good indication of the depth of the solution penetration with time. The low resistivity of the mortar mixtures, the early age of testing and possible leakage could have influenced the results.

Recommendations

1. To study the influence of limewater and simulated pore solution more thoroughly, it is suggested to case concrete rather than mortar and a wide range of mixture designs.
2. For the tests using internal sensors, it is suggested to place the embedded wires in such a way to prevent solution from entering at the interface of the wire and the surrounding concrete.

6 References

AASHTO T 277, (2007) “Standard Test Method for Electrical Indication of Concrete’s Ability to Resist Chloride”, American Association of State Highway and Transportation Officials, Washington, DC, 2007, 12 pp.

AASHTO, (2011) “Standard method of test for surface resistivity indication of concrete’s ability to resist chloride ion penetration”, AASHTO TP 95, Am. Assoc. State Highw. Transp. Off., 2011.

ASTM C1202-12, (2012) “Standard Test Method for Electrical Indication of Concrete’s Ability to Resist Chloride Ion Penetration”, ASTM International, West Conshohocken, PA, 2012, 8 pp.

ASTM, (2012) “Standard test method for bulk electrical conductivity of hardened concrete”, ASTM International, 2012.

Azarsa, P. and Gupta, R. (2017) “Electrical resistivity of concrete for durability evaluation: a review”. *Advances in Materials Science and Engineering*, 2017.

Banea, P. I. (2015) “The study of electrical resistivity of mature concrete".

Chini A. R., Muszynski L. C., and Hicks J. (2003) “Determination of Acceptance Permeability Characteristics for Performance-Related Specifications for Portland Cement Concrete”, Final report submitted to FDOT (MASc. Thesis), University of Florida, Department of Civil Engineering.

Claisse, P.A. (2014) “Letter: Using Electrical Tests as Durability Indicators”, *Concrete International*, V. 36, No. 10, Oct. 2014, p.17.

Cyr, M. (2013) “Eco-efficient concrete: 8. Influence of supplementary cementitious materials (SCMs) on concrete durability”. Elsevier Inc. Chapters; 2013 Feb 4.

Elkey W. and Sellevold, E.J. (1995) “Electrical resistivity of concrete”.

Gowers, K.R. and Millard, S.G. (1999) “Measurement of Concrete Resistivity for Assessment of Corrosion Severity of Steel Using Wenner Technique”, ACI Materials Journal, Technical paper, September - October 1999, Vol. 96, No. 5, pp. 536-541.

Larsen, B. W., White D. J., and Jahren C. T. (2007) “Embankment construction QC/QA using DCP and moisture control: Iowa case history for unsuitable soils”, In Proceedings of the 2007 Mid-Continent Transportation Research Symposium, pp. 714-730. 2007.

Layssi, H., Ghods, P., Alizadeh A. R. and Salehi, M. (2015) “Electrical resistivity of concrete”. *Concrete international*, *37*(5), pp.41-46.

Liu, Y. (2008) “Experiments and Modeling on Resistivity of Multi-layer Concrete with and without Embedded Rebar”, master’s thesis, Florida Atlantic University, Boca Raton, Fl, 2008, 91 pp.

Liu, Y., and Presuel-Moreno, F., “Evaluation of long-term hydration of concrete with SCMs by electrical resistivity method”.

Lu, X. (1997) “Application of the Nernst-Einstein Equation to Concrete”, *Cement and Concrete Research*, V. 27, No. 2, Feb. 1997, pp. 293-302.

McCarter, W. J. and Chrisp, M. (2000) “Monitoring water and ionic penetration into cover-zone concrete”. *Materials Journal*, 97(6), 668-674.

Mehta P. K. and Monteiro P. J. M. (2006) “Concrete: microstructure, properties, and materials”, McGraw-Hill, New York, NY, USA, 3rd edition.

Mohammadi, B., Nokken M. R. and Mivalad, S. (2017) “Development of in-situ water absorption method - laboratory study and field validation”, *Journal of Materials in Civil Engineering*, Vol. 29, Issue 10.

Monfore, G. E. (1968) “The electrical resistivity of concrete”. Skokie Ill: Portland Cement Association Research and Development Laboratories, 1968.

Morris, W., Moreno, E. I. and Sagues, A. A. (1996) “Practical Evaluation of Resistivity of Concrete in Test Cylinders Using a Wenner Array Probe”, *Cement and Concrete Research*, Vol. 26, No. 12, pp. 1779-1787.

Nadelman, E.I., and Kurtis, K.E. (2014) “A Resistivity-Based Approach to Optimizing Concrete Performance”, *Concrete International*, V. 36, No. 5, May 2014, pp. 50-54.

Noort, R. V., Hunger, M. and Spiesz, P. (2016) “Long-term chloride migration coefficient in slag cement-based and resistivity as an alternative test method”, *Construction and Building Materials*, vol. 115, pp. 746-759, 2016.

Qiao, C., Moradllo, M.K., Hall, H., Ley, M.T. and Weiss, W.J. (2019) “Electrical resistivity and formation factor of air-entrained concrete”. ACI Materials Journal, 116(3), pp.85-93.

Rajabipour, F., Weiss, J., Shane, J. D., Mason, T.O. and Shah, S.P. (2005) “Procedure to interpret electrical conductivity measurements in cover concrete during rewetting”, *Journal of materials in civil engineering*, 17(5), pp.586-594.

Rangelov, M. and Nassiri, S. (2018) “Empirical time-dependent tortuosity relations for hydrating mortar mixtures based on modified Archie’s law”. *Construction and Building Materials*, *171*, 825-838.

Resipod Operating Instructions. Proceq SA, Schwerzenbach, Switzerland, 2018.

Rupnow T. and Icenogle, P. (2012) “Evaluation of surface resistivity measurements as an alternative to the rapid chloride permeability test for quality assurance and acceptance”, Tech. Rep. 2290, Performing Organization Name and Address Louisiana Transportation Research Center, Baton Rouge, La, USA, 2012.

Sanchez Marquez J. M. and Nokken, M. R. (2014) “Evaluation of Saturation on Surface Electrical Resistivity Measurements”. CSCE Annual Conference, Halifax, NS, May 28 -31, 2014.

Spragg, R., Bu, Y., Snyder, K., Bentz, D. and Weiss, J., 2013. “Electrical Testing of Cement-Based Materials: Role of Testing Techniques, Sample Conditioning, and Accelerated Curing”, Final Report. Joint Transportation Research Program, Indiana Department of Transportation and Purdue University. Report Number: FHWA/IN/JRTP-2013/28. DOI: 10.5703/1288284315230. pp. 1- 19.

Spratt, R., Castro, J., Nantung, T. E., Paredes, M. and Weiss, W. J., 2011. “Variability Analysis of the Bulk Resistivity Measured Using Concrete Cylinders”, Tech. Rep., Purdue University Press, West Lafayette, Ind, USA, 2011.

Wang H., 2014. “The Study of Concrete Durability in the Case of Jinan Yellow River Highway Bridge”, master’s thesis.

Weydert R. and Gehlen, C., 1999. “Electrolytic resistivity of cover concrete: relevance, measurement, and interpretation”, *Durability of building materials and components* (Volume 1), 1999.

Whiting, D., 1981. “Rapid Determination of the Chloride Permeability of Concrete”, *Report No.* FHWA/RD-81/119, Federal Highway Administration, Washington, DC, 174 pp.